THE EFFECT OF IMPACT DAMPER IN FORCED VIBRATIONS

THE EFFECT OF IMPACT DAMPER IN FORCED VIBRATIONS

By

MAHENDRA D. SHAH, B. E.

A Thesis

Submitted to the Faculty of Graduate Studies

in Partial Fulfilment of the Requirements

for the Degree

Master of Engineering

McMaster University

March, 1968

MASTER OF ENGINEERING (1969) McMASTER UNIVERSITY

(CIVIL ENGINEERING) Hamilton, Ontario

TITLE: Composite Action in the Reinforced Concrete Beam

AUTHOR: A. Shakoor Uppal, B.Sc.Eng. (Panjab University)

SUPERVISOR: Dr. H. Robinson

NUMBER OF PAGES: xii, 195

SCOPE AND CONTENTS:

This thesis involves the treatment of the reinforced concrete beam as a composite beam with incomplete interaction. Influence of the loss of interaction and other parameters on the flexural cracking, and the moment capacity of the remaining uncracked portion of the reinforced concrete beam is studied analytically.

MASTER OF ENGINEERING (1968) McMASTER UNIVERSITY
(Mechanical Engineering) Hamilton, Ontario

TITLE: The Effect of Impact Damper in Forced Vibrations

AUTHOR: Mahendra D. Shah, B.E. (Electrical), B.E. (Mechanical)
M.S. University of Baroda, India

SUPERVISOR: Dr. M. A. Dokainish

NUMBER OF PAGES:

SCOPE AND CONTENTS:

An extensive experimental study is made of the general behaviour of the impact dampers, using a mechanical model. Coefficient of restitution, Mass-ratio, and Gap-factor are the parameters which were changed during the course of investigation and their effects were observed..

The noise level has been eliminated successfully. Dampers containing two particles in a single container are compared with single particle dampers and the latter are found to be relatively efficient. Results with the mass particle oscillating in the container filled with fluid indicate that friction forces acting on the mass-particle are detrimental to the efficiency of the damper.

ACKNOWLEDGEMENTS

The author wishes to express his gratitude to Dr. D. G. Huber, Chairman of Mechanical Engineering Department, whose advice, encouragement, and guidance were invaluable in the early stage of the work.

The author is deeply grateful to his supervisor, Dr. M. A. Dokainish, for the suggestion of the topic and constant guidance in all phases of this work.

The author is further indebted to the Department of Mechanical Engineering for the award of the scholarship and assistantship and to the National Research Council for support of this work under Grant No. A-2726.

Thanks are due to Mr. W. K. McDermid, of Polymer Corporation Limited, Sarnia, for the supply of rubber sheetings required for experimental purpose.

Thanks are due to Mrs. Anne Woodrow and Mrs. Carol Hedlund for their skillful typing.

TABLE OF CONTENTS

NOMENCLATURE

A	Displacement Amplitude of the Primary System in the Absence of the Impact Damper.
A_R	Displacement Amplitude of the Primary System in the Absence of the Impact Damper, at Resonance.
C	Inherent Equivalent Viscous Damping of the System.
C_{cr}	Critical Damping, $2\sqrt{KM}$
d	Clearance in Which the Particle is Free to Oscillate.
e	Coefficient of Restitution Between Container and m_i, $i = 1,2$.
e_3	Coefficient of Restitution Between m_1 and m_2.
F_o	Maximum Force of Excitation.
K	Spring Constant.
M	Mass of the Primary Vibrating System.
m	Mass of Particle.
m'	Added Mass Due to Fluid.
m_1) m_2)	Mass of Each Particle in Two-Particle System.
r	Frequency Ratio, $\frac{\Omega}{\omega}$
t	Time.
U, V, W	Absolute Velocities of Particles, as Defined in Figure 2.2.
X	Displacement of M.
X_o	Static Deflection, F_o/K.
X_R	Displacement of M, at Resonance.
Y_1	Displacement of Particle.

Y	Relative Displacement of Particle with Respect to M.
Z_i	Displacement of Particle m_i, i = 1,2.
α	Phase Angle Between Exciting Force and the First Impact.
δ	Critical Damping Ratio, C/C_{cr}.
μ	Mass Ratio, $m/M = \frac{m_1 + m_2}{M}$
μ_1	Mass Ratio, $\frac{m}{m + m'}$
μ_2	Mass Ratio, $\frac{m_1}{M} = \frac{m_2}{M}$
β	Gap Ratio, d/A
ρ_f	Density of Fluid in lbf. $Sec.^2/ft.^4$
ψ	Phase Angle (due to damping).
τ	Phase Angle, $\tau = \alpha - \psi$
ω	Natural Frequence, $\sqrt{K/M}$
Ω	Forcing Frequency.

I INTRODUCTION

I.1 HISTORY

The Impact Vibration Absorber, or Acceleration Damper, reduces the vibration of a mechanical system through momentum transfer by collision and conversion of mechanical energy into heat. A typical unit, Fig. 1.1, consists of a mass particle constrained to oscillate in a container which is fixed to the primary vibrating system. The effectiveness of the damper depends not only on the dissipation of energy in impacts but also on how the relative motion of the mass particle is tuned with respect to that of the container.

Paget [1]* was a pioneer in making experimental study of this damper. The free vibration of a simple harmonic oscillator attached with an impact vibration absorber was first investigated by Lieber and Jensen [2]. They considered only perfectly plastic impacts between the small mass and its container, and predicted theoretically that the maximum energy will be dissipated in a cycle when the container length is π times the amplitude of response. Results from experiments with lead spheres verified this theory.

Grubin [3] solved the viscously damped forced vibration problem by assuming that the impacts occured twice per cycle at

---

* Numbers in squre brackets designate reference at the end of the thesis.

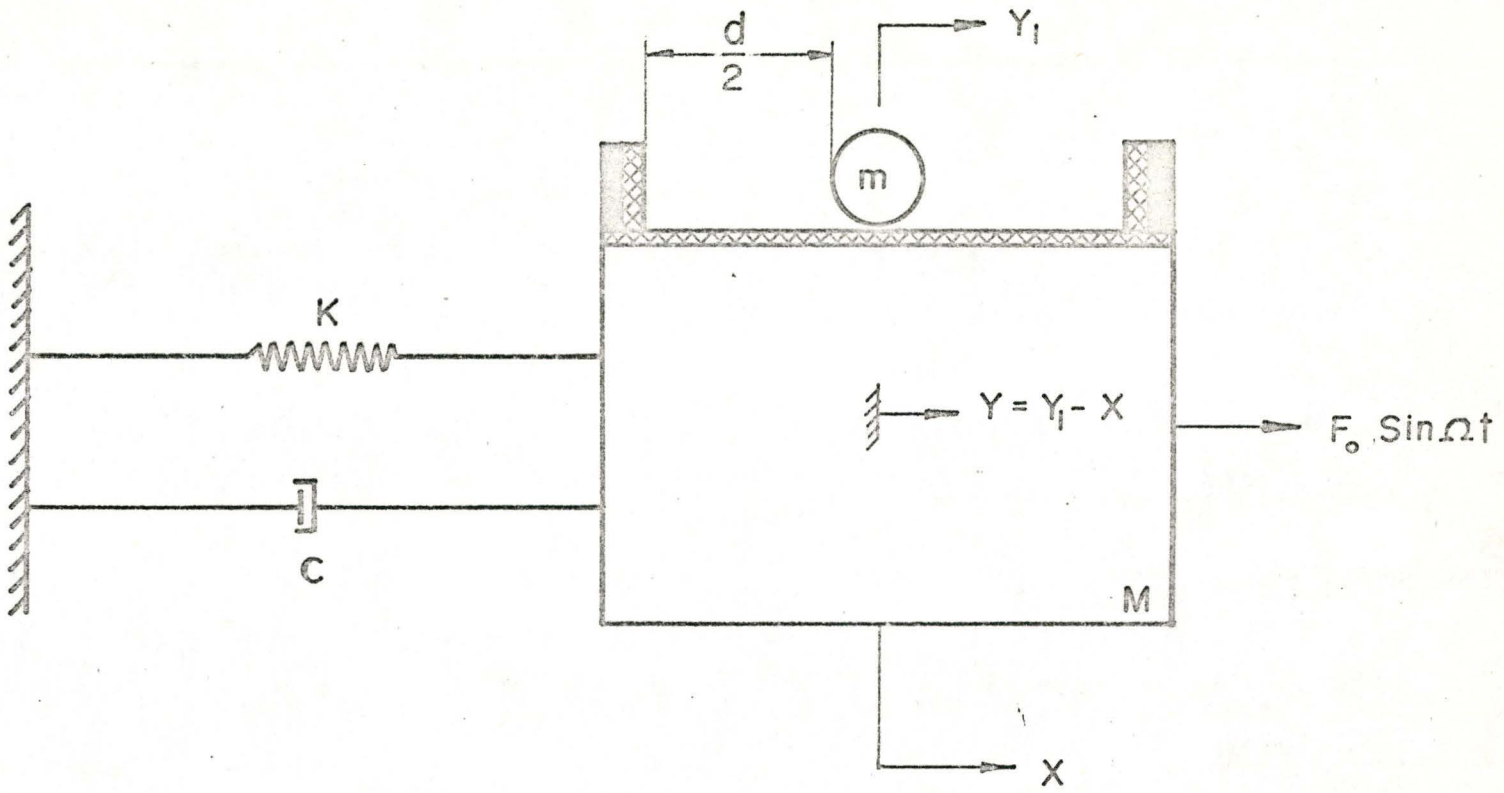

Fig. 1.1 Model of system

equal time intervals and by summing the effects of many impacts. It was shown that these assumptions result in two possible solutions but it could not be shown which one of these prevails, without solving the problem by a more exact but long numerical impact to impact method.

By introducing an unknown phase angle into the applied harmonic force and assuming steady state of two equispaced impacts per cycle and neglecting the inherent damping in the system, Arnold [4] analysed the problem. His experimental evidence did not agree with the theory.

A considerably simpler method for deriving the solution for two impacts per cycle motion, which requires only the consideration of two successive impacts, was suggested by Warburton [5].

Masri [6] has reported the stability analysis for two impacts per cycle solution and experiments with mechanical model and electric-analog simulation. Application of the stability criteria developed by him is numerically extensive because of the complicated functional dependence of the stability boundaries on the system's parameters. A very simple stability criterion for these solutions, neglecting the inherent damping in the system, was developed by Egle [10], and was used to determine the dependance of the stability boundaries on the parameters of the system.

The effectiveness of the impact damper on nonlinear systems is to be found in a recent work by Jha [18].

On the experimental side, the feasibility of using impact damping to reduce vibrations of such diverse systems as ship hulls, cantilever beams, single degree of freedom systems, and turbine buckets was investigated by McGoldrick [13], Lieber and Tripp [14], Sankey [15], and Duckwald [16]. Eastabrook and Plunkett [17] made an analytical study of impact damping in turbine buckets. Kaper [9] has reported the use of the impact damper in reducing vibrations of the reflectors of television receiving antennae.

All the previous investigators have reported excessive noise level while the impact damper is in operation.

I.2 OBJECTIVES

The objectives of the present study are to:

1. Extend and complement the work of other investigators in this field.
2. Study experimentally the general response of the damper to a wide range of its parameters including effect of the coefficient of restitution.
3. Investigate the behaviour of the two-particle impact damper.
4. Make the system usable in practice by reducing the noise level.
5. Study the effect of fluid resistance on the motion of the mass particle.

The objectives were accomplished by conducting experimental studies of two-particle and single-particle impact dampers. Coefficient of restitution e; Mass-ratio μ; and Gap-factor d/x_o; are the three parameters which were changed during the course of the experiments and their effects were observed. Coefficient of restitution was changed by using different rubber pads at the container ends where the collision occurs. The effect of friction was observed by allowing the mass particle to oscillate in a container filled with fluid.

The theoretical analysis and computed results are given in Chapter 2. The experimental procedure and apparatus are first described in Chapter 3 and then the results are plotted. The discussion is given in Chapter 4 and conclusions drawn from this investigation are stated in Chapter 5.

2 STEADY STATE SOLUTION

2.1 TWO-PARTICLE IMPACT DAMPER

The idealized model considered is shown in Figure 2.1. The equation of motion of primary mass M, between impacts, following the method suggested by Warburton [5], becomes

$$M\ddot{X} + C\dot{X} + KX = F_o \sin(\Omega t + \alpha) \tag{1}$$

and its complete solution is

$$X = e^{-\delta\omega t}\left[B_1 \sin\eta\omega t + B_2 \cos\eta\omega t\right] + A\sin(\Omega t + \tau) \tag{2}$$

where $\delta = C/C_{cr.}$; $C_{cr.} = 2\sqrt{KM}$

$\omega = \sqrt{K/M}$; $\eta = \sqrt{1-\delta^2}$

$r = \Omega/\omega$

$$A = \frac{F_o/K}{\sqrt{(1-r^2)^2 + (2\delta r)^2}}$$

$\tau = \alpha - \psi$

$\psi = \tan^{-1}\frac{2\delta r}{1-r^2}$

It is assumed that the two particles m_1 and m_2 are identical and that each particle has a single degree of freedom. Furthermore, it is assumed that, if there is a collision between, let us say, m_1 and the right hand side of the container at time t = 0, then the

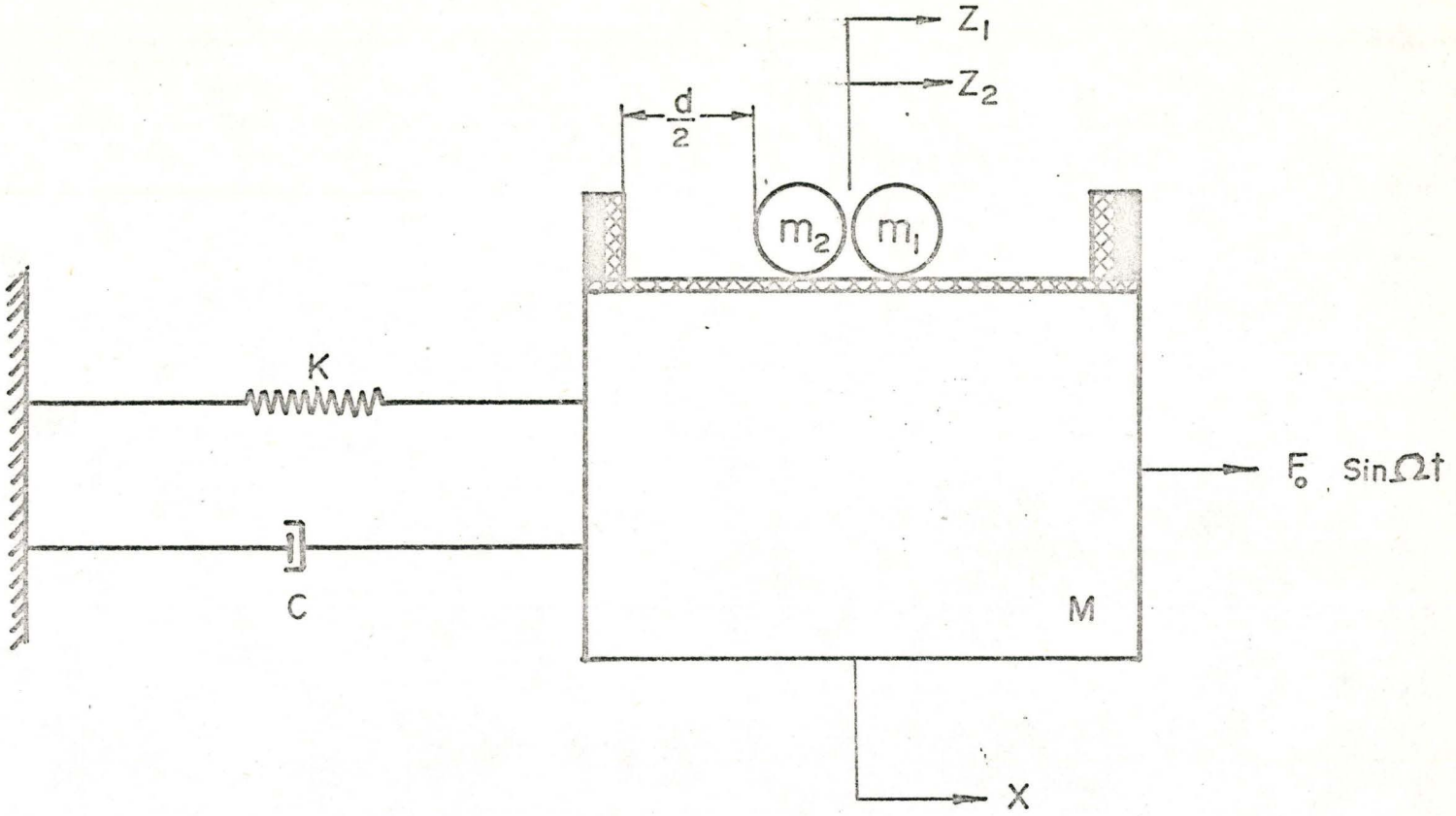

Fig. 2.1 Model Of System

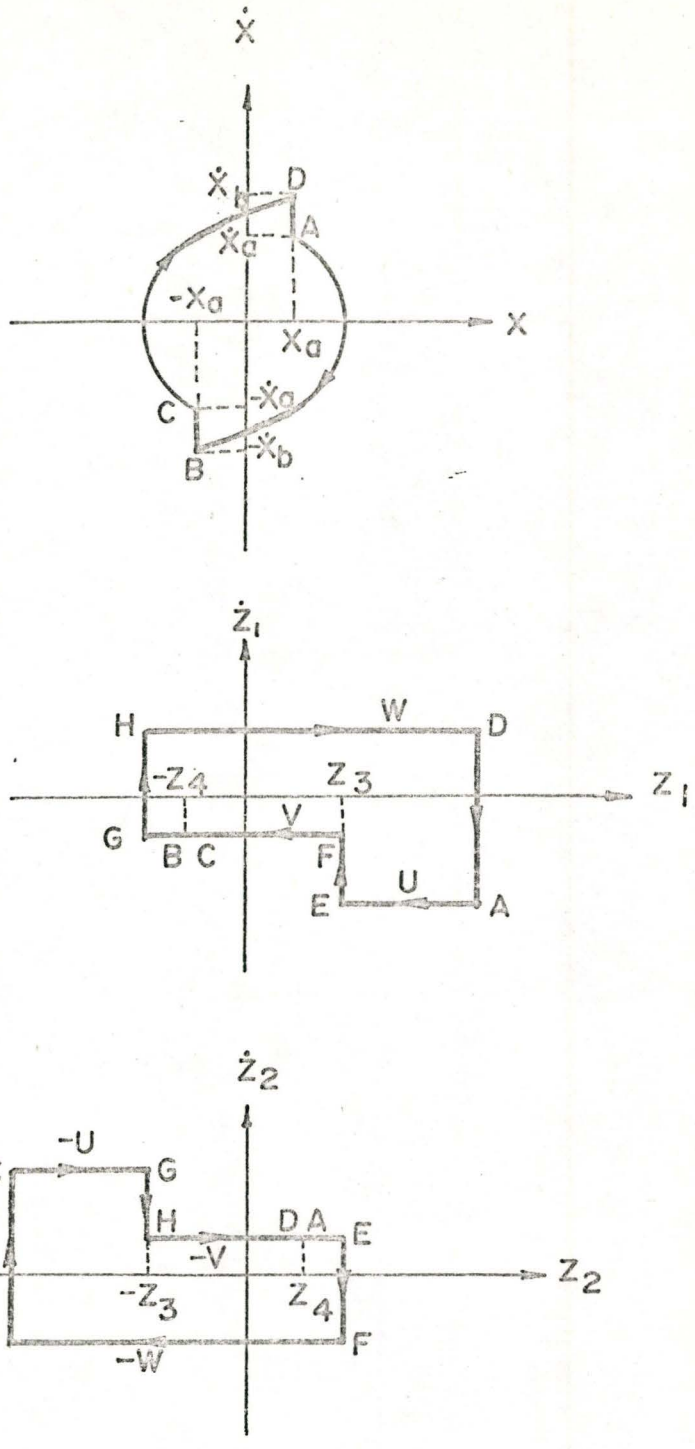

Fig. 2.2 PHASE PLANE REPRESENTATION OF PERIODIC 4 IMPACTS/CYCLE MOTION

next impact will occur at $t = \frac{\alpha_o}{\Omega}$ between the two particles. At $\Omega t = \pi$, there will be a collision between m_2 and the left hand side of the container; and at $\Omega t = \pi + \alpha_o$, the two particles will collide again. The phase plane representation of the corresponding periodic motion is shown in Figure 2.2.

The duration of impact is very small compared to the natural period of the primary system, hence it is reasonable to assume that at $t = 0_+$ the positions of M, m_1 and m_2 remain the same while their respective absolute velocities are discontinuously changing.

To summarize, the system should satisfy the following conditions:

t	X	$\dot{X}$	Z_1	$\dot{Z}_1$	Z_2	$\dot{Z}_2$
0_-	X_b	$\dot{X}_b$	$\frac{d}{2} + X_b$	W	Z_4	-V
0_+	X_b	$\dot{X}_a$	$\frac{d}{2} + X_b$	U	Z_4	-V
$\left(\frac{\alpha_o}{\Omega}\right)_-$			Z_3	U	Z_3	-V
$\left(\frac{\alpha_o}{\Omega}\right)_+$			Z_3	V	Z_3	-W
$\left(\frac{\pi}{\Omega}\right)_-$	$-X_b$	$-\dot{X}_b$	$-Z_4$	V	$-\frac{d}{2} - X_b$	-W
$\left(\frac{\pi}{\Omega}\right)_+$	$-X_b$	$-\dot{X}_a$	$-Z_4$	V	$-\frac{d}{2} - X_b$	-U

(3)

Since the motion of the system during impact must satisfy the momentum equation, then

$$M\dot{X}_- + m_i\dot{Z}_{i-} = M\dot{X}_+ + m_i\dot{Z}_{i+} \tag{4}$$

where i = 1 or 2 depending on the impinging mass particle, and for impact between the two mass particles;

$$\begin{aligned} & m_1\dot{Z}_{1-} + m_2\dot{Z}_{2-} = m_1\dot{Z}_{1+} + m_2\dot{Z}_{2+} \\ \text{or} \quad & \dot{Z}_{1-} + \dot{Z}_{2-} = \dot{Z}_{1+} + \dot{Z}_{2+} \end{aligned} \tag{5}$$

and from the definition of coefficient of restitution,

$$\dot{X}_+ - \dot{Z}_{i+} = -e(\dot{X}_- - \dot{Z}_{i-}) \tag{6}$$

similarly for impact between two masses

$$\dot{Z}_{1+} - \dot{Z}_{2+} = -e_3(\dot{Z}_{1-} - \dot{Z}_{2-}) \tag{7}$$

In steady state motion absolute speed of the particle is constant between impacts and can be given by,

$$U = \{Z_3 - (\frac{d}{2} + X_b)\}\frac{\Omega}{\alpha_0} \tag{8}$$

$$-V = \{Z_3 - Z_4\}\frac{\Omega}{\alpha_0} \tag{9}$$

$$V = \{-Z_4 - Z_3\}\frac{\Omega}{\pi-\alpha_0} \tag{10}$$

$$W = \{(\frac{d}{2} + X_b) + Z_3\} \frac{\Omega}{\pi - \alpha_0} \tag{11}$$

From equations (5), (7) and using conditons in (3),

$$U - V = V - W \tag{12}$$

$$V + W = -e_3(U + V) \tag{13}$$

substituting U, V, W in equation (13) from equations (8), (9), (10) and (11) we get,

$$\left\{(\frac{d}{2} + X_b) - Z_4\right\}\frac{\Omega}{\pi - \alpha_0} = -e_3\left\{-(\frac{d}{2} + X_b) + Z_4\right\}\frac{\Omega}{\alpha_0}$$

or $$\frac{1}{\pi - \alpha_0} = \frac{e_3}{\alpha_0}$$

$$\alpha_0(1 + e_3) = \pi e_3$$

$$\alpha_0 = \frac{\pi e_3}{1 + e_3} \tag{14}$$

Using equations (12) and (13)

$$V = \frac{1 - e_3}{3 + e_3} U = C_1 U \tag{15}$$

$$W = -\frac{1 + 3e_3}{3 + e_3} U = C_2 U \tag{16}$$

where

$$C_1 = \frac{1 - e_3}{3 + e_3}$$

$$C_2 = -\frac{1 + 3e_3}{3 + e_3}$$

Substituting W and U from equations (8), (11) into equation (16)

$$\left\{\left(\frac{d}{2} + X_b\right) + Z_3\right\}\frac{\Omega}{\pi - \alpha_o} = C_2\left\{Z_3 - \left(\frac{d}{2} + X_b\right)\right\}\frac{\Omega}{\alpha_o}$$

or

$$\left(\frac{d}{2} + X_b\right) + Z_3 = \frac{C_2}{e_3}\left\{-\left(\frac{d}{2} + X_b\right) + Z_3\right\}$$

or

$$\left(\frac{d}{2} + X_b\right)\left(1 + \frac{C_2}{e_3}\right) = Z_3\left(\frac{C_2}{e_3} - 1\right)$$

$$Z_3 = \left(\frac{d}{2} + X_b\right)\left(\frac{C_2 + e_3}{C_2 - e_3}\right)$$

$$Z_3 = \left(\frac{d}{2} + X_b\right)\left(\frac{1 - e_3^2}{1 + 6e_3 + e_3^2}\right) \qquad (17)$$

From equations (8) and (17),

$$U = \left(\frac{d}{2} + X_b\right)\left\{\frac{-2e_3(3+e_3)}{1 + 6e_3 + e_3^2}\right\}\frac{\Omega}{\alpha_o}$$

$$U = -\left(\frac{d}{2} + X_b\right)\left\{\frac{2e_3(3+e_3)}{2e_3(3+e_3) + 1 - e_3^2}\right\}\frac{\Omega}{\alpha_o}$$

$$U = -\left(\frac{d}{2} + X_b\right)\left\{\frac{1}{1 + \frac{(1+e_3)(1-e_3)}{2e_3(3+e_3)}}\right\}\frac{\Omega}{\alpha_o} \qquad (17\text{-a})$$

Using equations (14) , (15) and (17-a);

$$U = -\left(\frac{d}{2} + X_b\right)\left(\frac{1}{1 + \frac{\pi C_1}{2\alpha_0}}\right)\frac{\Omega}{\alpha_0}$$

$$U = -\left(\frac{d}{2} + X_b\right)\left(\frac{1}{\alpha_0 + \frac{\pi C_1}{2}}\right)\Omega \qquad (18)$$

simplifying equations (4), (6) to obtain relations for primary mass velocities before and after impact explicitly in terms of mass-particle velocities,

$$\dot{X}_- = \frac{(e-\mu_2)\dot{Z}_{i-} + (1+\mu_2)\dot{Z}_{i+}}{1+e} \qquad (19)$$

$$\dot{X}_+ = \frac{e(1+\mu_2)\dot{Z}_{i-} + (1-\mu_2 e)\dot{Z}_{i+}}{1+e} \qquad (20)$$

where $\mu_2 = \frac{m_1}{M} = \frac{m_2}{M}$ and $\mu = \frac{m_1 + m_2}{M}$

Now from equations (16), (18), (19) and (3) at t = 0,

$$\dot{X}_b = \left(\frac{e-\mu_2}{1+e}\right)W + \left(\frac{1+\mu_2}{1+e}\right)U$$

$$\dot{X}_b = (K_1 C_2 + K_2)U$$

where

$$K_1 = \frac{e-\mu_2}{1+e}$$

and $$K_2 = \frac{1+\mu_2}{1+e}$$

$$\dot{X}_b = -\left(\frac{d}{2} + X_b\right)\left\{\frac{\Omega\,(K_1 C_2 + K_2)}{\alpha_o + \frac{\pi C_1}{2}}\right\}$$

$$X_b + \left\{\frac{\alpha_o + \frac{\pi C_1}{2}}{\Omega\,(K_1 C_2 + K_2)}\right\}\dot{X}_b = -\frac{d}{2} \qquad (21)$$

similarly from equations (16), (18), (20) and (3) at t = 0,

$$X_b + \left\{\frac{\alpha_o + \frac{\pi C_1}{2}}{\Omega\,(K_3 C_2 + K_4)}\right\}\dot{X}_a = -\frac{d}{2} \qquad (22)$$

where $$K_3 = \frac{e\,(1+\mu_2)}{1+e}$$

and $$K_4 = \frac{1-\mu_2 e}{1+e}$$

An expression describing the velocity of M can be obtained by differentating equation (2) with respect to t.

Thus

$$\dot{X} = -\delta\omega e^{-\delta\omega t}\,(B_1 \sin\eta\omega t + B_2 \cos\eta\omega t)$$

$$+ e^{-\delta\omega t}\,(B_1\eta\omega\cos\eta\omega t - B_2\eta\omega\sin\eta\omega t) + A\Omega\cos(\Omega t+T) \qquad (23)$$

From equations (2), (23) and using conditions (3),

$$X(0_+) = X_b = B_2 + A\sin(T) \qquad (24)$$

$$X\left\{\left(\frac{\Pi}{\Omega}\right)_-\right\} = -X_b = e^{-\frac{\delta\Pi}{r}}\left(B_1 \sin \eta\frac{\Pi}{r} + B_2 \cos \eta\frac{\Pi}{r}\right) - A \sin(T) \tag{25}$$

$$\dot{X}(0_+) = \dot{X}_a = -\delta\omega B_2 + B_1 \eta\omega + A\Omega \cos(T) \tag{26}$$

$$\begin{aligned}\dot{X}\left\{\left(\frac{\Pi}{\Omega}\right)_-\right\} = -\dot{X}_b = &-\delta\omega e^{-\frac{\delta\Pi}{r}}\left[B_1 \sin \eta\frac{\Pi}{r} + B_2 \cos \eta\frac{\Pi}{r}\right] \\ &+ \eta\omega e^{-\frac{\delta\Pi}{r}}\left[B_1 \cos \eta\frac{\Pi}{r} - B_2 \sin \eta\frac{\Pi}{r}\right] \\ &- A\Omega \cos(T)\end{aligned} \tag{27}$$

From equations (24), (27), (25), (26), (21), and (22),

$$\begin{aligned} X_b - B_2 - SA &= 0 \\ \dot{X}_b + \theta_1 B_1 + \theta_2 B_2 - CA &= 0 \\ X_b + h_1 B_1 + h_2 B_2 - SA &= 0 \\ \dot{X}_a - \eta\omega B_1 + \delta\omega B_2 - CA &= 0 \\ X_b + C_3 \dot{X}_b &= -\frac{d}{2} \\ X_b + C_4 \dot{X}_a &= -\frac{d}{2} \end{aligned} \tag{28}$$

where $S = \sin(T)$; $C = \Omega \cos(T)$

$$h_1 = e^{-\frac{\delta\Pi}{r}} \sin \eta\frac{\Pi}{r} \quad ; \quad h_2 = e^{-\frac{\delta\Pi}{r}} \cos \eta\frac{\Pi}{r}$$

$$C_3 = \left\{\frac{\alpha_0 + \frac{\Pi C_L}{2}}{\Omega(K_1 C_2 + K_2)}\right\}$$

$$C_4 = \left\{\frac{\alpha_0 + \frac{\Pi C_1}{2}}{\Omega(K_3 C_2 + K_4)}\right\}$$

$$\theta_1 = \omega e^{-\frac{\delta\pi}{r}}\left[-\delta \sin \eta\frac{\pi}{r} + \eta \cos \eta\frac{\pi}{r}\right]$$

$$\theta_2 = \omega e^{-\frac{\delta\pi}{r}}\left[-\delta \cos \eta\frac{\pi}{r} - \eta \sin \eta\frac{\pi}{r}\right]$$

Equation (28) can be put in the form of matrix,

$$\begin{bmatrix} 1 & 0 & 0 & 0 & -1 & -S \\ 0 & 0 & 1 & -\eta\omega & \delta\omega & -C \\ 1 & 0 & 0 & h_1 & h_2 & -S \\ 0 & 1 & 0 & \theta_1 & \theta_2 & -C \\ 1 & C_3 & 0 & 0 & 0 & 0 \\ 1 & 0 & C_4 & 0 & 0 & 0 \end{bmatrix} \begin{Bmatrix} X_b \\ \dot{X}_b \\ \dot{X}_a \\ B_1 \\ B_2 \\ A \end{Bmatrix} = \begin{Bmatrix} 0 \\ 0 \\ 0 \\ 0 \\ -d/2 \\ -d/2 \end{Bmatrix} \tag{29}$$

From these equations A, B_1, and B_2 in terms of the known parameters can be obtained. Thus

$$A = \frac{N(A)}{\Delta} \tag{30}$$

$$B_1 = \frac{N(B_1)}{\Delta} \tag{31}$$

$$B_2 = \frac{N(B_2)}{\Delta} \tag{32}$$

where $N(A) = \frac{d}{2}[h_1(C_3\theta_2 - C_4\omega\delta) - (C_3\theta_1 + \eta C_4\omega)(1+h_2)]$

$$N(B_1) = \frac{d}{2}(1+h_2)(C_4 - C_3)C$$

$$N(B_2) = \frac{d}{2}h_1(C_3 - C_4)C$$

$$\Delta = h_1[C(C_4 - C_3) - (S + CC_4)C_3\theta_2 + (S + CC_3)\delta\omega C_4]$$

$$+(1+h_2)[(S + CC_4)C_3\theta_1 + (S + CC_3)\eta\omega C_4]$$

Equation (30) can be put in the form

$2 \sin T + H \cos T = -\delta$ .....(33), where $\delta = \frac{d}{A}$ and

$$H = 2\Omega\left\{\frac{[(C_4 - C_3) + C_3C_4(\delta\omega - \theta_2)]h_1 + [C_3C_4(\theta_1 + \eta\omega)](1+h_2)}{[\delta C_4\omega - C_3\theta_2]h_1 + [C_3\theta_1 + \eta C_4\omega](1+h_2)}\right\}$$

Solution of equation (31) for T results in:

$$\sin T = \frac{-2\delta \pm H\sqrt{H^2+4-\delta^2}}{H^2+4}$$

$$\cos T = \frac{-\delta H \mp 2\sqrt{H^2+4-\delta^2}}{H^2+4}$$

$$T = \tan^{-1}\left[\frac{-2\delta \pm H\sqrt{H^2+4-\delta^2}}{-\delta H \mp 2\sqrt{H^2+4-\delta^2}}\right] \qquad (34)$$

In order to have real values for sin T and cos T, the clearance d cannot be arbitrarily large; it should satisfy the relation

$S^2 \leq H^2 + 4$. The physical interpretation of this restriction is that, for d exceeding this limit, the actual system will not have a four-impacts per cycle steady state motion.

With the value of T determined from equation (34), B_1 and B_2 can be found from equations (31) and (32), and with the help of equation (2) the motion of the primary mass is determined.

Without introducing damping, the behaviour of damper at resonance (r=1) can be determined by putting $r = 1 + \varepsilon$ and letting $\varepsilon \to 0$. It is found that

$$\frac{X}{X_0} = \left(\frac{\pi^2}{8\mu_2} - \frac{1}{2}\frac{d}{X_0}\right)\cos\omega t - \frac{(1-e-2\mu_2 e)\pi}{4\mu_2(1+e)}\sin\omega t - \frac{1}{2}\omega t \sin\omega t \quad (35)$$

where $X_0 = F_0/K$ $\qquad 0 \leq \omega t \leq \pi$

Differentating equation (35) with respect to ωt, it can be shown that the maximum displacement occurs when $\omega t = \pi/2$, if

$$\frac{d}{X_0} = 1 + \frac{\pi^2}{4\mu_2} \quad (36)$$

From equation (35), the maximum displacement occurs at $\omega t = \pi/2$,

$$\left|X/X_0\right|_{max.} = \frac{\pi(1+\mu_2)(1-e)}{4\mu_2(1+e)} \quad (37)$$

2.2 SINGLE-PARTICLE IMPACT DAMPER

Following the method of Warburton [5], complete solution of the system is derived by Masri [6]. The equation of motion of the primary mass M between two impacts is

$$M\ddot{X} + C\dot{X} + KX = F_o \sin(\Omega t + \alpha)$$

and its complete solution is

$$X = e^{-\delta\omega t}\left[B_1 \sin \eta\omega t + B_2 \cos \eta\omega t\right] + A \sin(\Omega t + T) \qquad (38)$$

where δ, ω, η, A and r are as defined before and B_1 and B_2 are unknown constants.

Evaluating equation (38) and its derivative at $\Omega t = 0$ and π, and by using the definition of coefficient of restitution and the momentum equation, we obtain six relationships involving the six unknowns x_a, $\dot{x}_b$, $\dot{x}_a$, B_1, B_2 and T. The value of B_1, B_2 and T in the present case will be given by equations (31), (32), and (34) if their constants C_3 and C_4 are replaced by the new constants σ_1 and σ_2 respectively

where

$$\sigma_1 = \frac{\pi}{2\Omega}\,\frac{1+e}{1-e+2\mu}$$

$$\sigma_2 = \frac{\pi}{2\Omega}\,\frac{1+e}{1-e-2\mu e} \qquad \text{and} \qquad \mu = \frac{m}{M}$$

2.3 EFFECT OF VARIOUS PARAMETERS

Using the steady state solutions of section 2.1 and 2.2, to study the effect of various parameters, computation was done with the aid of digital computer IBM7040, at the computing center of the McMaster University. The computer programmes written in FORTRAN IV language are given in Appendix D.

The two sets of sign appearing in equation (34) correspond to two distinct steady state solutions. The upper sign is used in computation, as suggested by previous investigators, since only a part of the curve with upper signs results in a stable solution.

A check is introduced in the computer programmes which ensured that $\beta^2 \leq H^2+4$ and hence real values for T. Violation of above condition resulted in a note stating that the gap d is too big and the motion is unsteady.

In Figure 2.3, two-particle and single-particle systems are compared for various mass-ratios. It is seen that single-particle system is twice as effective as that of two-particle system.

In Figures 2.4 and 2.10, effect of coefficient of restitution is plotted. In both the systems it is seen that increase in value of e increases the efficiency of the damper, provided that the proper gap d is selected. Even with the value of e = 0 for both single-particle and two-particle systems the maximum reduction in amplitude is 59% and 42% respectively. It is observed that for

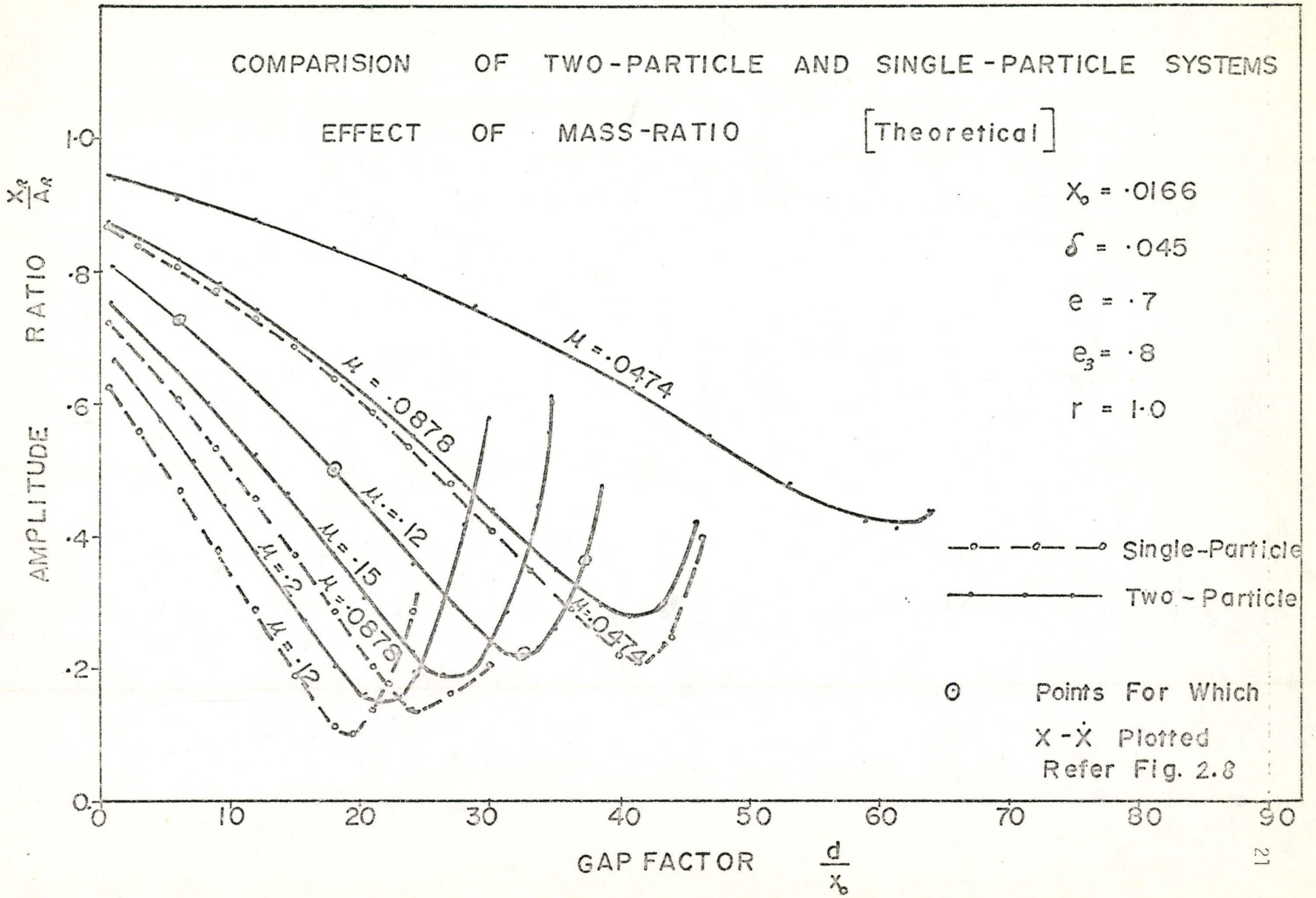
COMPARISION OF TWO-PARTICLE AND SINGLE-PARTICLE SYSTEMS
EFFECT OF MASS-RATIO [Theoretical]
X_0 = ·0166
δ = ·045
e = ·7
e_3 = ·8
r = 1·0
μ = ·0474
μ = ·0878
μ = ·12
μ = ·15
μ = ·2
μ = ·0878
μ = ·0474
μ = ·12
Single-Particle
Two-Particle
Points For Which X-Ẋ Plotted Refer Fig. 2.8
AMPLITUDE RATIO $\frac{X_R}{A_R}$
GAP FACTOR $\frac{d}{X_0}$
0
·2
·4
·6
·8
1·0
0
10
20
30
40
50
60
70
80
90

Fig. 2.3

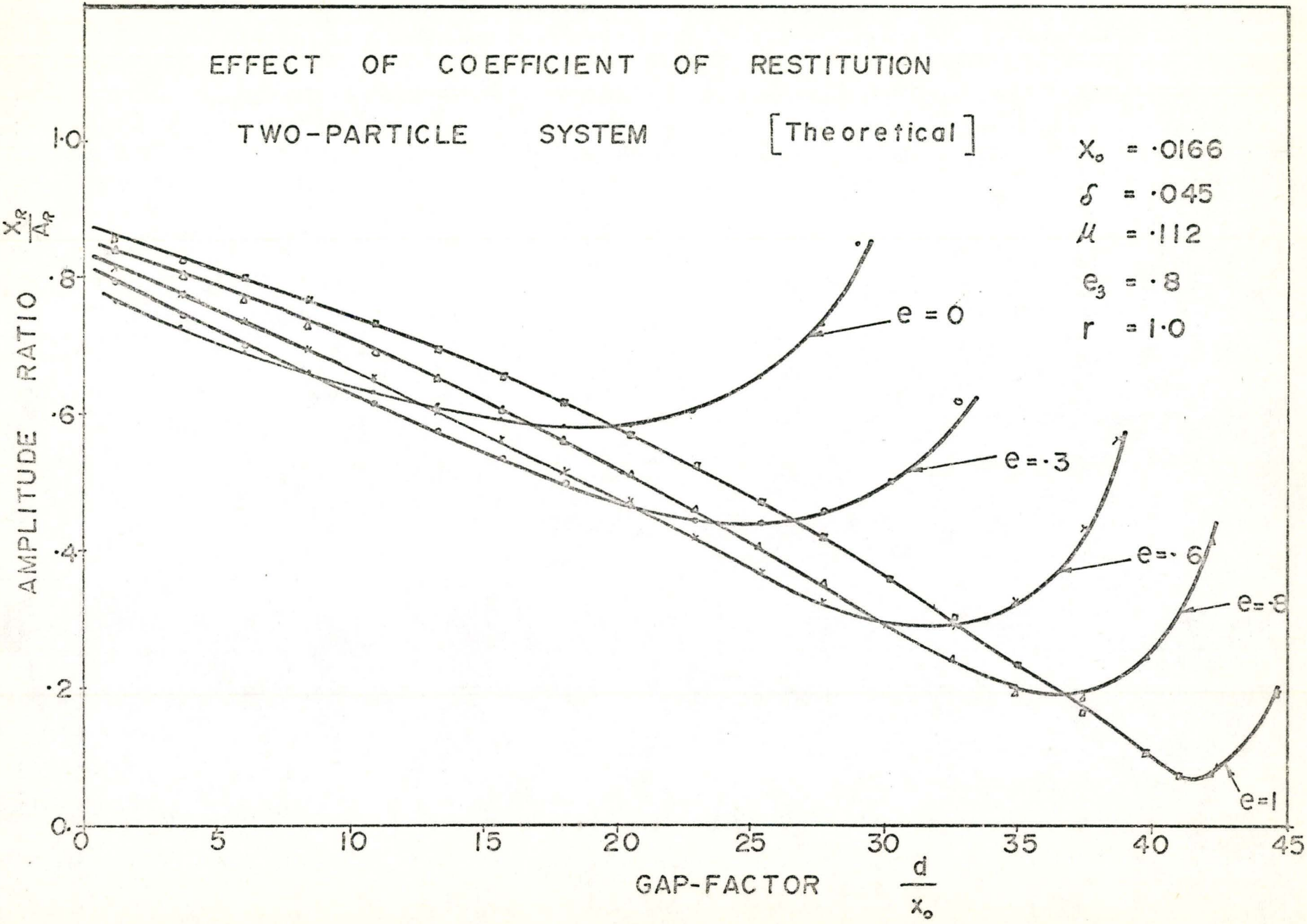
EFFECT OF COEFFICIENT OF RESTITUTION
TWO-PARTICLE SYSTEM [Theoretical]
X_o = ·0166
δ = ·045
μ = ·112
e_3 = ·8
r = 1·0
e = 0
e = ·3
e = ·6
e = ·8
e = 1
AMPLITUDE RATIO $\frac{X_R}{A_R}$
GAP-FACTOR $\frac{d}{x_o}$
1·0
·8
·6
·4
·2
0·
0
5
10
15
20
25
30
35
40
45

Fig 2.4

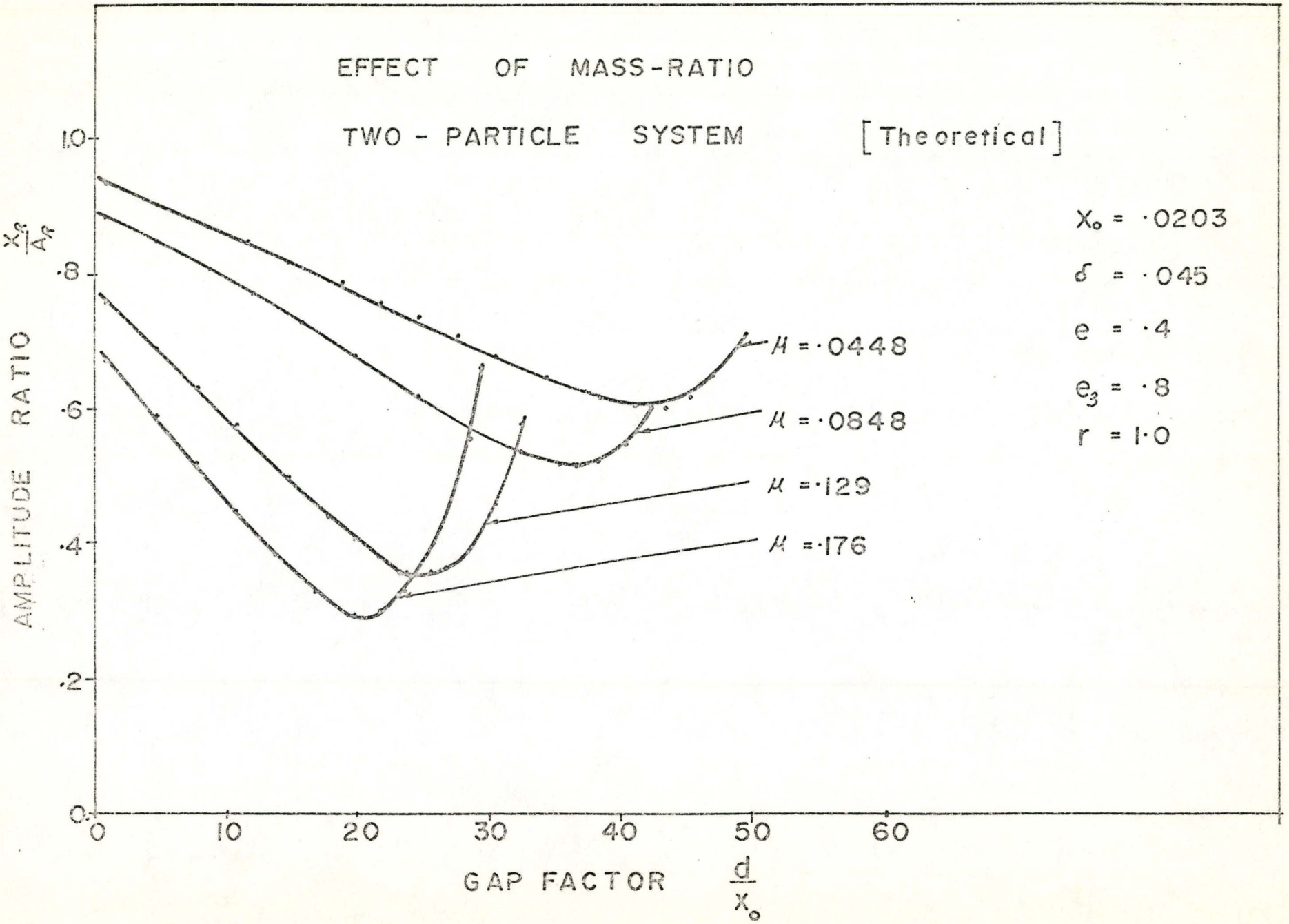
EFFECT OF MASS-RATIO
TWO - PARTICLE SYSTEM [Theoretical]
X_0 = ·0203
δ = ·045
e = ·4
e_3 = ·8
r = 1·0
μ = ·0448
μ = ·0848
μ = ·129
μ = ·176
AMPLITUDE RATIO $\frac{X_2}{A_2}$
1·0
·8
·6
·4
·2
0
0
10
20
30
40
50
60
GAP FACTOR $\frac{d}{X_0}$

Fig. 2.5

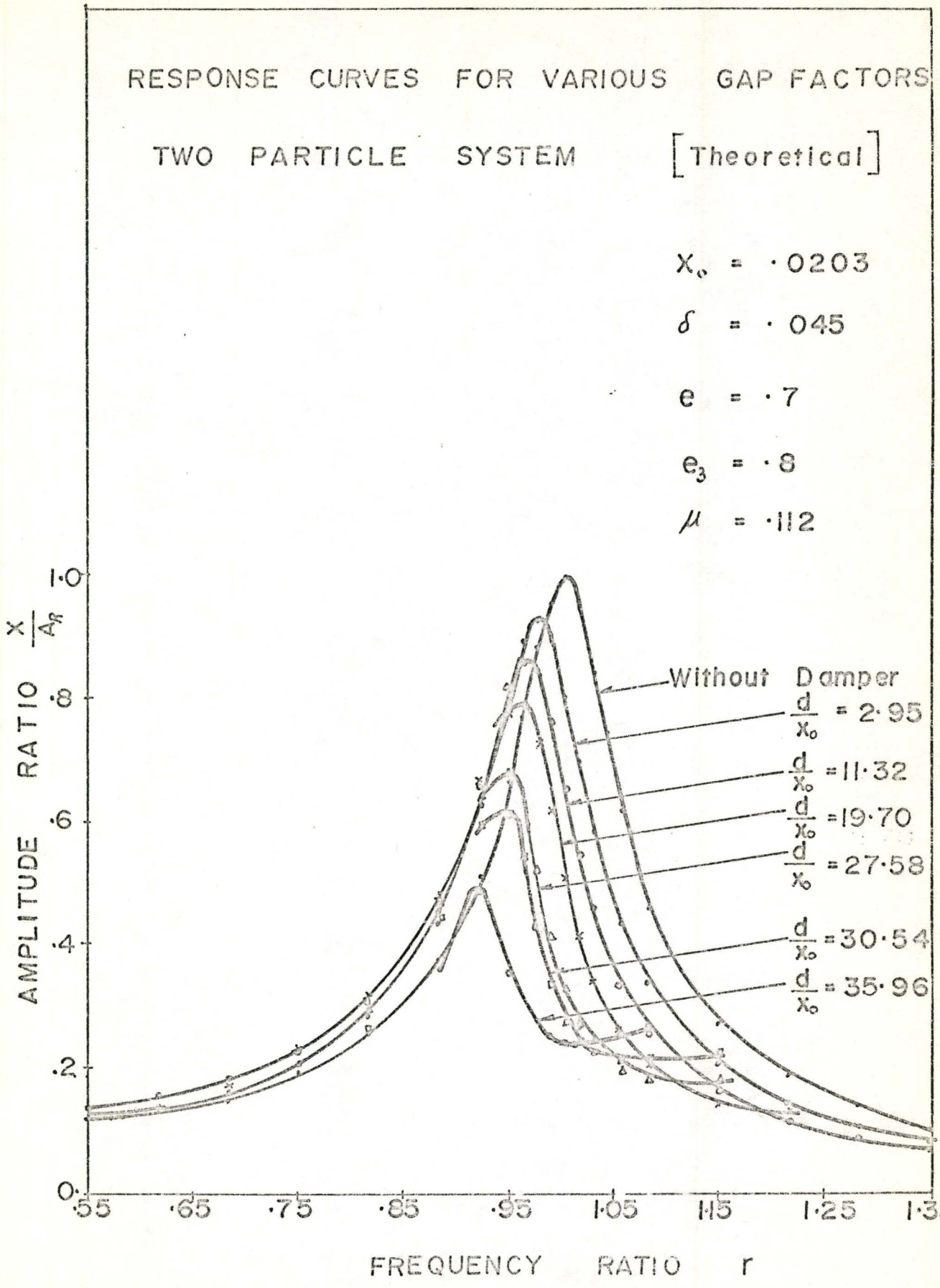
RESPONSE CURVES FOR VARIOUS GAP FACTORS
TWO PARTICLE SYSTEM [Theoretical]
X_0 = ·0203
δ = ·045
e = ·7
e_3 = ·8
μ = ·112
AMPLITUDE RATIO $\frac{X}{A_R}$
1·0
·8
·6
·4
·2
0·
Without Damper
$\frac{d}{X_0}$ = 2·95
$\frac{d}{X_0}$ = 11·32
$\frac{d}{X_0}$ = 19·70
$\frac{d}{X_0}$ = 27·58
$\frac{d}{X_0}$ = 30·54
$\frac{d}{X_0}$ = 35·96
·55
·65
·75
·85
·95
1·05
1·15
1·25
1·35
FREQUENCY RATIO r

Fig. 2.6

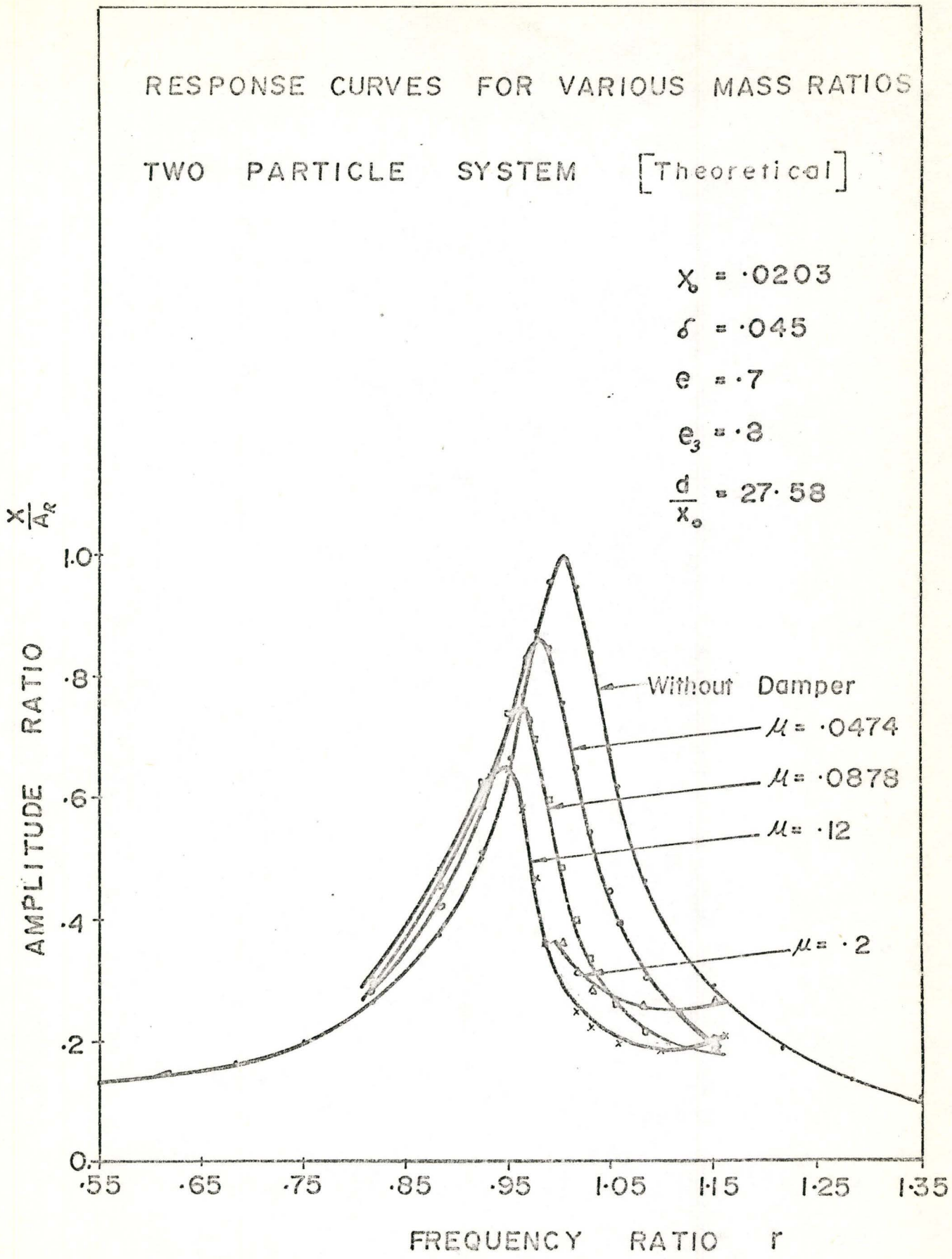
RESPONSE CURVES FOR VARIOUS MASS RATIOS
TWO PARTICLE SYSTEM [Theoretical]
X_0 = ·0203
δ = ·045
e = ·7
e_3 = ·8
$\frac{d}{x_0}$ = 27·58
$\frac{x}{A_R}$
AMPLITUDE RATIO
1.0
·8
·6
·4
·2
0.
Without Damper
μ = ·0474
μ = ·0878
μ = ·12
μ = ·2
·55
·65
·75
·85
·95
1·05
1·15
1·25
1·35
FREQUENCY RATIO r

Fig. 2.7

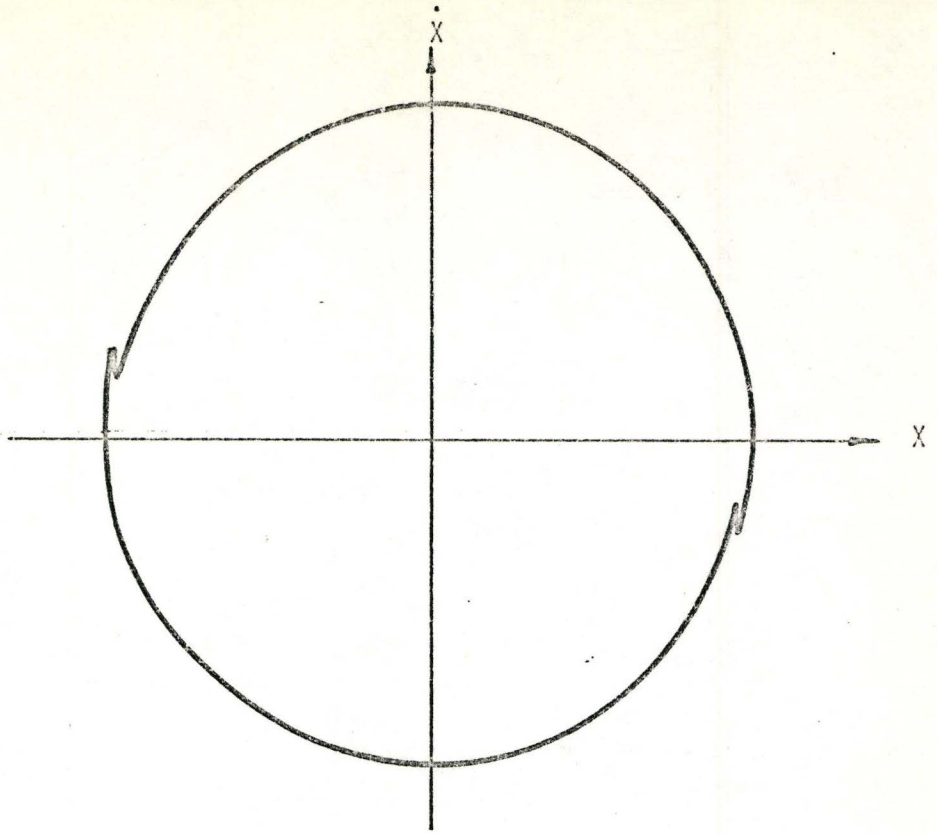

(a) $d/x_o = 6.0241$

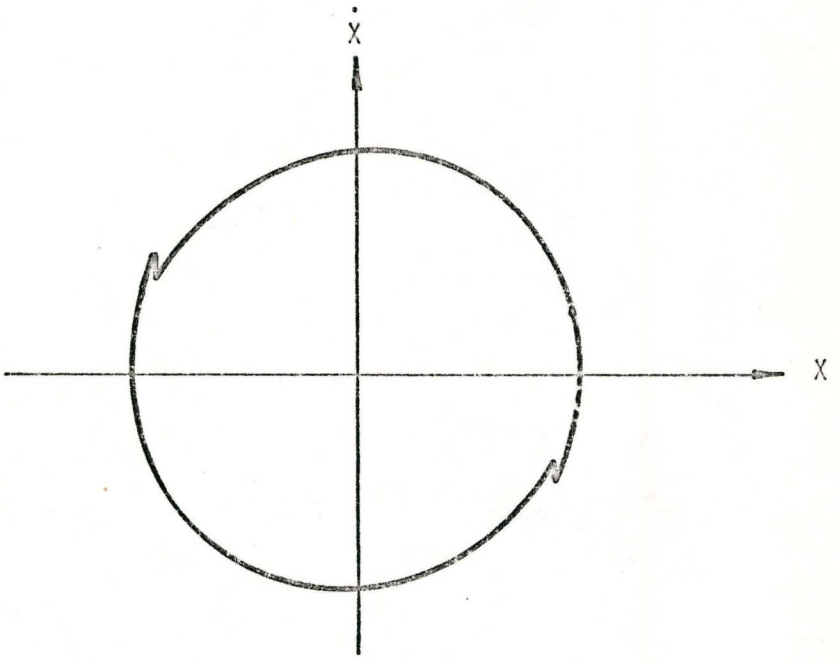

(b) $d/x_o = 18.0723$

Fig. 2.8 (a), (b).

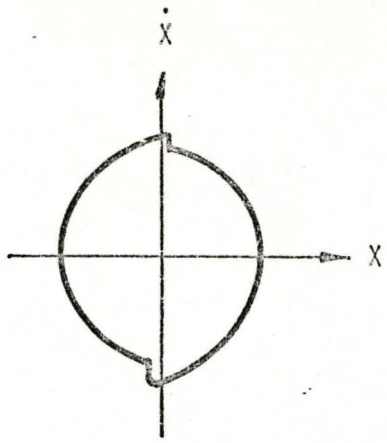

(c) $d/X_o = 32.53$

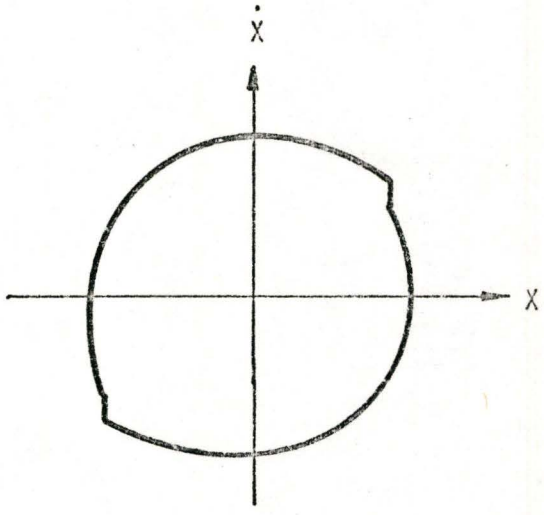

(d) $d/X_o = 37.35$

Figure 2.8 (a),(b),(c),(d) Phase Plane Diagrams for Primary Mass Motion [Theoretical]

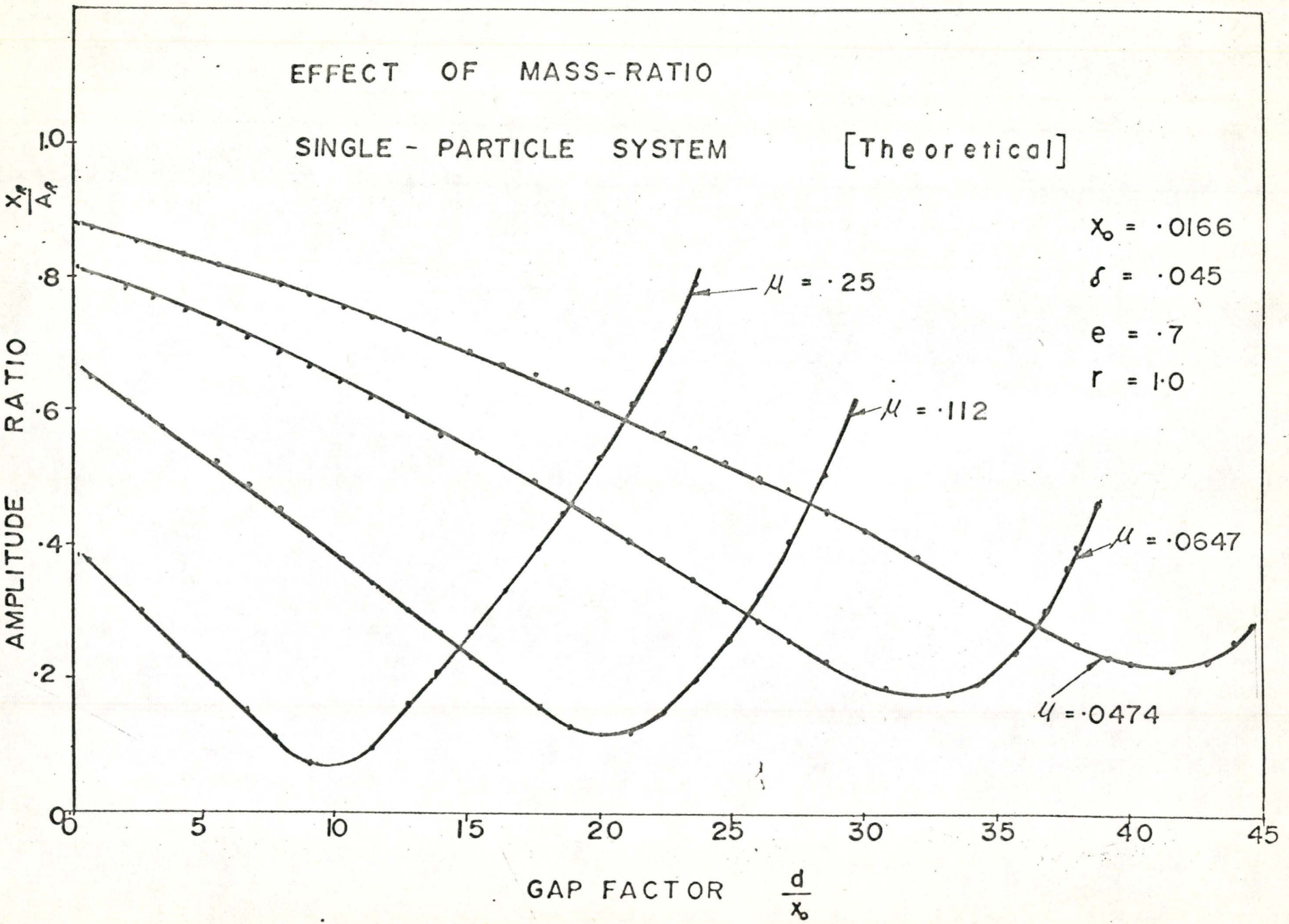
EFFECT OF MASS-RATIO
SINGLE - PARTICLE SYSTEM [Theoretical]
X_0 = ·0166
δ = ·045
e = ·7
r = 1·0
μ = ·25
μ = ·112
μ = ·0647
μ = ·0474
AMPLITUDE RATIO $\frac{X_p}{A_p}$
1.0
·8
·6
·4
·2
0
0
5
10
15
20
25
30
35
40
45
GAP FACTOR $\frac{d}{X_0}$

Fig. 2.9

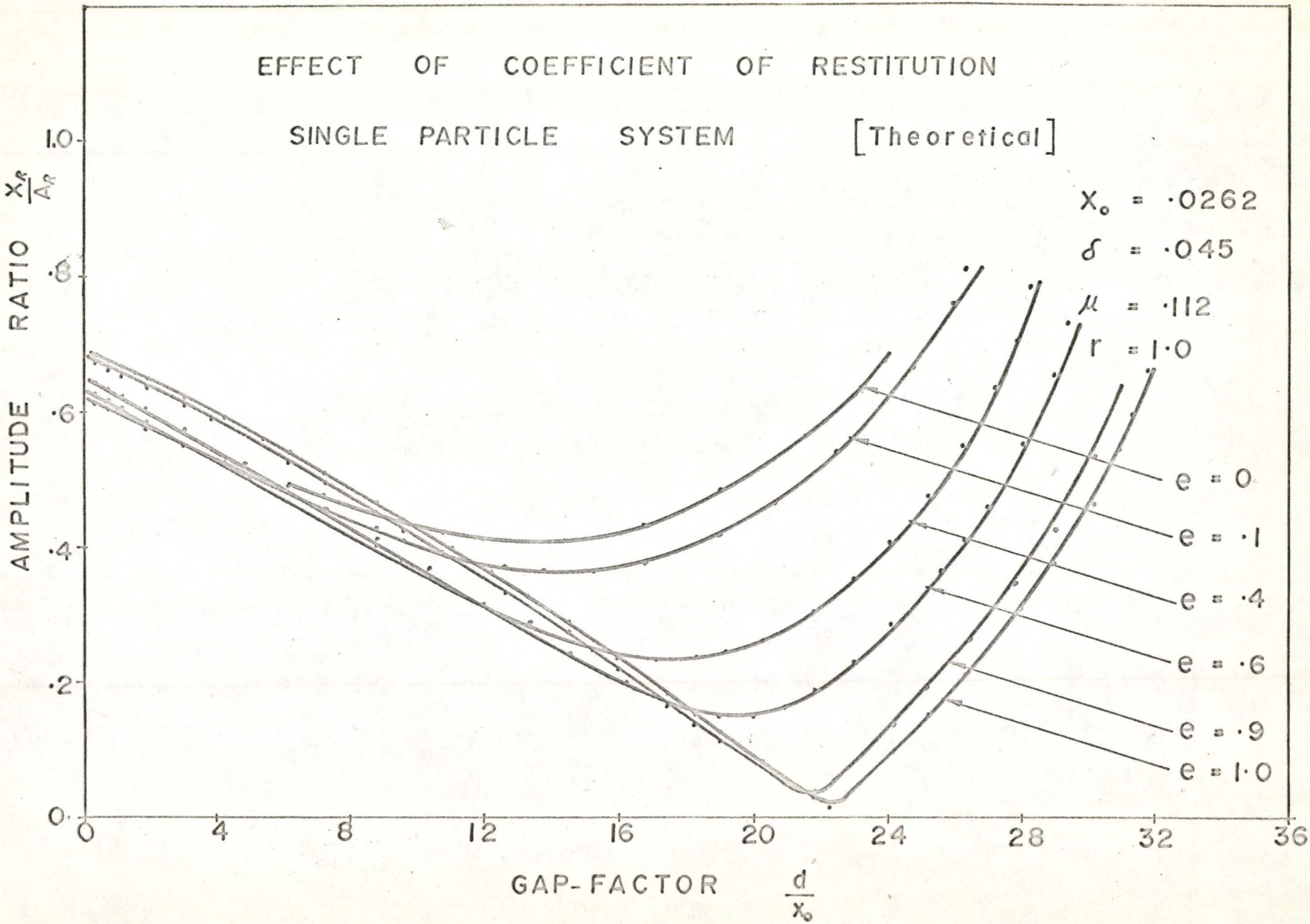
EFFECT OF COEFFICIENT OF RESTITUTION
SINGLE PARTICLE SYSTEM [Theoretical]
AMPLITUDE RATIO $\frac{X_r}{A_r}$
1.0
.8
.6
.4
.2
0
0
4
8
12
16
20
24
28
32
36
GAP-FACTOR $\frac{d}{X_0}$
X_0 = ·0262
δ = ·045
μ = ·112
r = 1·0
e = 0
e = ·1
e = ·4
e = ·6
e = ·9
e = 1·0

Fig. 2.10

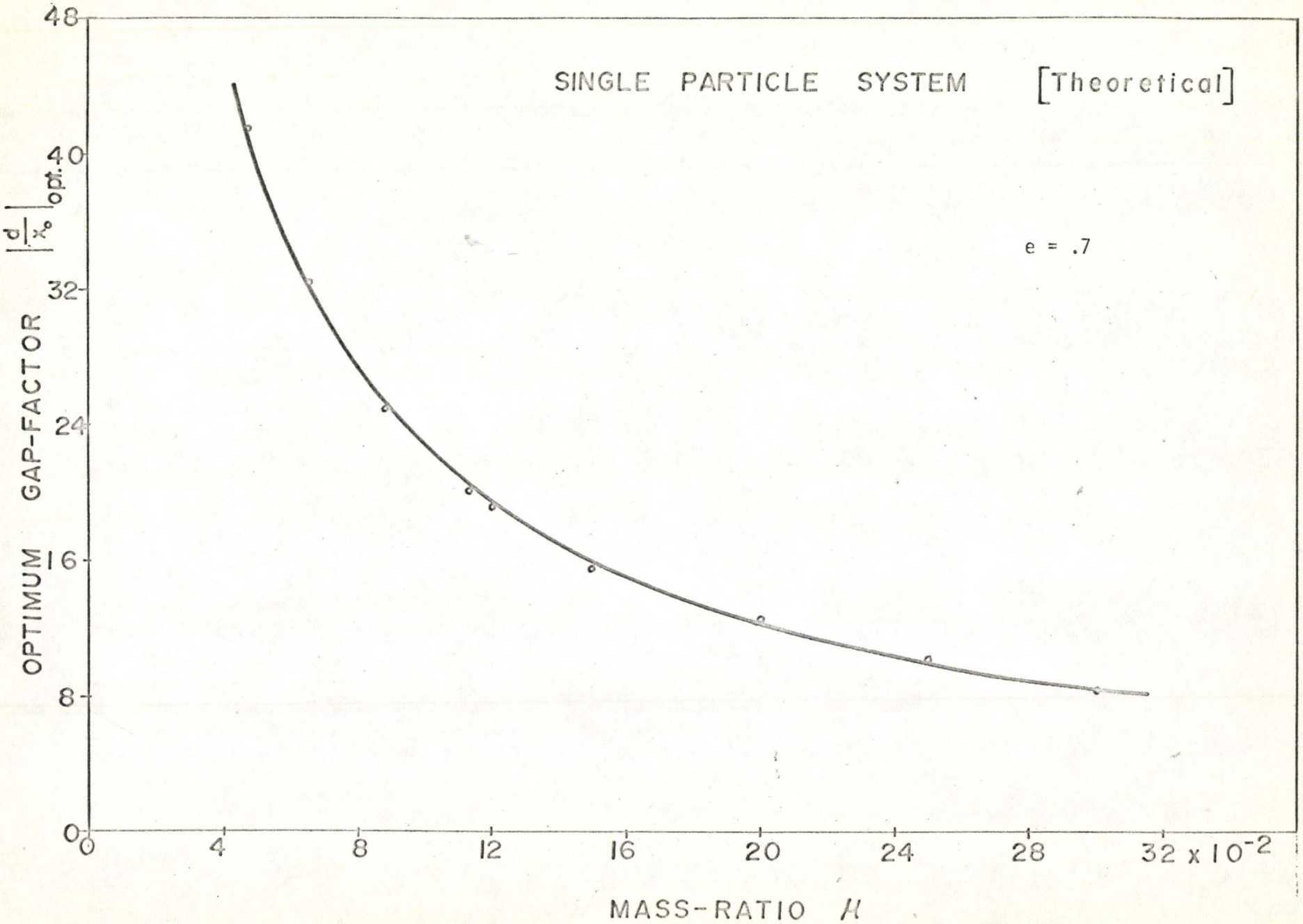
SINGLE PARTICLE SYSTEM [Theoretical]
e = .7
OPTIMUM GAP-FACTOR $\left|\frac{d}{x_0}\right|_{opt.}$
MASS-RATIO μ
0
8
16
24
32
40
48
4
12
20
28
32×10^{-2}

Fig. 2.11

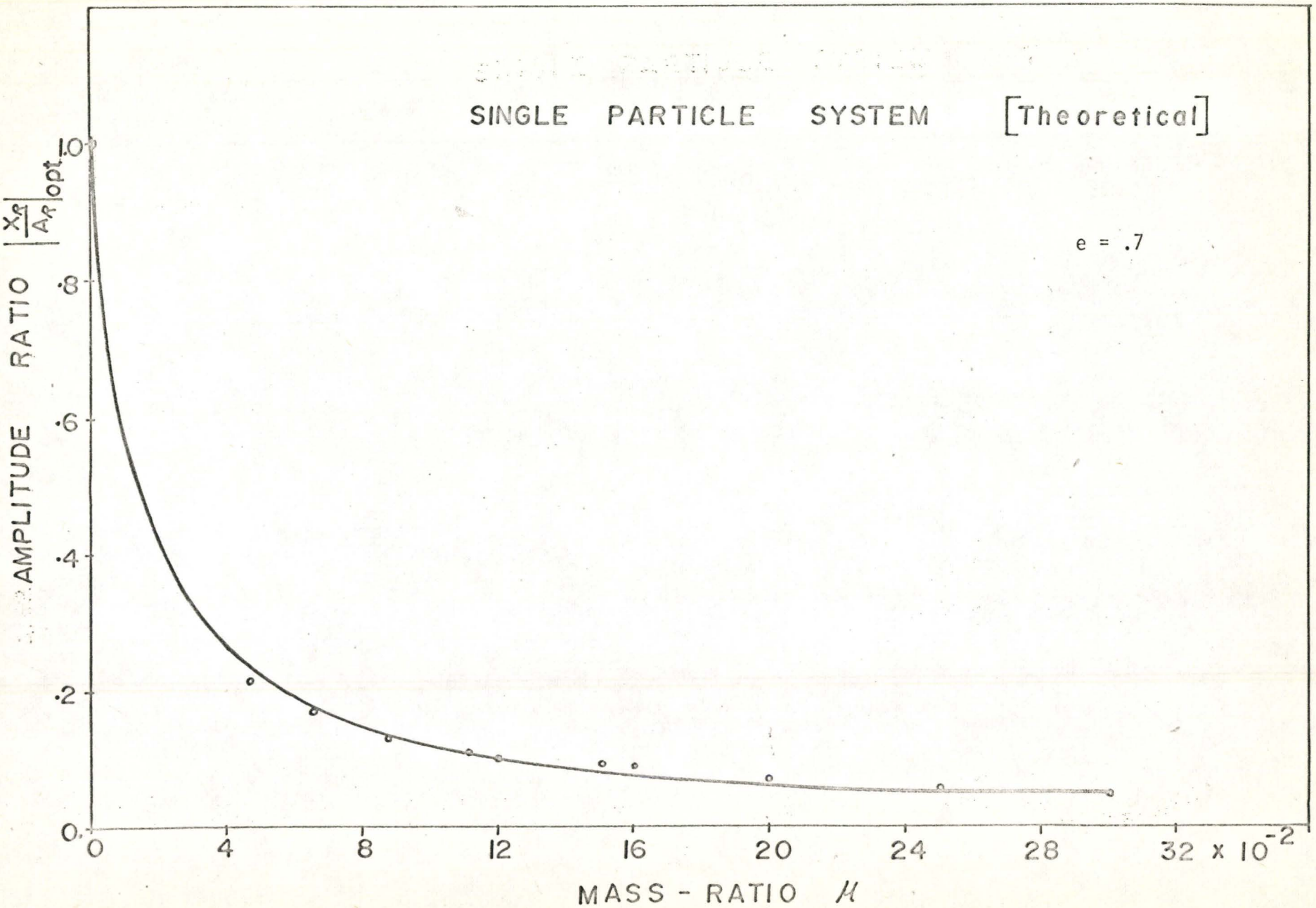
SINGLE PARTICLE SYSTEM [Theoretical]
e = .7
AMPLITUDE RATIO $\left|\frac{X_R}{A_R}\right|_{opt}$
1.0
.8
.6
.4
.2
0.
0
4
8
12
16
20
24
28
32 x 10^{-2}
MASS - RATIO μ

Fig. 2.12

e=1, the curve is V shaped; as e decreases the curve becomes flat. It is worth noting that the efficiency of damper in this range of optimum performance - where the curves are flat - is not sensitive to the parameters of the damper, so that a small change in these parameters will not affect the performance of the damper in an appreciable manner.

Figures 2.5, 2.9 show the effect of mass-ratio on the effectiveness of impact damper for two particles and single particle systems, respectively.

Figures 2.6, 2.7 are response curves for various gap-factors and mass-ratios for two-particle system.

Figures 2.8 (a), (b), (c) and (d) show X-$\dot{X}$ phase plane diagrams computed, for two-particle system, for four points as marked in figure 2-3. For these four phase plane diagrams, gap is varied keeping all other parameters constant. It is noted that the change in gap changes the amplitude and the position of impacts. For the optimum gap factor the impacts occur near the peak velocity, causing the greatest possible dissipation of kinetic energy.

As the single-particle impact damper is found to be more effective, its computed results are summarized in Figures 2.11 and 2.12. The former curve shows the variation of the optimum gap-factor, at which maximum reduction of amplitude ratio is achieved, for various mass ratios. This shows that the optimum gap-factor decreases continuously with the increase of mass-ratio. The second curve shows the variation of minimum amplitude ratio, i.e. at optimum d/x_o, for

various mass-ratios. This curve shows that the amplitude ratio decreases with the increase of the mass-ratio until a certain limit after which any more increase in μ is not advantageous.

3 EXPERIMENTAL STUDIES

3.1 EXPERIMENTAL TECHNIQUE

A schematic diagram of the mechanical model used and a photograph of actual structure are shown respectively in Figures 2.1 and 3.2 (a), (b) and (c).

Since the response of a single degree of freedom oscillator is not altered when the excitation is applied either to the base or directly to the mass, the former type of excitation was used in this case, as a matter of convenience.

The mass M is primarily a rectangular box with adjustable stops as its ends, that constrain the movement of the free mass particle M to oscillate within a certain clearance. The free mass particles used are hardened-steel balls, of the type normally used in ball bearings.

The base of the structure was excited by a vibration exciter. The electro-magnetic coil of the exciter was energized through an RC-generator and amplifier. The voltage and frequency supplied to the exciter could be controlled with the help of RC-generator.

The relative displacement of the primary mass, with respect to base, was measured with the help of a transducer which converts the variations of displacement into variations of capacitance. The transducer thus acts as an electrical reactance which varies in accordance

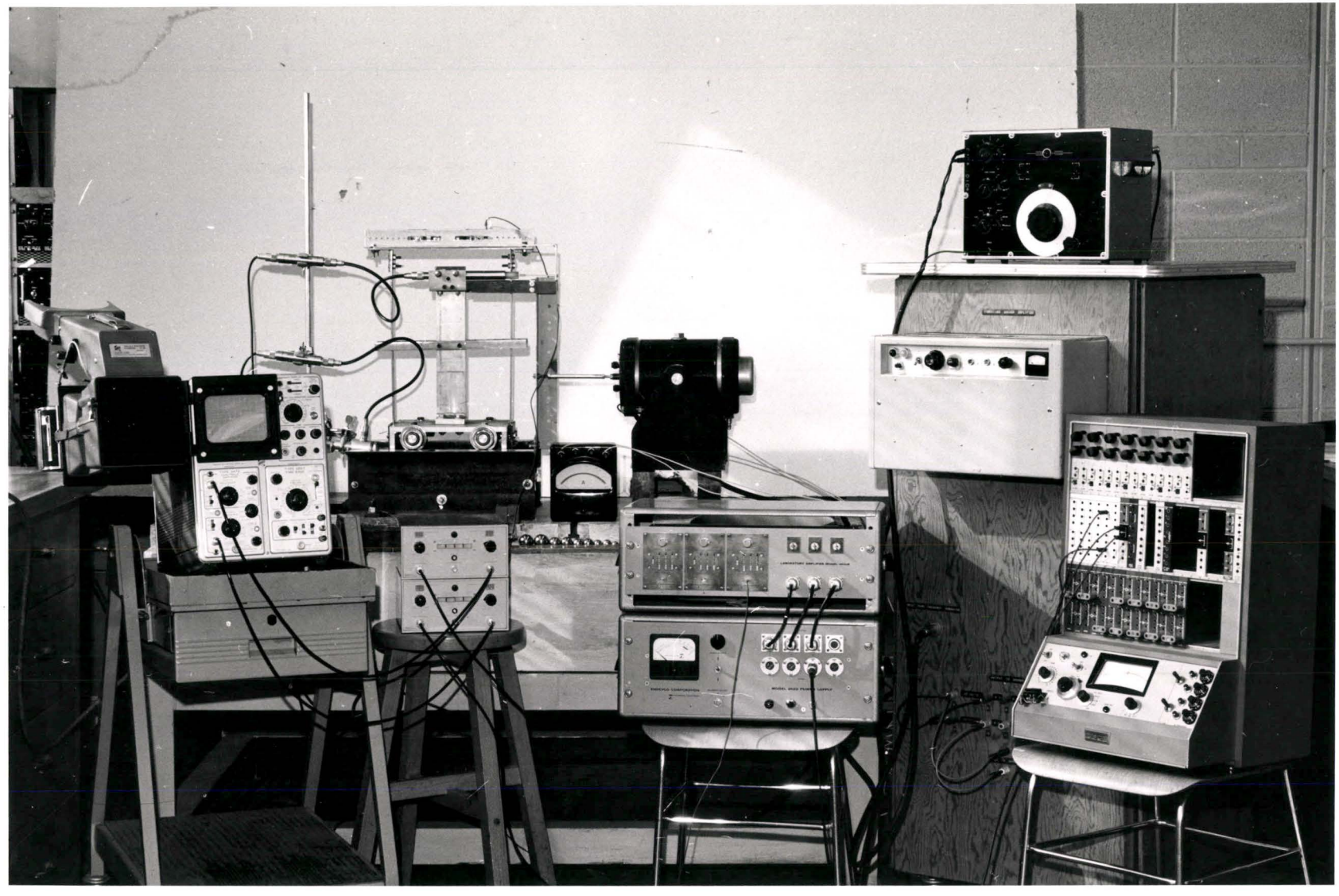

(a) GENERAL VIEW

Figure 3.2 Photograph of Mechanical Model

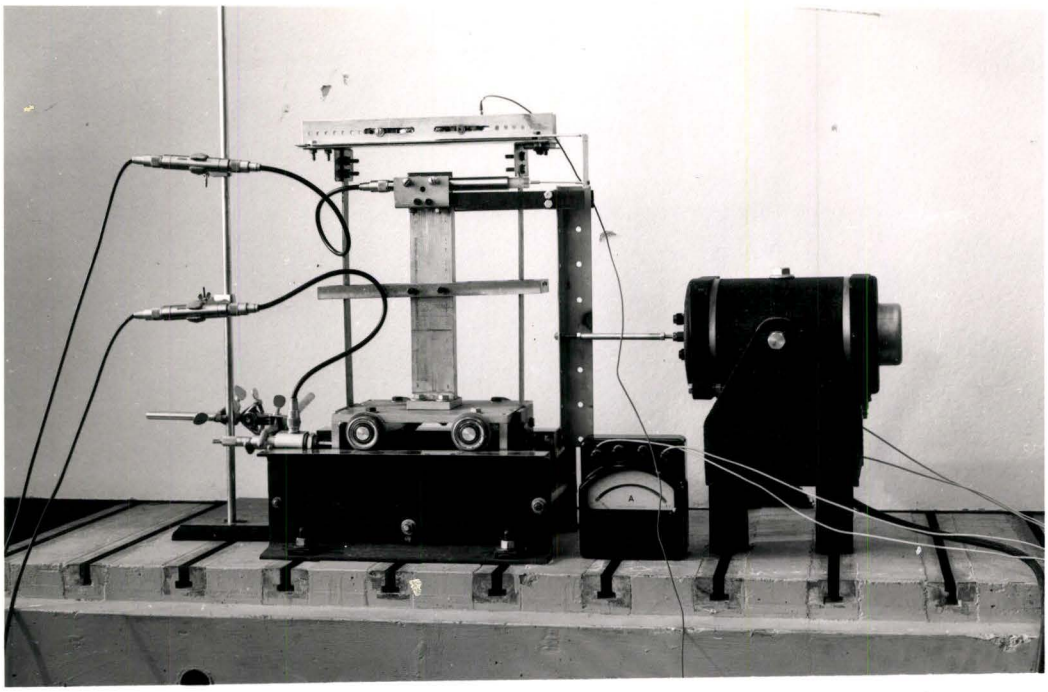

Fig. 3.2 (b). Front View of the Mechanical Model

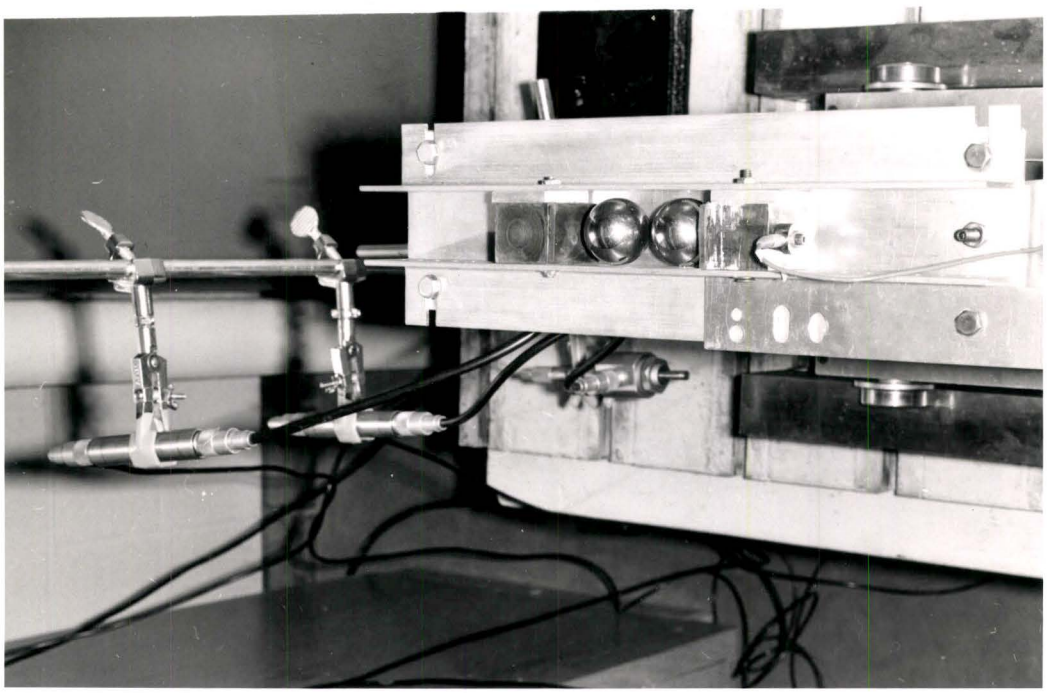

Fig. 3.2 (c). Plan of the Container

with the phenomenon to be measured (displacement in our case). The fluctuating reactance of the transducer is connected in series with a fixed reactance of a tuning plug to form an electrical resonant circuit, the resonant frequency of which determines the operating frequency of an RF oscillator. Thus change in physical quantity to be measured is converted to a frequency shift in the signal delivered by oscillator. The frequency modulated signal is fed to the reactance converter which in turn is converted to a d.c. voltage pulsating in accordance with the said signal. Output of reactance converter is connected to the d.c. coupled oscilloscope amplifier, which amplifies the pulsating d.c. voltages and its output terminals are connected to the cathode-ray-tube. The output on the screen of oscilloscope was calibrated by giving a known displacement to the transducer. Appropriate adjustments were made on reactance converter to insure that it was operating in a linear region.

The velocity wave form for the primary mass was obtained by integrating the output of a piezoelectric accelerometer attached to the primary mass. The integration was accomplished by an integrating network and an operational amplifier.

A list of the equipment used is given in Appendix C.

3.2 TWO-PARTICLE IMPACT DAMPER

Figure 2.1 shows the mechanical model used to obtain experimental results on the impact vibration absorber. These experiments were motivated by the desire to investigate the various aspects and effectiveness of two-particle impact dampers and to compare their behaviour with those of equivalent single particle dampers.

The effects of various parameters of the impact damper, viz μ, $\frac{d}{x_0}$ and e were investigated when the vibrating system was in a state of forced vibrations. Amplitudes of vibration of the system were measured on the screen of the oscilloscope for various excitation frequencies and the response curves of the system are plotted.

Figures 3.3, 3.4 are the two sets of response curves obtained by keeping the mass ratio μ constant for each set, and varying the gap-factor d/x_0. With the increase in damping the peak shifts to lower values of r. After optimum gap is reached there is a decrease in damping and peak is expected to shift towards higher values of r. The response curve for the vibrating system, without inserting the free mass, was also

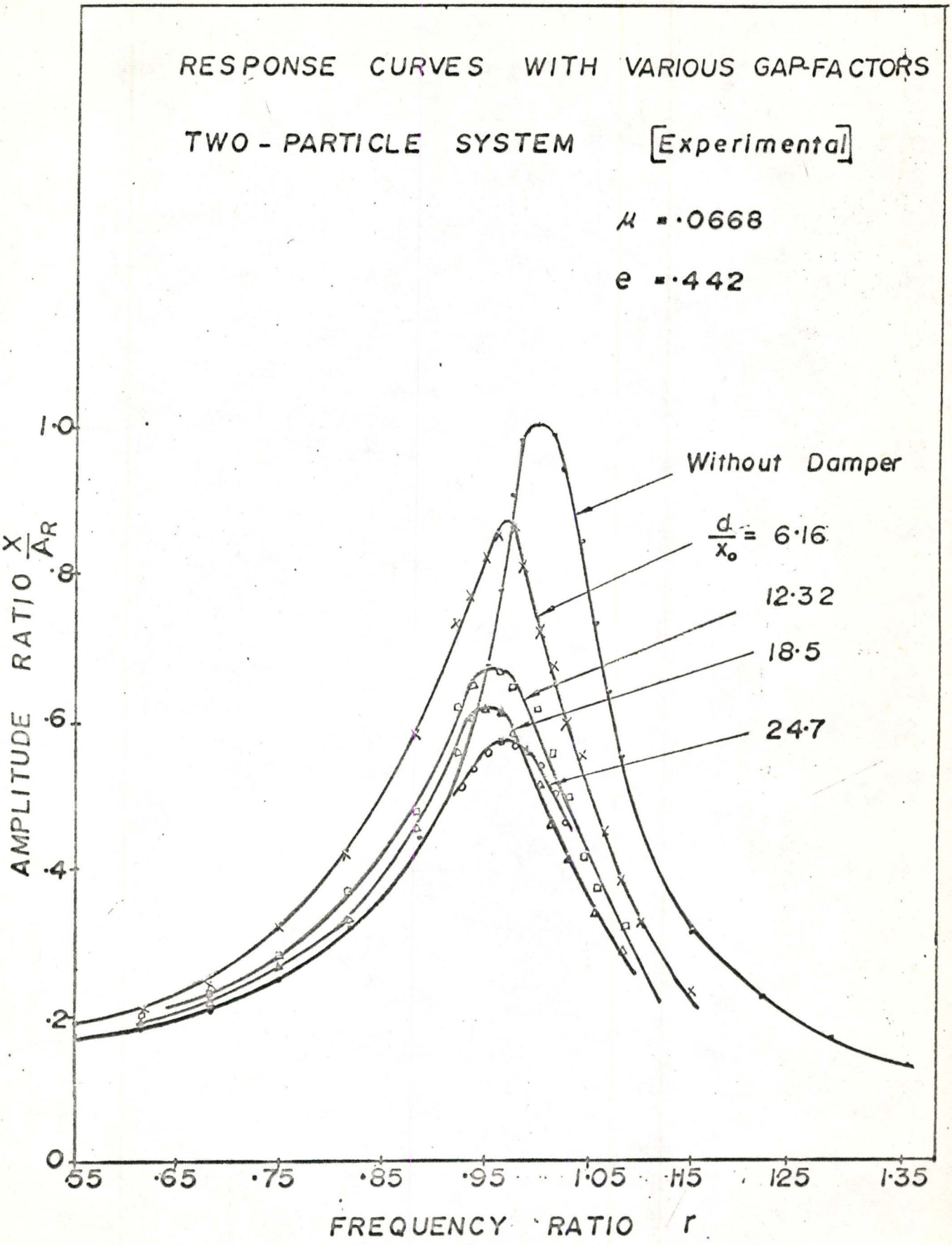
RESPONSE CURVES WITH VARIOUS GAP-FACTORS
TWO - PARTICLE SYSTEM [Experimental]
μ = ·0668
e = ·442
Without Damper
d/x₀ = 6·16
12·32
18·5
24·7
AMPLITUDE RATIO X/A_R
1·0
·8
·6
·4
·2
0
·55
·65
·75
·85
·95
1·05
1·15
1·25
1·35
FREQUENCY RATIO r

Fig. 3.3

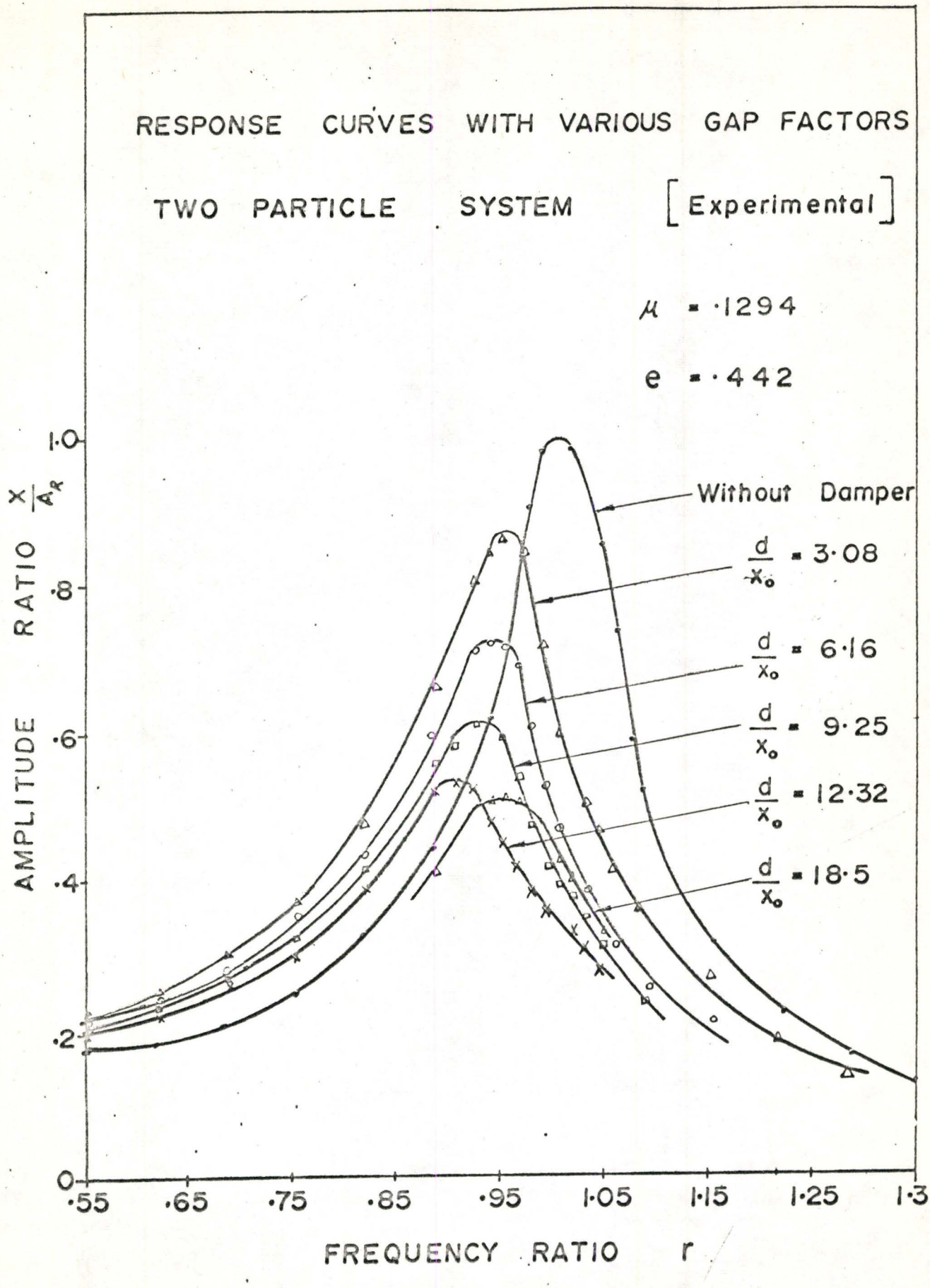
RESPONSE CURVES WITH VARIOUS GAP FACTORS
TWO PARTICLE SYSTEM [Experimental]
μ = ·1294
e = ·442
Without Damper
d/x₀ = 3·08
d/x₀ = 6·16
d/x₀ = 9·25
d/x₀ = 12·32
d/x₀ = 18·5
AMPLITUDE RATIO X/A
0
·2
·4
·6
·8
1·0
·55
·65
·75
·85
·95
1·05
1·15
1·25
1·35
FREQUENCY RATIO r

Fig. 3.4

obtained experimentally and is shown superimposed on the response curves with impact damper to demonstrate the effectiveness of the impact damper.

Similarly, Figures 3.5, 3.6 are the two sets of response curves obtained, while keeping d/x_0 constant for each set and varying μ .

At resonance, the ratio of amplitudes with the impact damper in and out of action, for various values of μ , are plotted versus the gap-factor d/x_0, in Figure 3.7. A curve shown in dotted line for single-particle system with μ = .0647, is also shown superimposed in Figure 3.7.

By making the single-particle and two-particle systems equivalent, i.e. by using same d/x_0 and μ in both cases, a set of response curves are plotted as Figure 3.8, to compare the behaviour of the two systems in the frequency range.

In Figure 3.9 response curves for different values of coefficient of restitution, e, for constant μ and d/x_0 are shown. Figure 3.10 shows the effect of e on the amplitude of vibration, for complete range of d/x_0.

The coefficient of restitution was varied by using different rubber pads at the ends of the container where the mass particle collides. The method and calculations for coefficient of restitution is given in Appendix B.

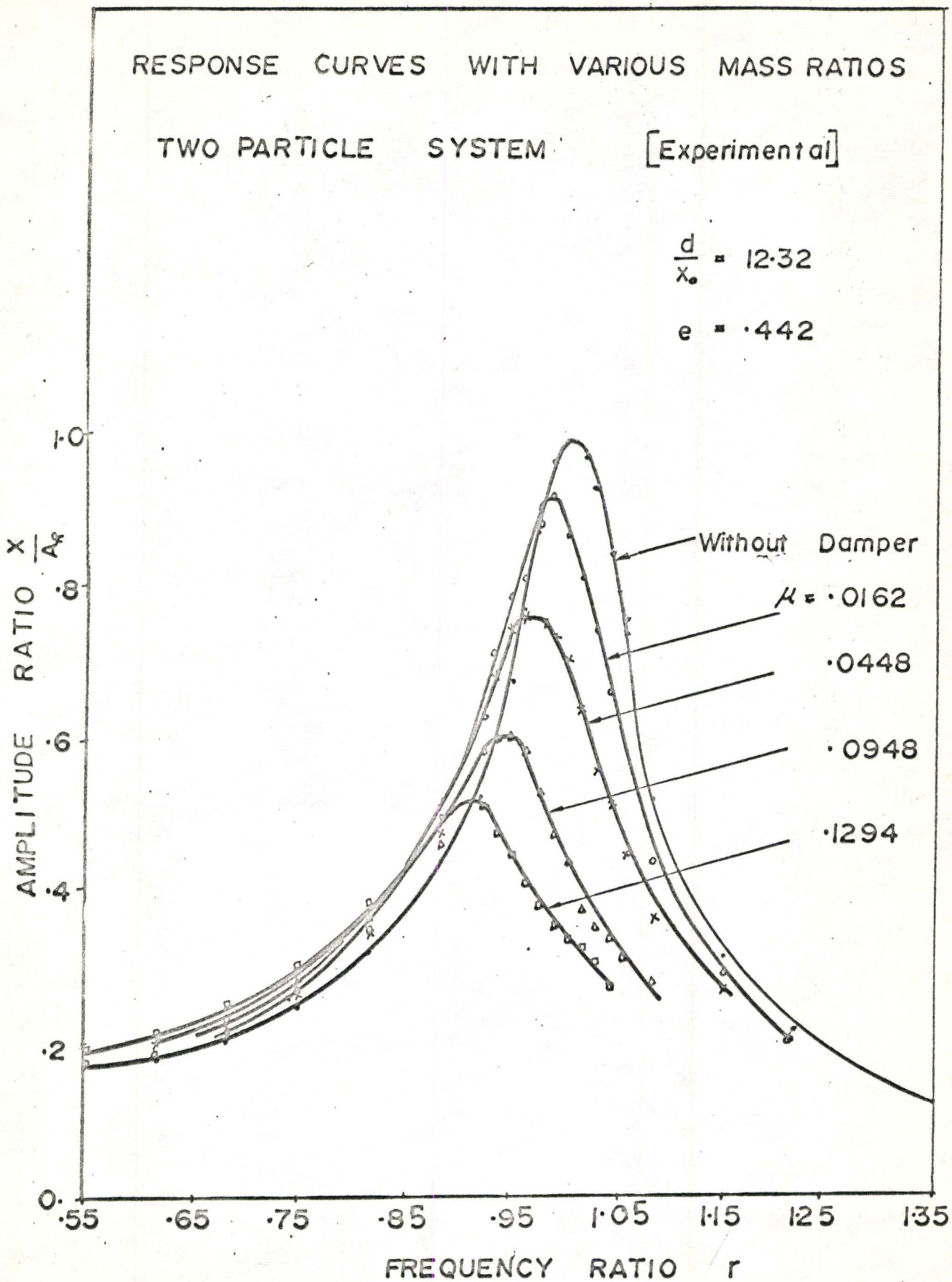
RESPONSE CURVES WITH VARIOUS MASS RATIOS
TWO PARTICLE SYSTEM [Experimental]
d/x₀ = 12·32
e = ·442
AMPLITUDE RATIO X/A
1·0
·8
·6
·4
·2
0·
Without Damper
μ = ·0162
·0448
·0948
·1294
·55
·65
·75
·85
·95
1·05
1·15
1·25
1·35
FREQUENCY RATIO r

Fig. 3.5

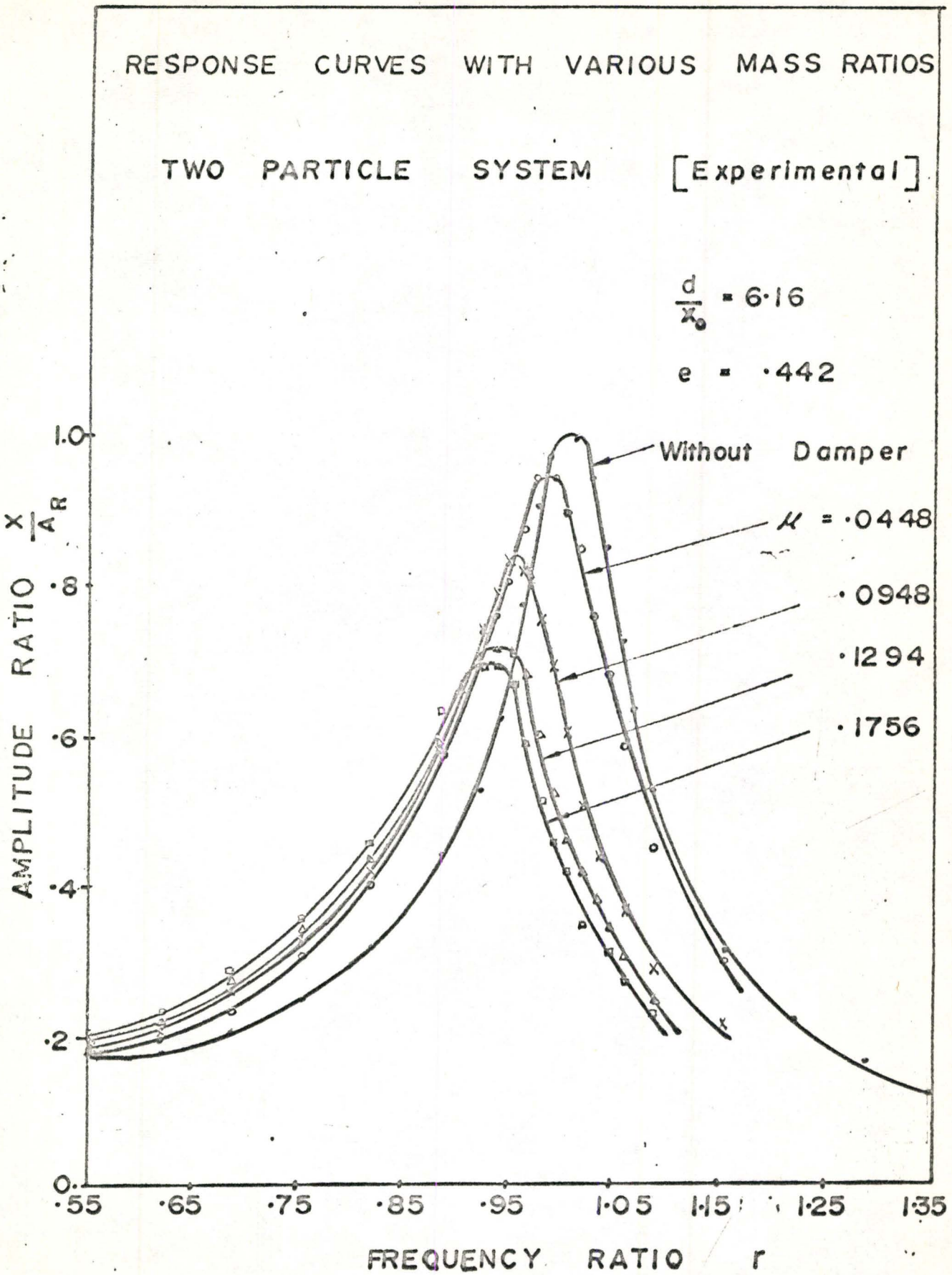
RESPONSE CURVES WITH VARIOUS MASS RATIOS
TWO PARTICLE SYSTEM [Experimental]
d/x0 = 6·16
e = ·442
Without Damper
μ = ·0448
·0948
·1294
·1756
AMPLITUDE RATIO X/AR
1.0
·8
·6
·4
·2
0
·55
·65
·75
·85
·95
1·05
1·15
1·25
1·35
FREQUENCY RATIO r

Fig. 3·6

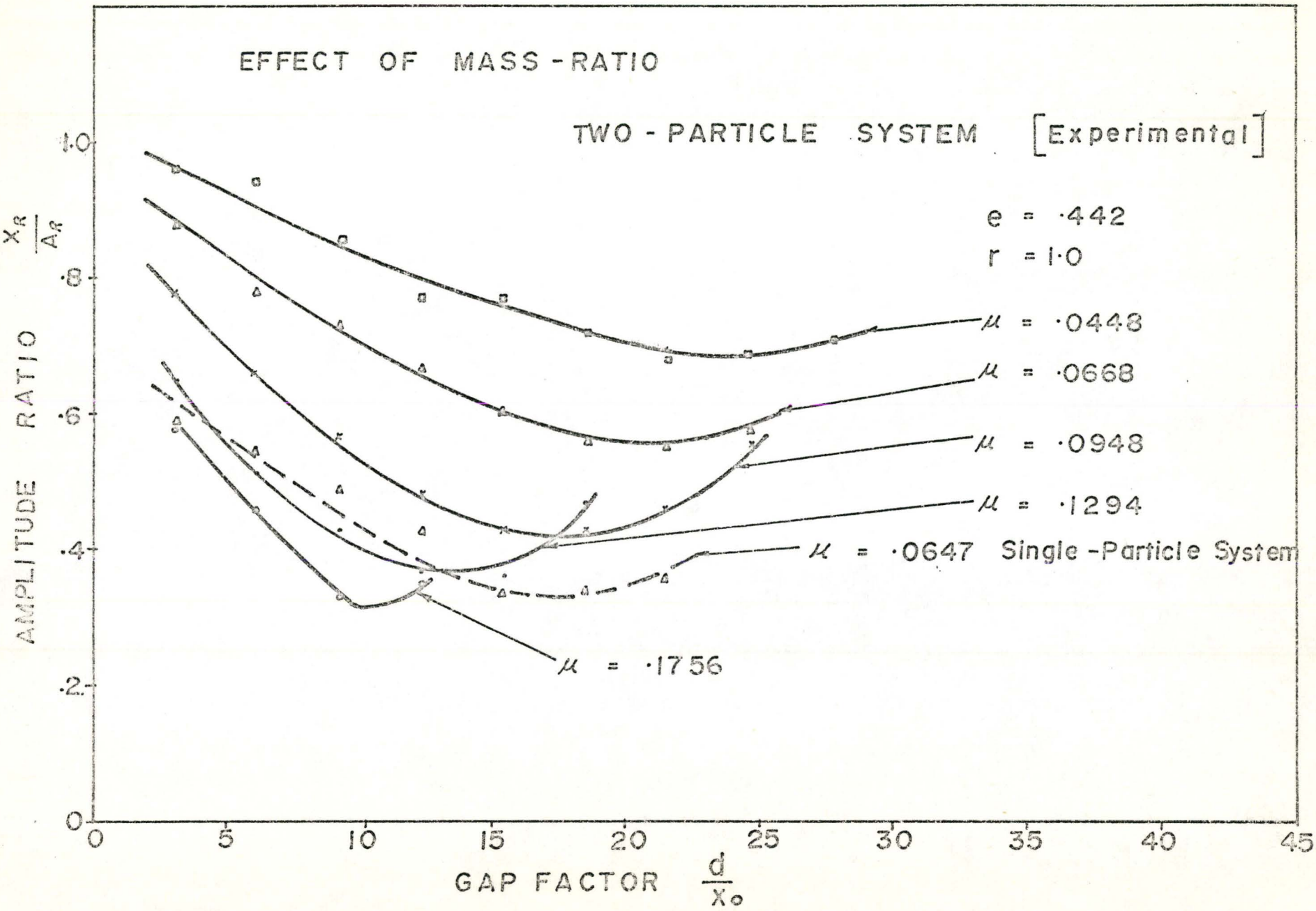
EFFECT OF MASS-RATIO
TWO-PARTICLE SYSTEM [Experimental]
e = ·442
r = 1·0
μ = ·0448
μ = ·0668
μ = ·0948
μ = ·1294
μ = ·0647 Single-Particle System
μ = ·1756
AMPLITUDE RATIO $\frac{X_R}{A_R}$
GAP FACTOR $\frac{d}{X_0}$
0
·2
·4
·6
·8
1·0
0
5
10
15
20
25
30
35
40
45

Fig. 3.7

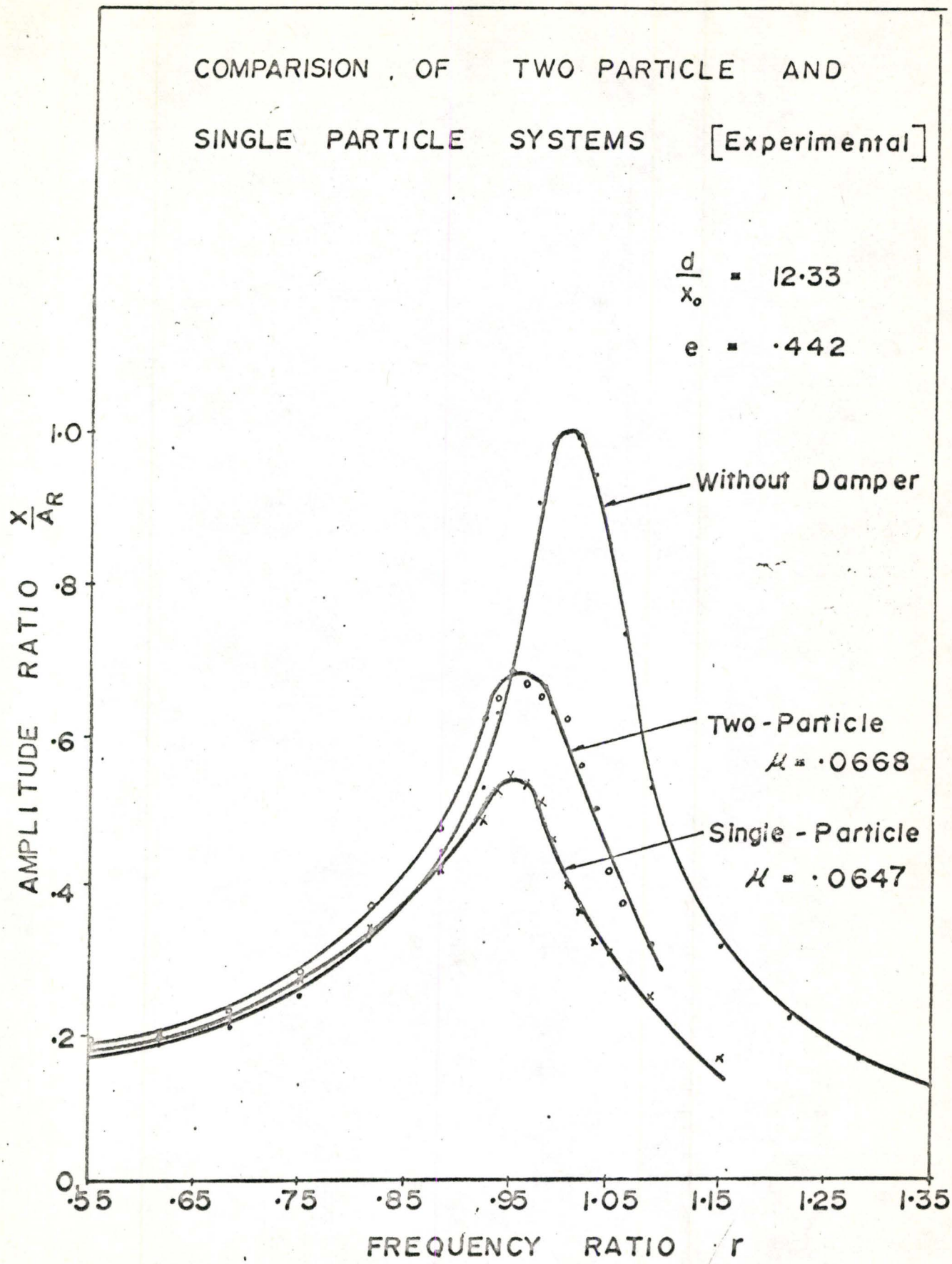
COMPARISION . OF TWO PARTICLE AND
SINGLE PARTICLE SYSTEMS [Experimental]
d/x₀ = 12·33
e = ·442
Without Damper
Two-Particle
μ = ·0668
Single-Particle
μ = ·0647
AMPLITUDE RATIO X/A_R
1·0
·8
·6
·4
·2
0
·55
·65
·75
·85
·95
1·05
1·15
1·25
1·35
FREQUENCY RATIO r

Fig. 3.8

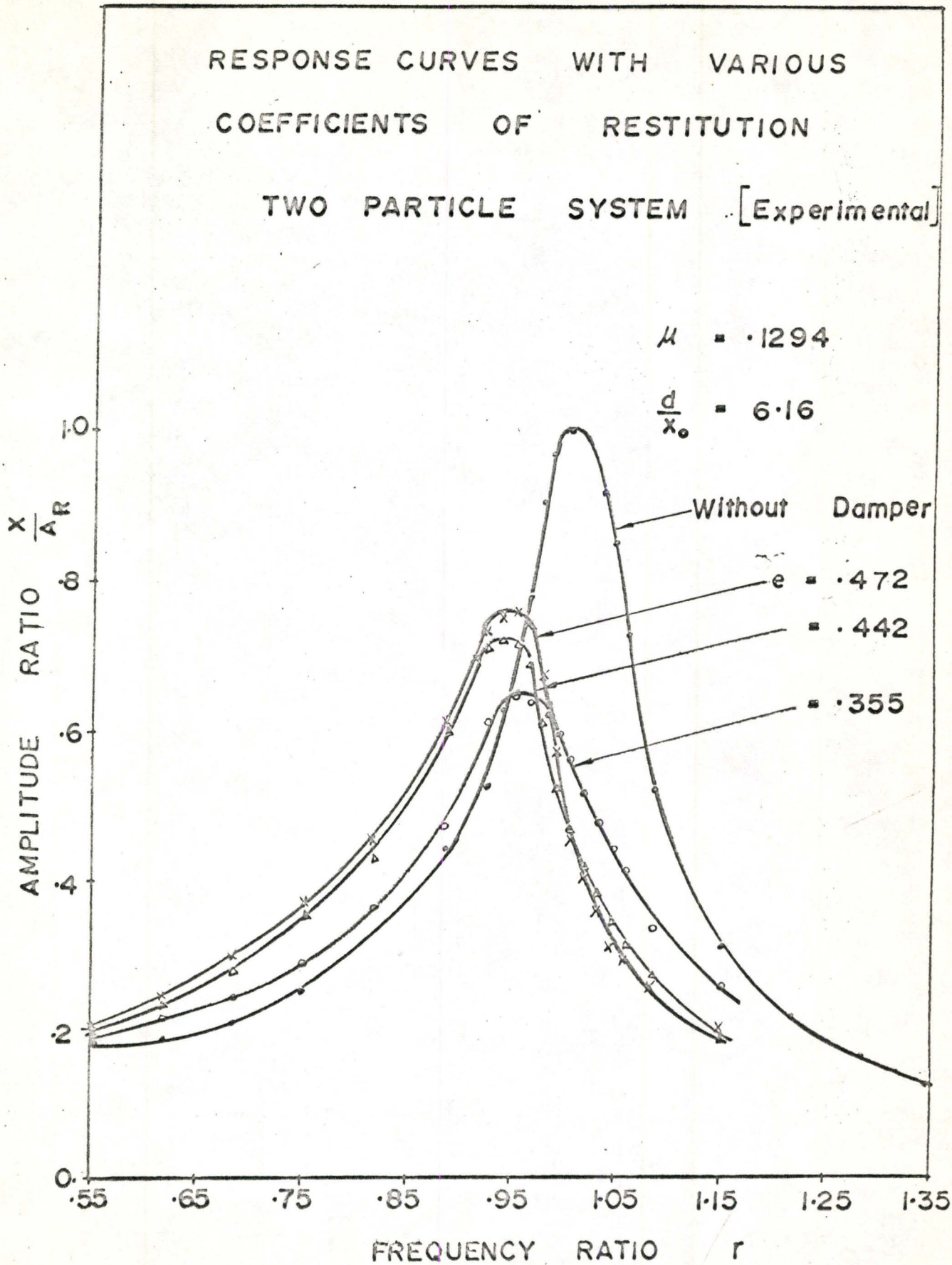
RESPONSE CURVES WITH VARIOUS
COEFFICIENTS OF RESTITUTION
TWO PARTICLE SYSTEM [Experimental]
μ = ·1294
d/x₀ = 6·16
Without Damper
e = ·472
= ·442
= ·355
AMPLITUDE RATIO X/A_R
0·
·2
·4
·6
·8
1·0
·55
·65
·75
·85
·95
1·05
1·15
1·25
1·35
FREQUENCY RATIO r

Fig. 3.9

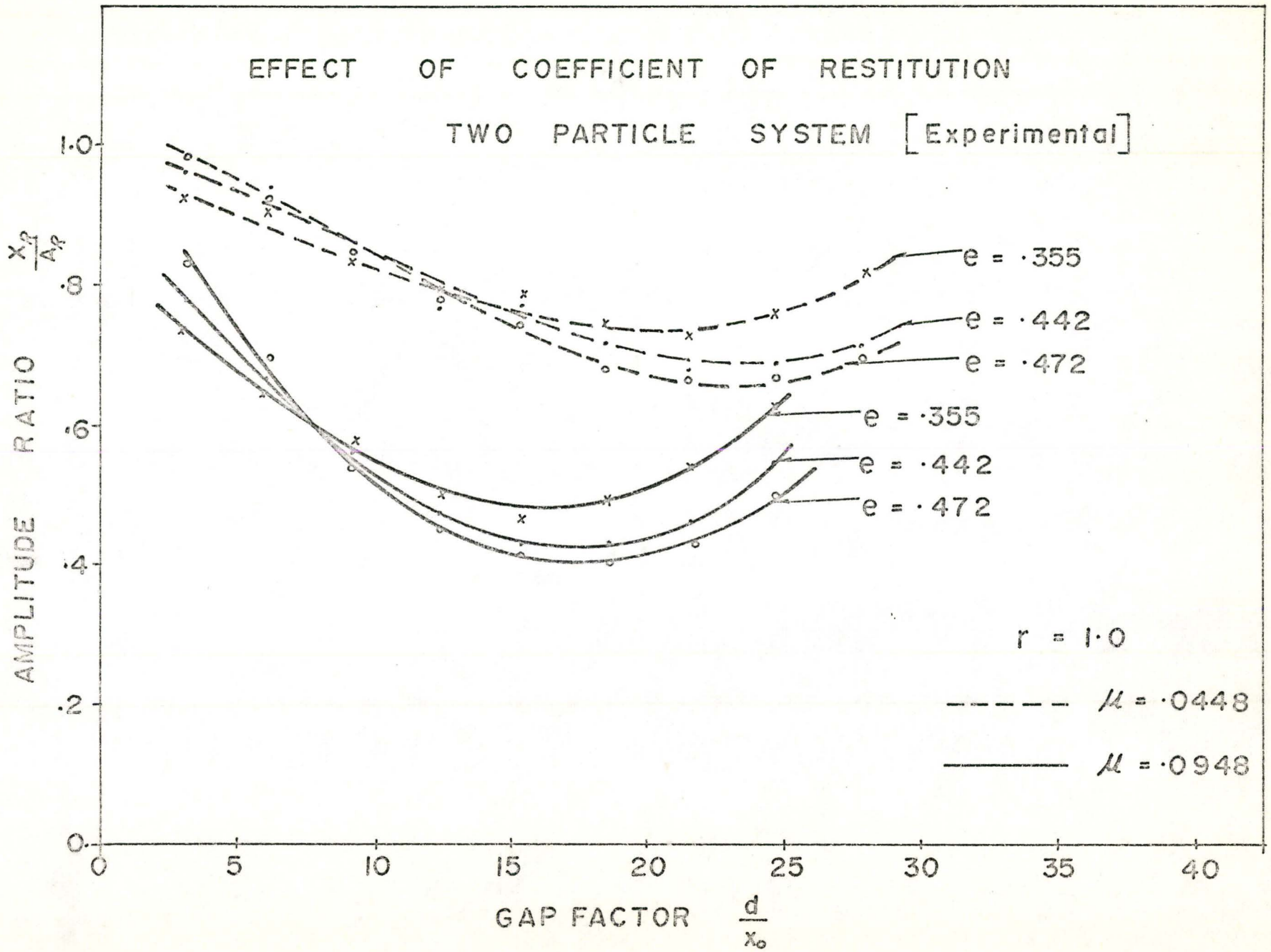
EFFECT OF COEFFICIENT OF RESTITUTION
TWO PARTICLE SYSTEM [Experimental]
AMPLITUDE RATIO $\frac{X_p}{A_p}$
GAP FACTOR $\frac{d}{x_0}$
1·0
·8
·6
·4
·2
0
0
5
10
15
20
25
30
35
40
e = ·355
e = ·442
e = ·472
e = ·355
e = ·442
e = ·472
r = 1·0
μ = ·0448
μ = ·0948

Fig. 3.10

In case of two-particle impact damper, it is observed that, when steady state motion is established, the symmetric four impacts per cycle motion predominates and confirms the validity of assumption in theoretical analysis, as shown in phase plane diagram in Figure 2.2.

3.3 SINGLE-PARTICLE IMPACT DAMPER

These sets of experiments were motivated by the desire to investigate the possibility of reduction of noise level, reported by previous investigators, due to the impacts between hard surfaces. For this purpose different Butyl rubber sheetings, supplied by Polymer Corporation, were used as soft material at the ends of the container where the mass particle collides. The effect of wide range of various parameters, ViZ. $\frac{d}{x_0}$, μ, and e, were also investigated.

Figures 3.11, 3.12 are two sets of response curves, for the single-particle system, obtained by keeping μ constant for each set and by varying d/x_0. Similarly, response curves are plotted in Figures 3.13, 3.14 for constant d/x_0 and varying μ in each case.

Figure 3.15 is a summing up of results and the curves show the effect of varying the gap-factor on the amplitude ratio X_R/A_R, for various mass ratios at resonance. An optimum gap-factor is observed in this set of curves for each μ. However, an optimum gap could not be reached for highest mass ratio $\mu = .112$, since the beating started earlier. This can be explained by the fact that the higher is the value of μ more energy the free mass will require to travel through the specific gap.

Effect of difference values of e, on amplitude ratio for the entire range of gap-factor is plotted in Figure 3.16.

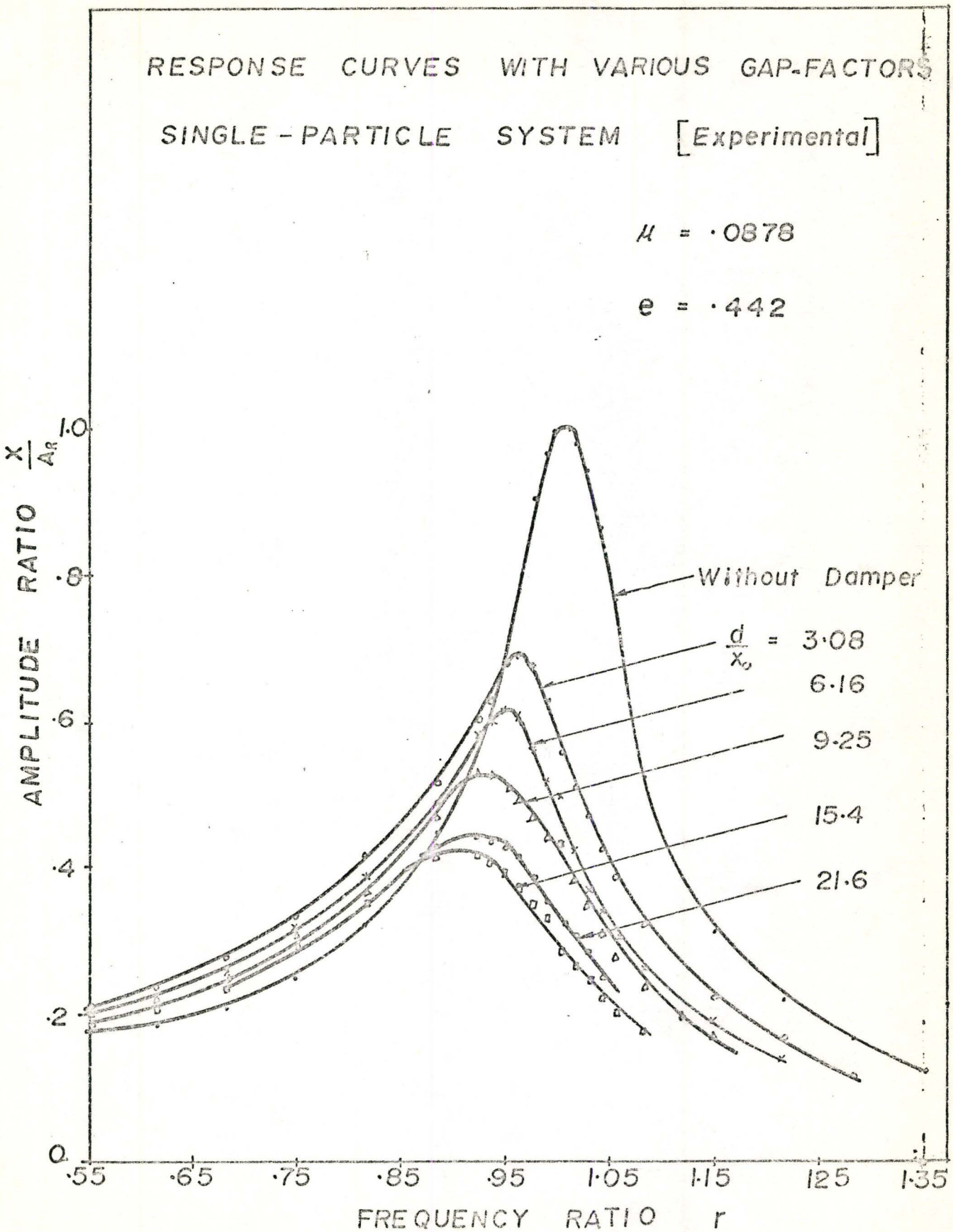

Fig. 3.11

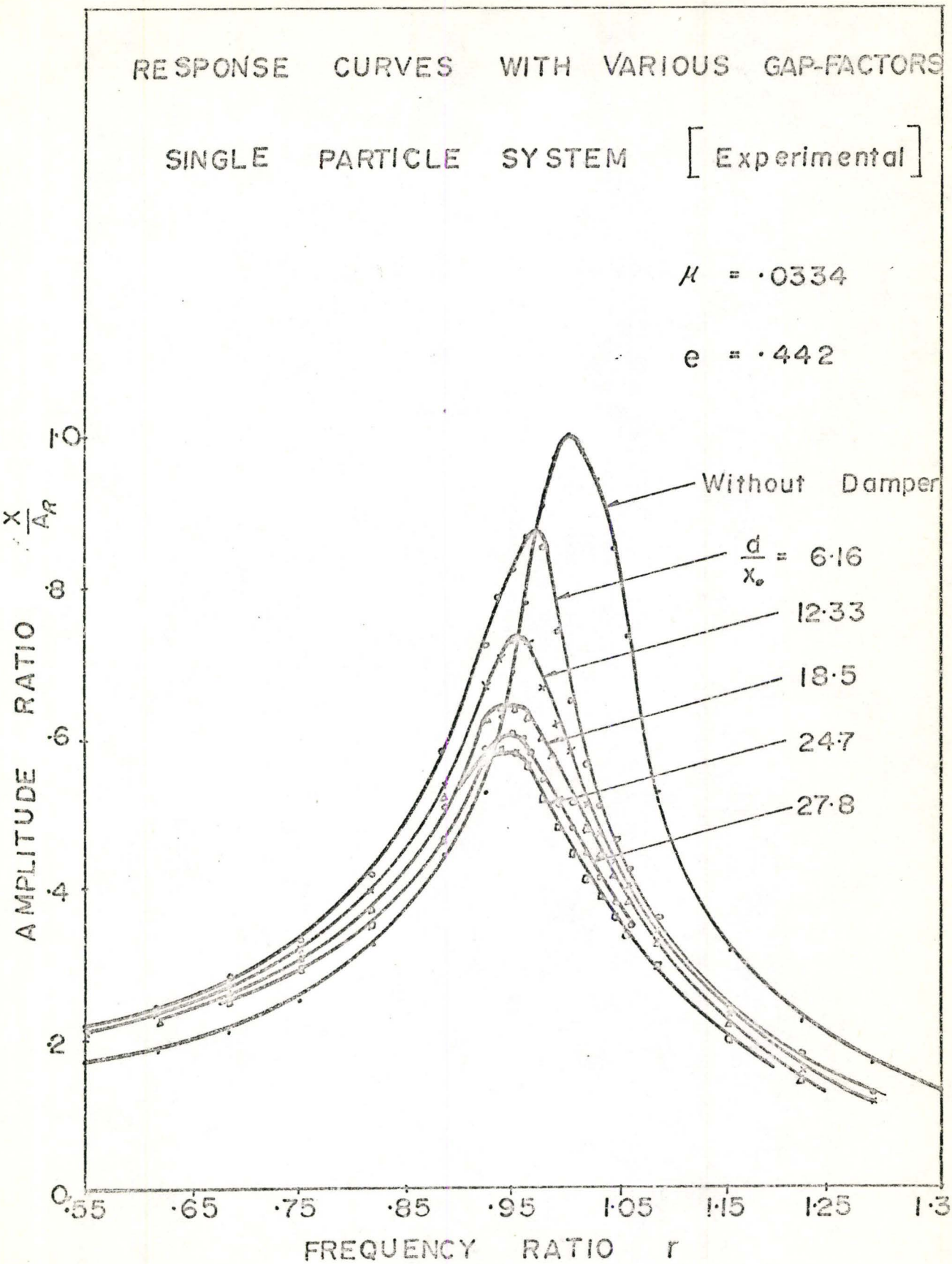
RESPONSE CURVES WITH VARIOUS GAP-FACTORS
SINGLE PARTICLE SYSTEM [Experimental]
μ = ·0334
e = ·442
Without Damper
d/x₀ = 6·16
12·33
18·5
24·7
27·8
AMPLITUDE RATIO X/A_R
0
·2
·4
·6
·8
1·0
·55
·65
·75
·85
·95
1·05
1·15
1·25
1·35
FREQUENCY RATIO r

Fig. 3.12

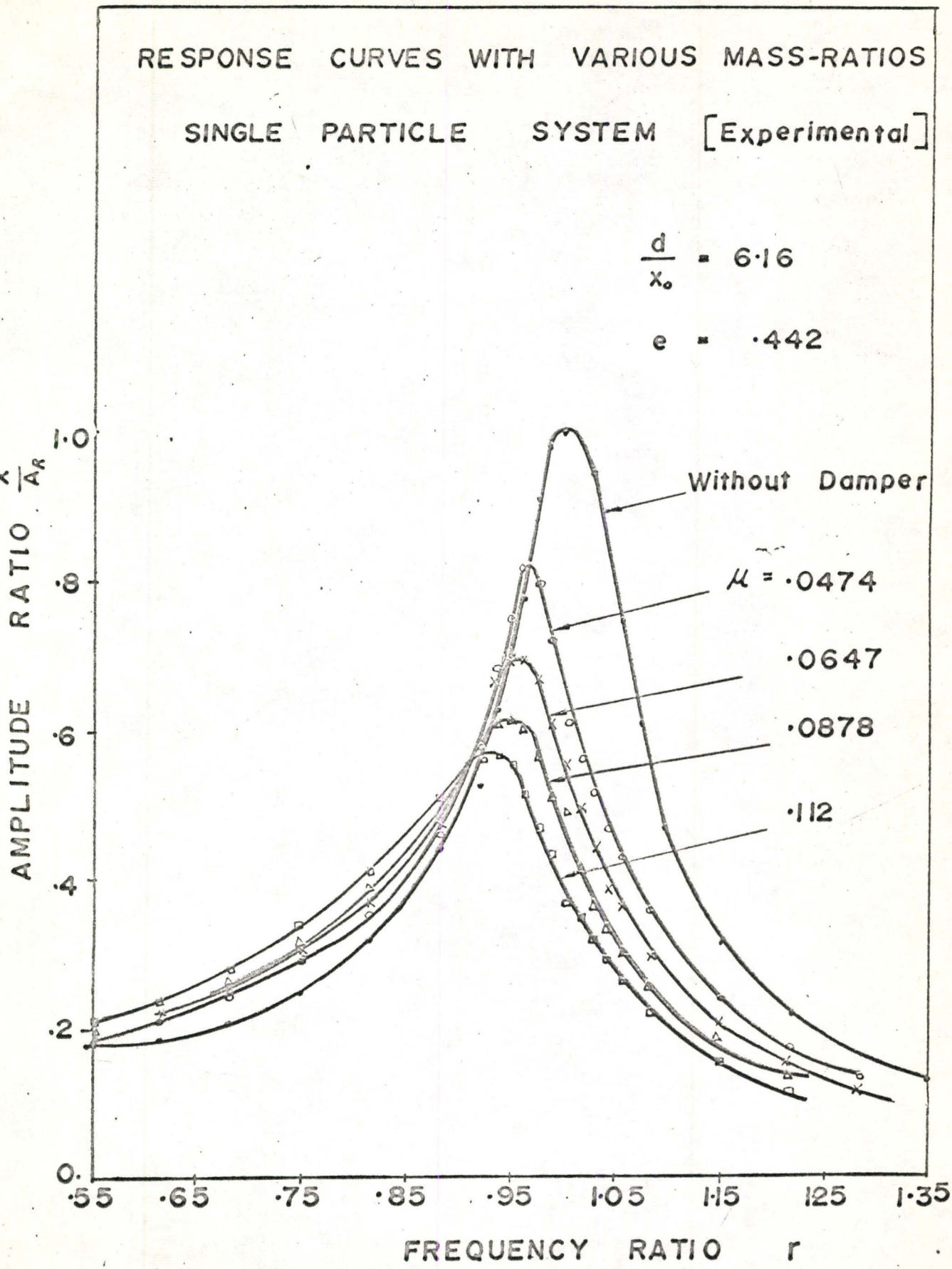
RESPONSE CURVES WITH VARIOUS MASS-RATIOS
SINGLE PARTICLE SYSTEM [Experimental]
d/X₀ = 6·16
e = ·442
Without Damper
μ = ·0474
·0647
·0878
·112
AMPLITUDE RATIO X/A_R
1·0
·8
·6
·4
·2
0.
·55
·65
·75
·85
·95
1·05
1·15
1·25
1·35
FREQUENCY RATIO r

Fig. 3.13

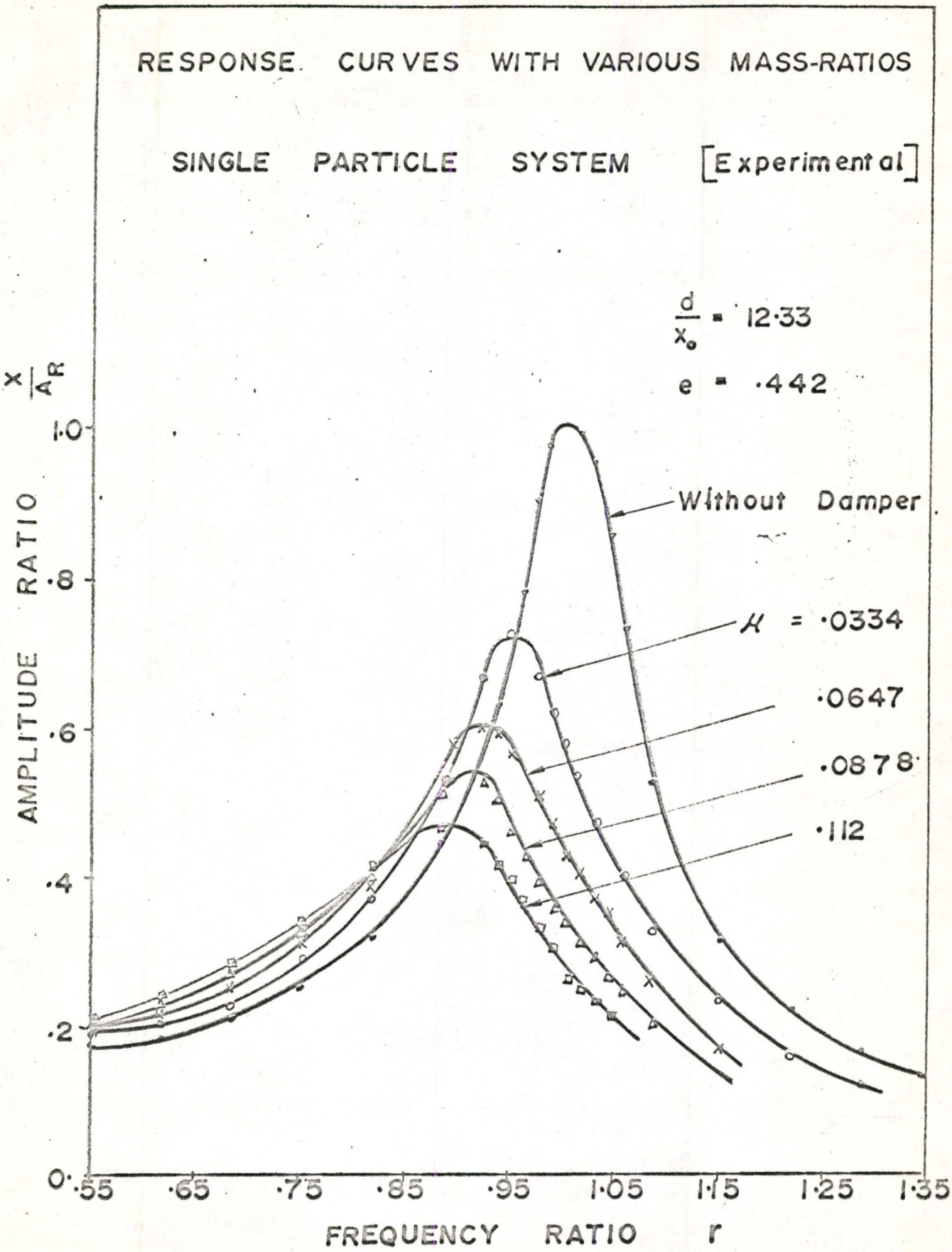
RESPONSE CURVES WITH VARIOUS MASS-RATIOS
SINGLE PARTICLE SYSTEM [Experimental]
d/x0 = 12·33
e = ·442
x/AR
AMPLITUDE RATIO
1·0
·8
·6
·4
·2
0
Without Damper
μ = ·0334
·0647
·0878
·112
·55
·65
·75
·85
·95
1·05
1·15
1·25
1·35
FREQUENCY RATIO r

Fig. 3.14

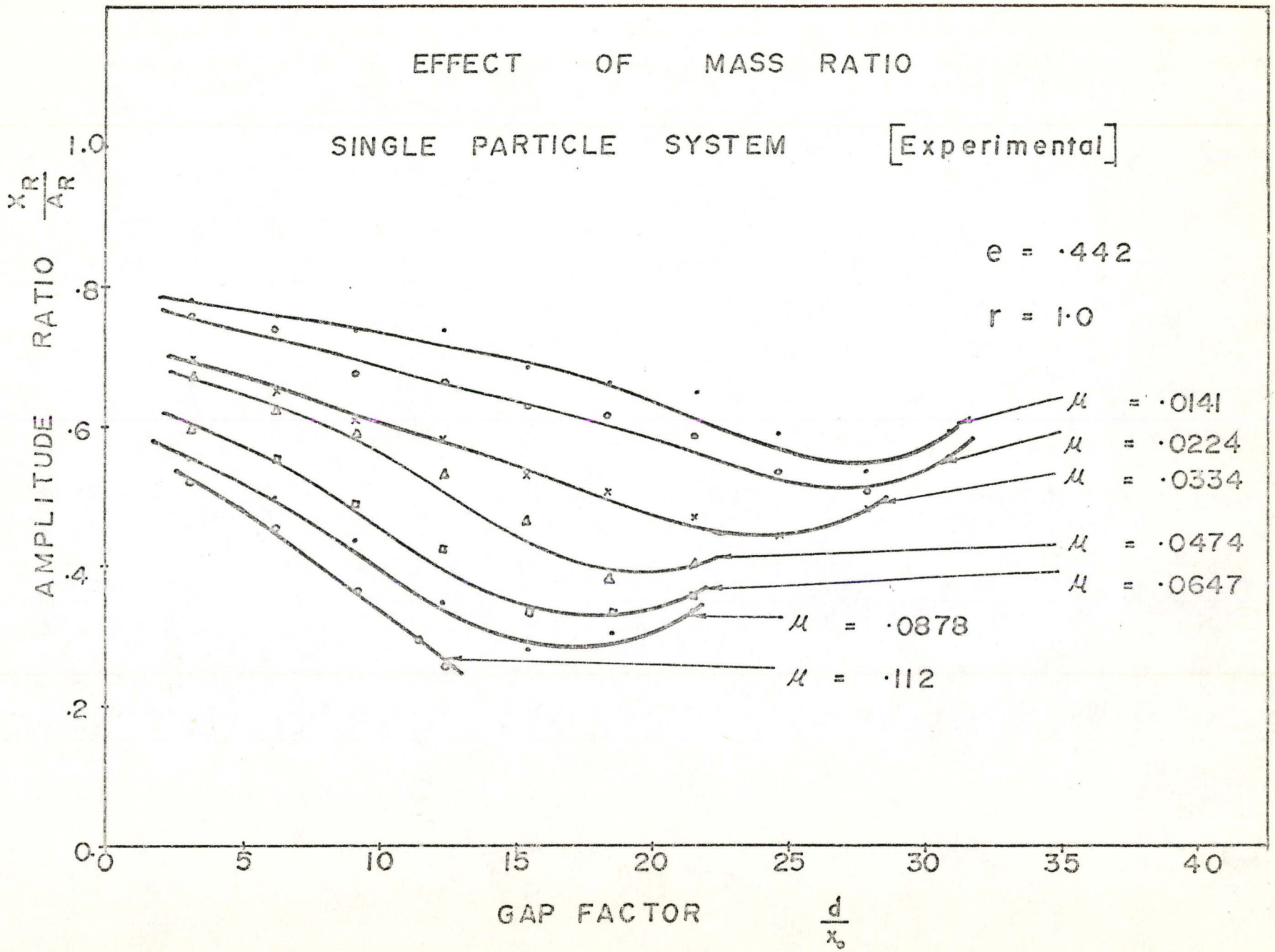
EFFECT OF MASS RATIO
SINGLE PARTICLE SYSTEM [Experimental]
e = ·442
r = 1·0
μ = ·0141
μ = ·0224
μ = ·0334
μ = ·0474
μ = ·0647
μ = ·0878
μ = ·112
AMPLITUDE RATIO $\frac{x_R}{A_R}$
GAP FACTOR $\frac{d}{x_0}$
0·0
·2
·4
·6
·8
1·0
5
10
15
20
25
30
35
40

Fig. 3.15

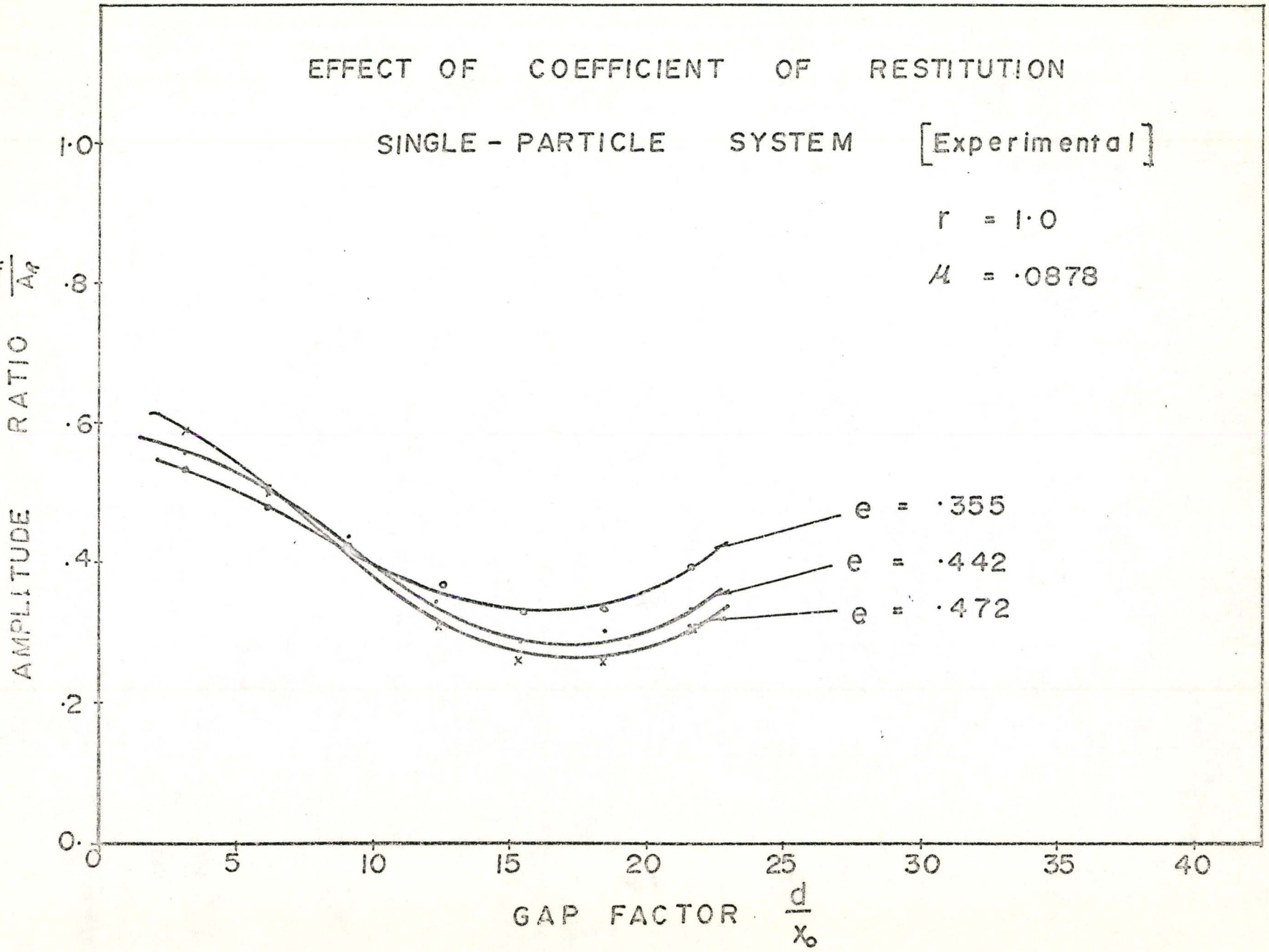
EFFECT OF COEFFICIENT OF RESTITUTION
SINGLE - PARTICLE SYSTEM [Experimental]
r = 1·0
μ = ·0878
e = ·355
e = ·442
e = ·472
AMPLITUDE RATIO $\frac{X_R}{A_P}$
GAP FACTOR $\frac{d}{X_0}$
1·0
·8
·6
·4
·2
0·
0
5
10
15
20
25
30
35
40

Fig. 3.16

3.4 SINGLE PARTICLE SYSTEM WITH FLUID

This set of experiments was motivated by the desire to study the effect of friction on the motion of mass particle. To accomplish this, the container was filled with fluid and the mass particle was allowed to oscillate between two stops. The fluid resistance gave the effect of friction on the mass particle. The fluid used was No. 1 diesel oil, supplied by Texaco, with density (ρ_f) equal to 1.563 lbf. sec^2/ft^4 and kinematic viscosity equal to 4.9×10^{-4} ft^2/sec.

Amplitude ratio X_R/A_R is plotted versus the gap-factor d/x_o, for various mass ratios, in Figure 3.17. A curve, with $\mu = 0.0666$ and without fluid in the container, is shown superimposed in the same figure to compare the effects. Response curves for the equivalent systems, i.e. keeping μ and d/x_o same in both systems, with and without fluid are plotted in Figure 3.18, to compare the effect in the complete frequency range.

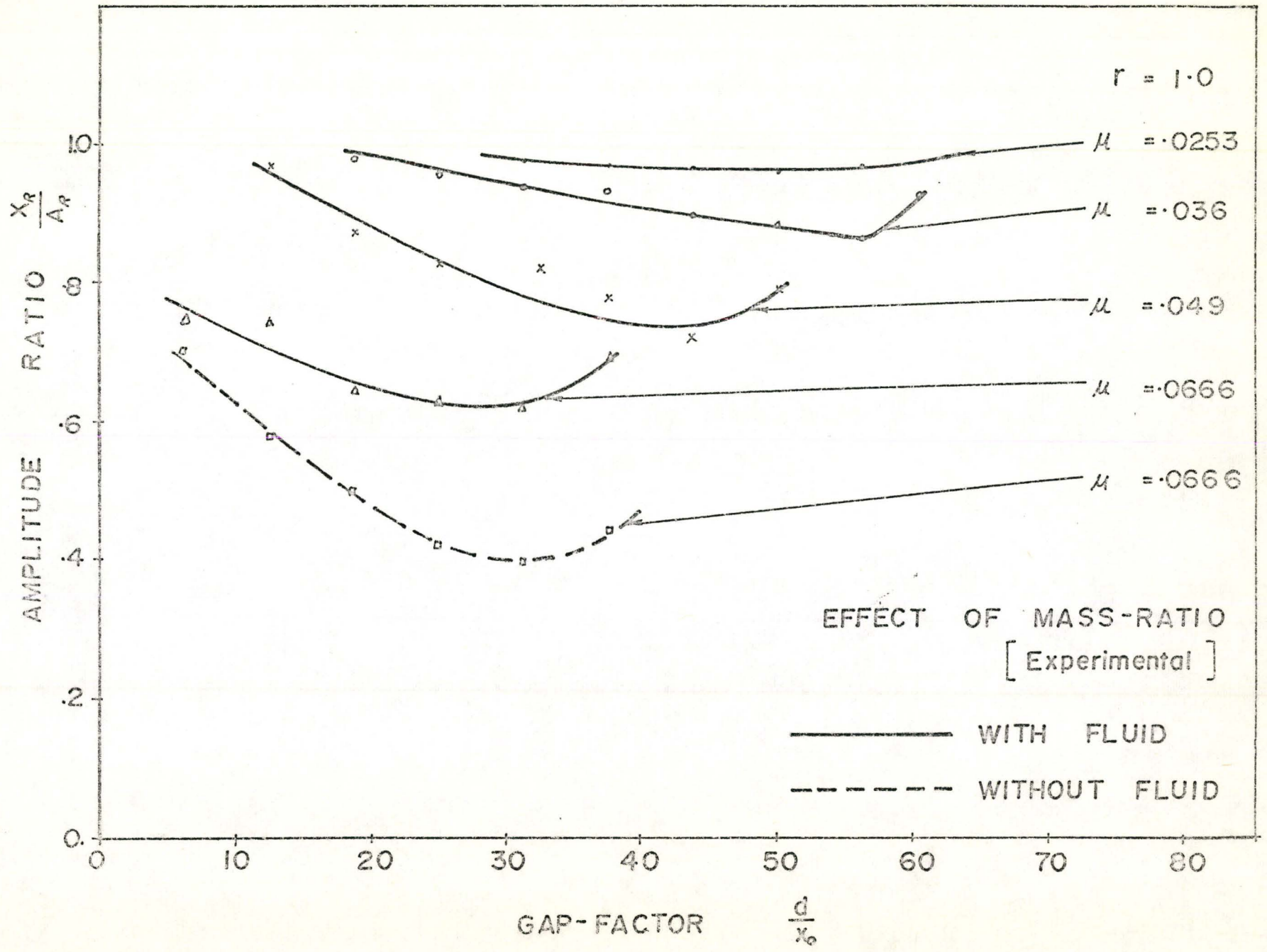
r = 1·0
μ = ·0253
μ = ·036
μ = ·049
μ = ·0666
μ = ·0666
EFFECT OF MASS-RATIO
[Experimental]
WITH FLUID
WITHOUT FLUID
AMPLITUDE RATIO $\frac{X_R}{A_R}$
GAP-FACTOR $\frac{d}{x_0}$
0.
·2
·4
·6
·8
1·0
0
10
20
30
40
50
60
70
80

Fig. 3.17

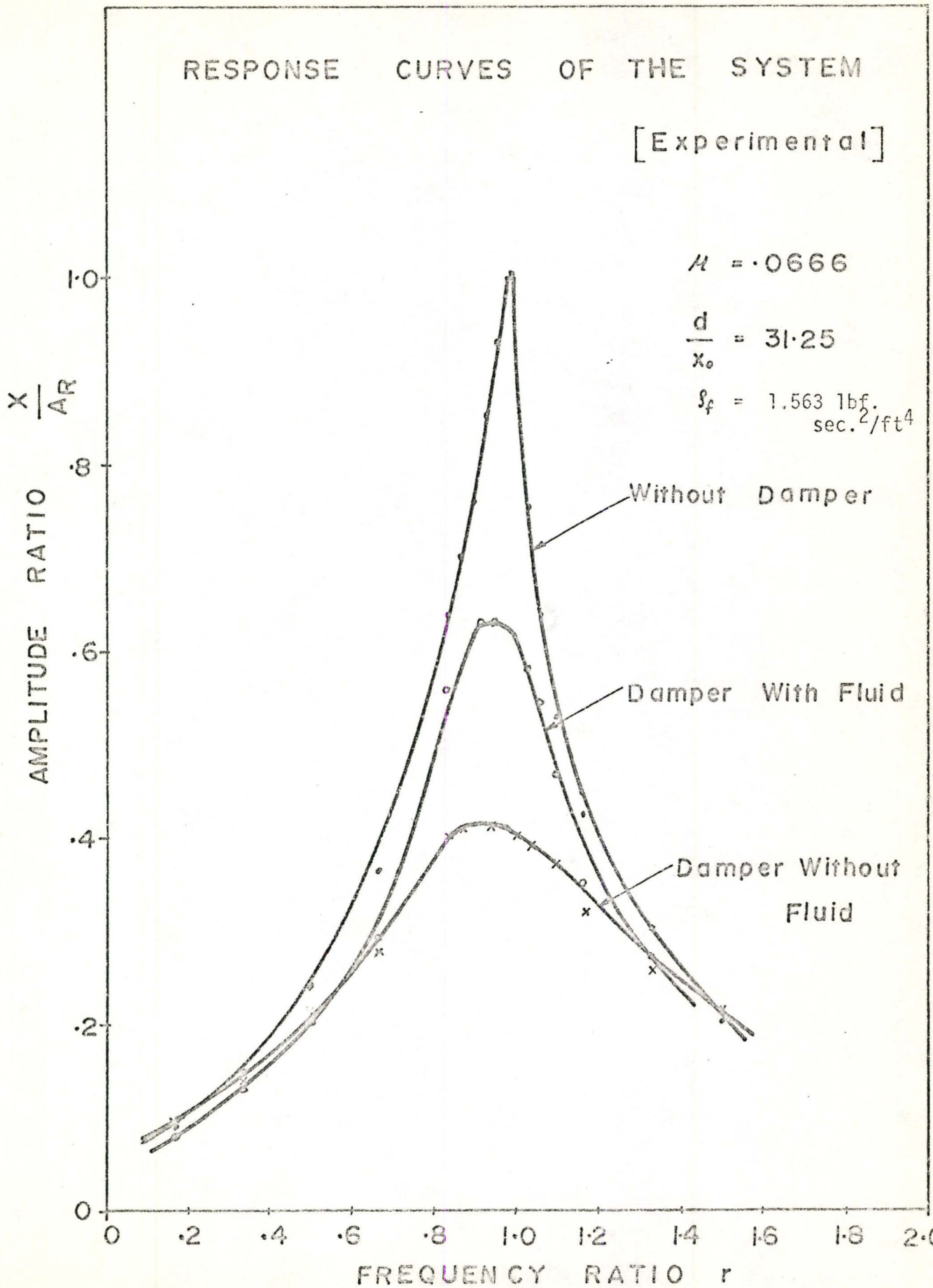
RESPONSE CURVES OF THE SYSTEM
[Experimental]
μ = ·0666
$\frac{d}{x_o}$ = 31·25
ρ_f = 1.563 lbf. sec.^{2}/ft^4
Without Damper
Damper With Fluid
Damper Without Fluid
AMPLITUDE RATIO $\frac{X}{A_R}$
1·0
·8
·6
·4
·2
0
0
·2
·4
·6
·8
1·0
1·2
1·4
1·6
1·8
2·0
FREQUENCY RATIO r

4 DISCUSSION OF RESULTS

By examining the various response curves, it is seen that the peak - which is always present - moves to the lower value of r as μ increases. Before the peak is reached, the amplitude is generally slightly above the amplitude without impact damper. After the peak amplitude is reached the damper is really effective and the amplitude is always less than that without the impact damper. This is in agreement with the theoretical prediction. One more point to be noted is that, with constant d/x_o, the peak amplitude decreases constantly with increase in μ. However, after a certain value of μ, any further increase in the value of μ does not necessarily increase the proportional effectiveness of the damper. It is generally seen that the damping tends to smooth out the sharpness of the undamped curves for amplitude response.

It can be seen from Figures 3.7, 3.15, 3.16, that with the increase in gap from zero the damper becomes more effective. This situation continues until an optimum condition is reached, after which the peak amplitude of vibration increases with increase in gap. The points on the extreme right of the curves in Figures 3.7, 3.15 and 3.16 are for the gap-factor beyond which any increase in gap results in erratic behaviour or 'beating' of the damper. This stems from the fact that the energy imparted

to the free mass at one impact is inadequate to force the free mass to the opposite end of the damper container. The free mass then starts to oscillate while the amplitude of the primary system builds up until subsequent impacts occur between the damper container ends and the vibrational amplitude decreases subsequently, resulting in a vibration wave form that resembles that of the beating phenomenon. Pictures of the beating phenomenon are shown in Figure 4.1 (a), (b), which indicates the building up of amplitude while there is no impact.

Figures 4.2 (a), (b) are photographs taken from the screen of the oscilloscope, showing the reduction in amplitude when the impact damper comes into action. Two photographs show the effect of two different mass-ratios as marked on the figures.

Figures 4.4 (a), (b), (c), (d) show the phase plane diagrams obtained by experimentation with a different pair of μ and d/x_o. Various X-t and $\dot{X}$-t wave forms are shown in Figures 4.3 (a), (b), (c) and (d). These were obtained from the screen of the oscilloscope for different values of d, for the same value of μ. It is observed that two impacts per cycle, with the stops, occur at equal time intervals. This behaviour is observed to repeat for wide range of parameters for which impact damper is in action, so it justifies the assumption of equispaced impacts in analytical derivation. The actual wave form of the response is sinusoidal, and the assumption that the velocity changes discontinuously is

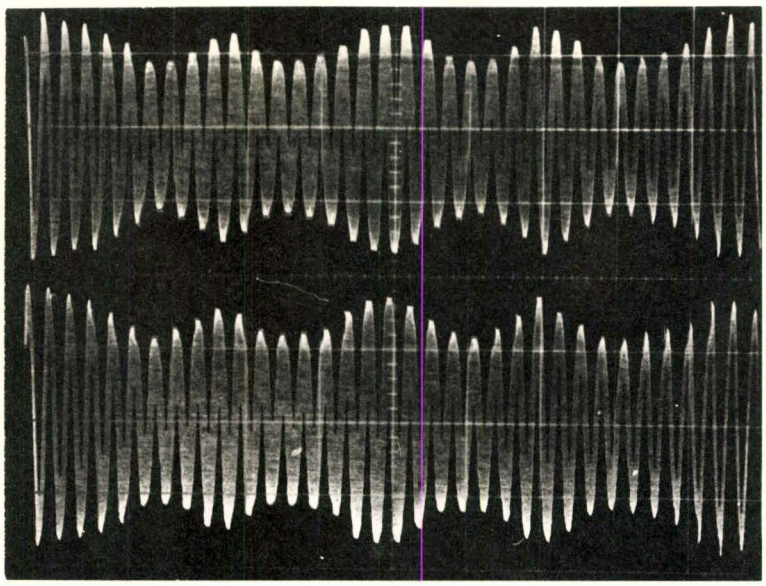

X

$\dot{X}$

Figure 4.1 (a) Two-Particle System, X, $\dot{X}$ Motion of Primary Mass for μ = .1294, d/X_o = 24.7, r=1

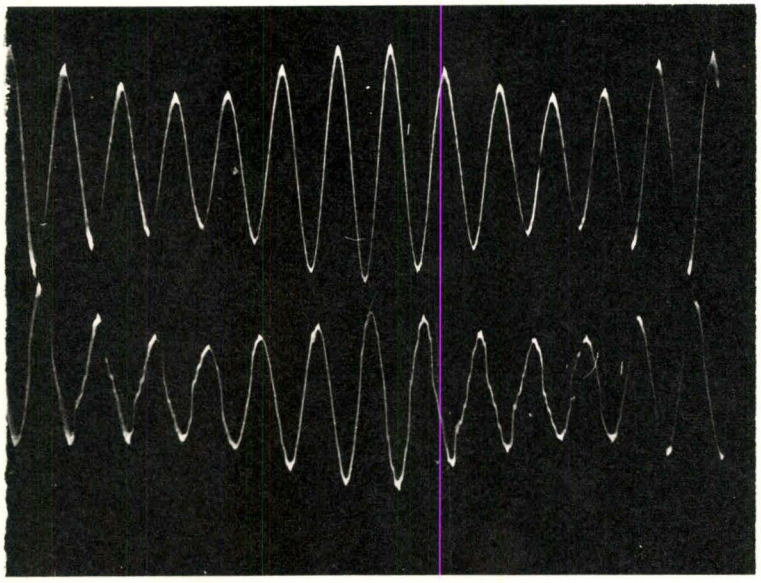

X

$\dot{X}$

Figure 4.1 (b) Single-Particle System, X, $\dot{X}$ Motion of Primary Mass for μ = .112, d/X_o = 18.5, r=1

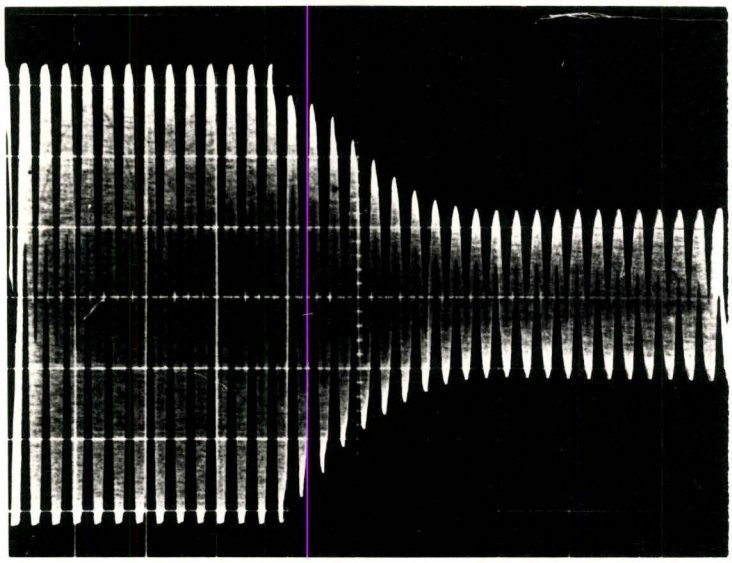

(a)

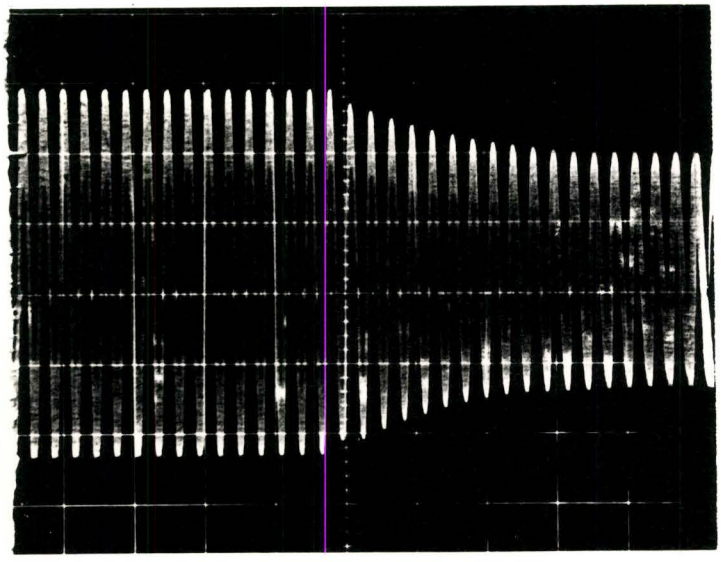

(b)

Figure 4.2 Motion of Primary Mass M

(a) Effect of Introducing μ = .0878

(b) Effect of Introducing μ = .0224; for $\frac{d}{X_o}$ = 12.3

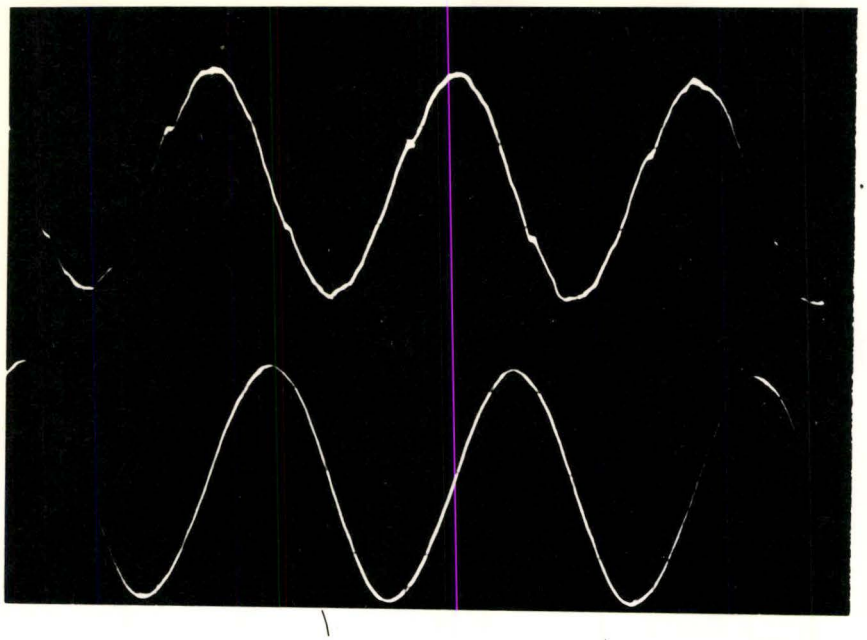

(a) $d/X_o = 3.08$

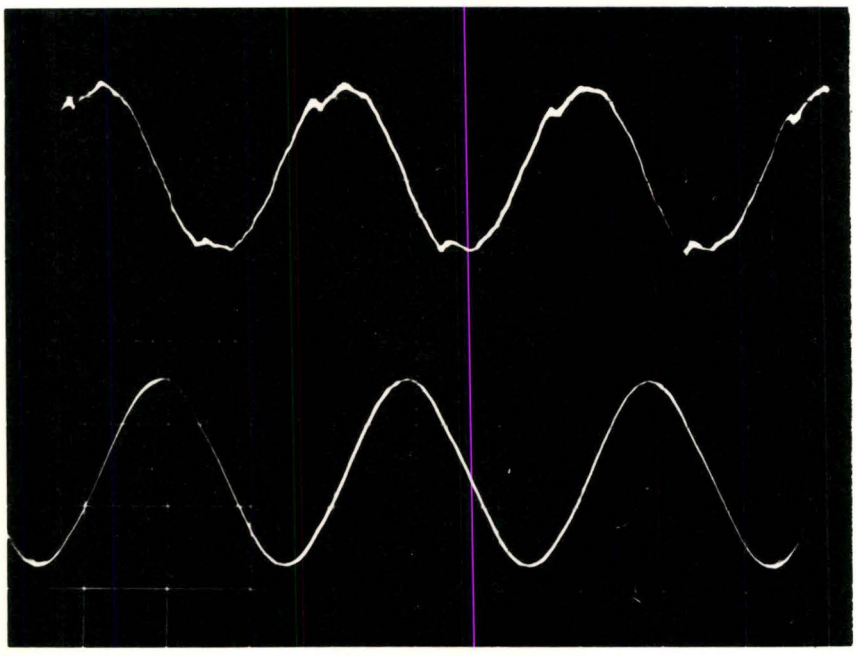

(b) $d/X_o = 9.25$

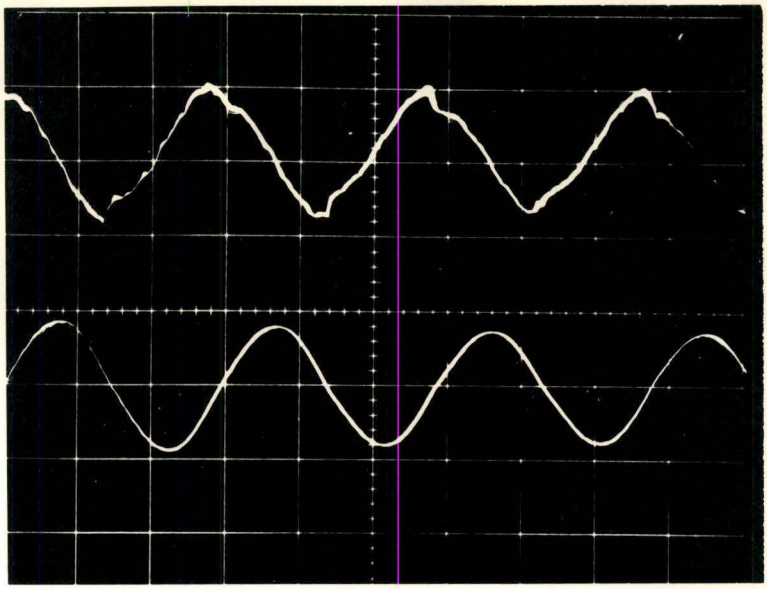

$\dot{X}$

X

(c) $d/X_o = 12.32$

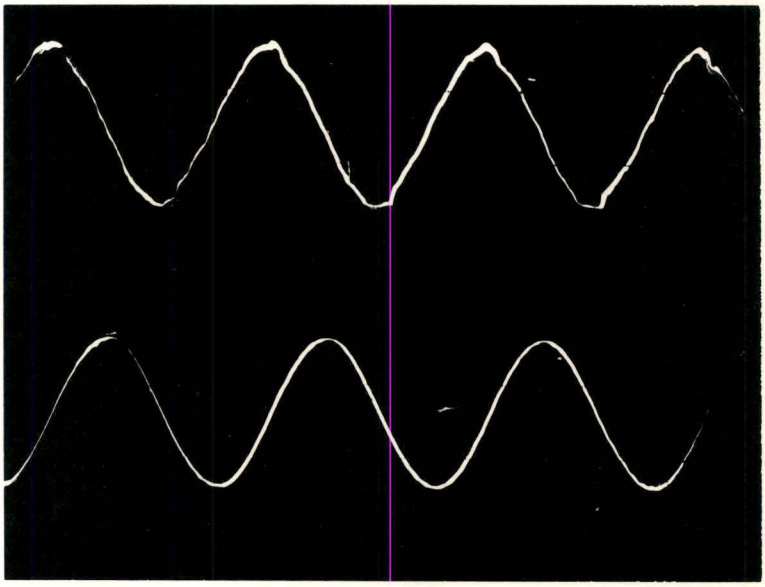

$\dot{X}$

X

(d) $d/X_o = 15.4$

Figure 4.3 (a),(b),(c),(d) Two-Particle System X, $\dot{X}$ Wave Forms as Photographed from The Screen of C.R.O. for $\mu = .1294$

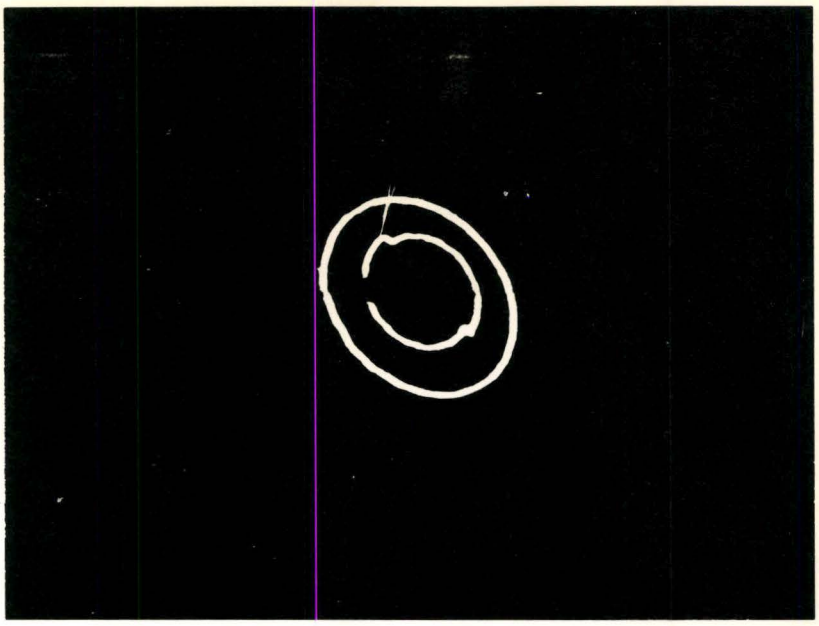

(a) Single-Particle System

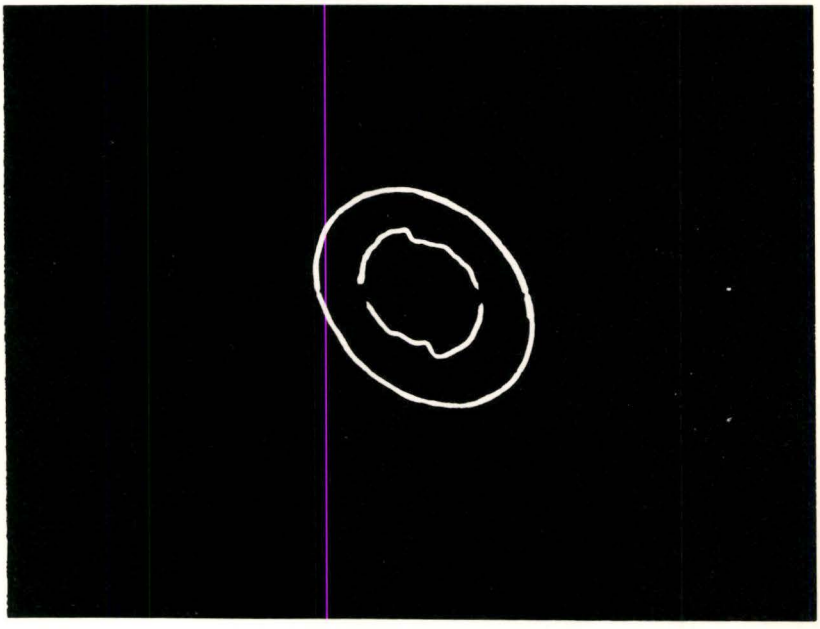

(b) Single-Particle System

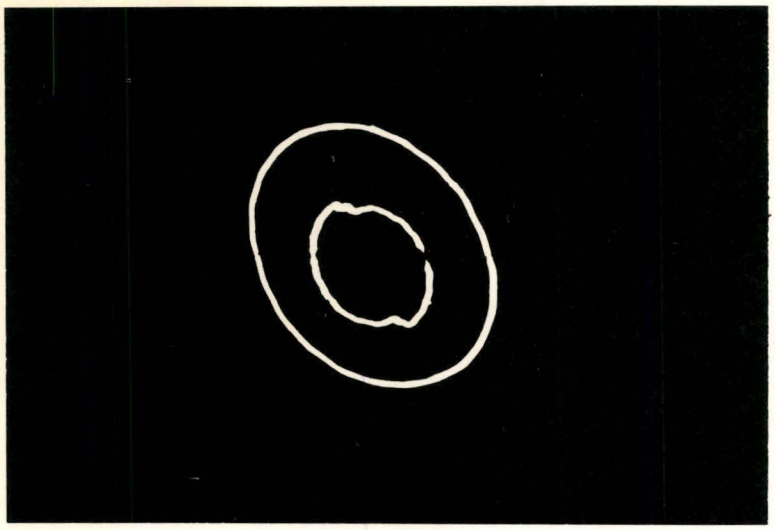

(c) Two-Particle System

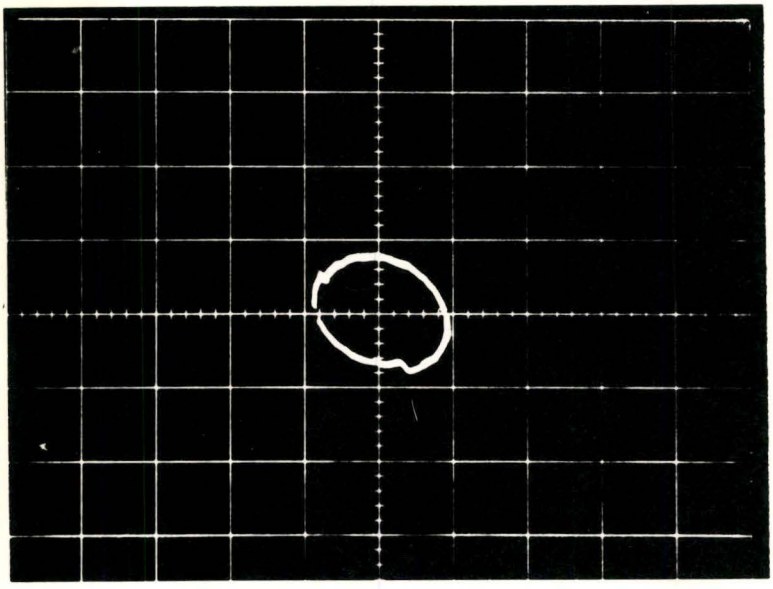

(d) Single-Particle System

Figure 4.4. Limit Cycles of Impact Damper
(a), (b), (c) $X - \dot{X}$ With $\mu=0$ & $\mu \neq 0$
(d) $X - \dot{X}$ with $\mu \neq 0$

justifiable . This is seen in Figures 4.3 and 4.4.

It is to be noted that a change in gap changes the position of impact and for optimum gap the impacts occur near the peak velocity. This shows that at resonance, when the optimum damping is called for to improve the behaviour of the vibrating system, the impacts occur when the velocity of the vibrating system is maximum thereby causing the greatest possible dissipation of kinetic energy.

It is clear from Figures 3.7, 3.15 that the increase in μ causes a decrease in maximum gap-factor that can be reached before beating starts. Similarly, optimum gap decreases, and, for the same gap, more efficient behaviour of the damper is achieved. This is to be expected since increasing the free mass weight will cause higher dissipation of energy from the vibrating system in order to traverse the free mass through this specific gap.

From Figure 3.16 it is seen that increase in value of e improves the performance of the damper for wide range of gap-factor. However, for smaller gap - where the damper is not so efficient - the effect of increase in e is not favourable.

In Figures 3.7, 3.8, two-particle system is compared with the single-particle system for the mass ratios marked on the figure. The behaviour of the two systems are qualitatively similar for the range used. The comparision of the two systems shows that, if the same total mass is used in both cases, the single

particle damper is more efficient than the two-particle damper for a complete range of frequencies and gap-factors.

All through the experiments, rubber pads were used at the stops. The biggest gain in the system, with single-particle impact damper, is that the noise is eliminated and hence the impact damper becomes more practical in light of its use in the presence of human beings.

It is noted in the case of the two-particle impact damper, that in spite of use of rubber pads, the system is still noisy due to the intermediate impacts between two mass particles.

Due to the resistance of the fluid on the motion of mass particle, the system is less efficient in its purpose of reducing the amplitude of vibration. These experiments suggest that the impact damper is effective even in the presence of fluid and that there is a little reduction in noise. However, the use of the fluid in the container, for such a damper, is not recommended because of two reasons. Firstly, noise reduction is not significant compared to loss of efficiency. Secondly, the presence of fluid complicates the design and maintenance of the damper which otherwise is quite simple.

The experiments generally tend to confirm the theory and the behaviour is qualitatively comparable. The amplitude at resonance is markedly reduced while the amplitude at frequencies

close to resonance is larger. For frequencies above resonance there is no indication of increased amplitudes.

5 CONCLUSIONS

As a result of the experimental investigation, the following conclusions could be made.

1. Experiments with rubber pads at the ends of the container indicate that the system behaves similarly to one with rigid stops. In this system noise is eliminated, as the impact is on soft surfaces. All the previous investigators have reported excessive noise level while the damper is functioning; with the use of this system and by proper selection of the soft materials (with high coefficient of restitution), the damper becomes less noisy and hence more practical.

   Choosing a practical value of μ, say .1 to .2, and materials giving high coefficient of restitution, it will be seen that the use of the correctly designed impact damper considerably reduces the vibrations at resonance.

2. With higher value of e, the efficiency of the damper improves.

3. Experiments with a pair of mass-particles in the container show that even if the same total mass is used in a single-particle as in two-particle impact damper, the former will be more effective in reducing the amplitude of vibrations.

4. In the case of the two-particle impact damper, the intermediate impacts between two mass particles, makes the system noisy and hence for continuous operation will require muffling. This is true even if rubber pads are used at the ends.

5. Experiments with the mass particle moving in a fluid suggest that the friction forces acting on the mass particle are detrimental to the efficiency of the damper.

6. The significant advantage of the impact vibration absorber over the conventional dynamic absorber is the reduction of the amplitude of the primary system both at resonance and at higher frequencies.

7. Since in practical applications the resulting amplitude rather than the existence of stable periodic motions is of prime concern, the impact damper fulfilled its role even when its motion was not steady.

8. Some of the main advantages, of impact damper, would be the relative simplicity of installation, maintenance and facility of variation of damper parameters.

With more investigation and development, the future of the impact damper appears quite promising. For further studies, it would be worth considering the effects of various soft materials as impacting surfaces and two-mass particle system with each particle in a separate channel.

APPENDIX A

THEORETICAL SOLUTION FOR THE SYSTEM WITH FLUID

The equation of motion of primary mass M, between impacts, is

$$M\ddot{X} + C\dot{X} + KX = F_0 \sin\Omega t \tag{41}$$

when the mass particle is oscillating in the container filled with fluid the equation of motion for mass particle, between impacts, is

$$m\ddot{y} + \frac{1}{2}\rho_f \frac{\pi d_o^3}{6}\ddot{y} = -m\ddot{X} \tag{42}$$

or

$$(m + m')\ddot{y} = -m\ddot{X}$$

where $m' = \frac{1}{2}\rho_f \frac{\pi d_o^3}{6}$ added mass due to fluid.

The complete solution of equation (41) is,

$$X = e^{-\delta\omega t}[B_1 \sin \eta\omega t + B_2 \cos \eta\omega t] + A \sin (\Omega t - \psi) \tag{43}$$

using the initial conditions at impact,

$X(t_{i+}) = X_i$; $\dot{X}(t_{i+}) = \dot{X}_i$, the constants B_1 and B_2 can be evaluated.

Differentiating the equation (43) w.r.t. t,

$$\dot{X} = e^{-\delta\omega t}[-\delta\omega B_1 \sin\eta\omega t - \delta\omega B_2 \cos\eta\omega t + \eta\omega B_1 \cos\eta\omega t - \eta\omega B_2 \sin\eta\omega t] + A\Omega\cos(\Omega t - \psi) \tag{44}$$

Substituting initial conditions in (43) and (44),

$$B_1 = e^{\delta\omega t_i}\left[E_i \sin \eta\omega t_i + D_i \cos \eta\omega t_i\right]$$

$$B_2 = e^{\delta\omega t_i}\left[E_i \cos \eta\omega t_i - D_i \sin \eta\omega t_i\right]$$

where $$E_i = X_i - A \sin(\Omega t_i - \psi)$$

$$D_i = \frac{1}{\eta}\left[\delta E_i + \frac{\dot{X}_i}{\omega} - Ar \cos(\Omega t_i - \psi)\right]$$

Hence

$$X = e^{-\delta\omega(t-t_i)}\left[D_i \sin \eta\omega(t-t_i) + E_i \cos \eta\omega(t-t_i)\right] + A \sin(\Omega t - \psi) \qquad (45)$$

For the solution of equation (42), using the initial conditions at the time t_{i+} immediately after ith impact,

$$X(t_{i+}) = X_i \ , \qquad \dot{X}(t_{i+}) = \dot{X}_i \ ;$$

$$Y(t_{i+}) = Y_i \ , \qquad \dot{Y}(t_{i+}) = \dot{Y}_i \ .$$

Integrating twice equation (42)

$$(m + m')\dot{y} = -m\dot{x} + C_1$$

$$(m + m')y = -mx + C_1 t + C_2$$

Applying initial conditions

$$C_1 = (m + m')\dot{Y}_i + m\dot{X}_i \qquad \text{and}$$

$$C_2 = (m + m')Y_i + mX_i - \{(m + m')\dot{Y}_i + m\dot{X}_i\} t_i$$

Hence

$$(m + m')y = -mX + mX_i + (m + m')y_i$$

$$+ \{(m + m')\dot{y}_i + m\dot{X}_i\}(t - t_i)$$

letting

$$\mu_1 = \frac{m}{m + m'}$$

$$Y = -\mu_1 X + \mu_1 X_i + Y_i + (\dot{Y}_i + \mu_1 \dot{X}_i)(t - t_i) \qquad (46)$$

In equation (42) potential flow analysis is used. This has been justified* by several reported experimental investigations conducted in water and other low viscosity fluid, as in our case, and in such cases viscous effects are negligible and results would easily be within one percent of potential flow solution.

The solutions (45)and (46) are valid only up to $t_{(i+1)}$-, time immediately before next impact. From the impact conditions,

---

* Reference: "Added Mass of a Sphere in a Bounded Viscous Fluid" by McConnel and Young, Journal of Engineering Mechanics Division, August 1965, page 263.

at $t_{(i+1)_+}$,

$$
\begin{aligned}
X(t_{(i+1)+}) &= X(t_{(i+1)-}) \\
Y(t_{(i+1)+}) &= Y(t_{(i+1)-}) \\
\dot{X}(t_{(i+1)+}) &= \dot{X}(t_{(i+1)-}) + \frac{\mu(1+e)}{1+\mu}\dot{Y}(t_{(i+1)-}) \\
\dot{Y}(t_{(i+1)+}) &= -e\dot{y}(t_{(i+1)-})
\end{aligned}
\tag{47}
$$

Using the new initial conditions from equation (47) the solution can be obtained for the time interval $t_{(i+1)+}$ to $t_{(i+2)-}$. This procedure can be continued and the motion can be determined from collision to collision.

A digital computer programme for this method is given in Appendix D. A check is introduced in the programme so that when the periodic solution reaches steady state conditions, the programme would then discontinue that solution and start constructing a new one correpsonding to a new set of parameters.

A typical digital computer output for two systems with and without fluid is given in Appendix AII. The two sets of curves obtained from similar computation are shown as Figures (A1) and (A-2) Experimentally obtained curves, with and without fluid, for the same parameters, are superimposed in figure A1.

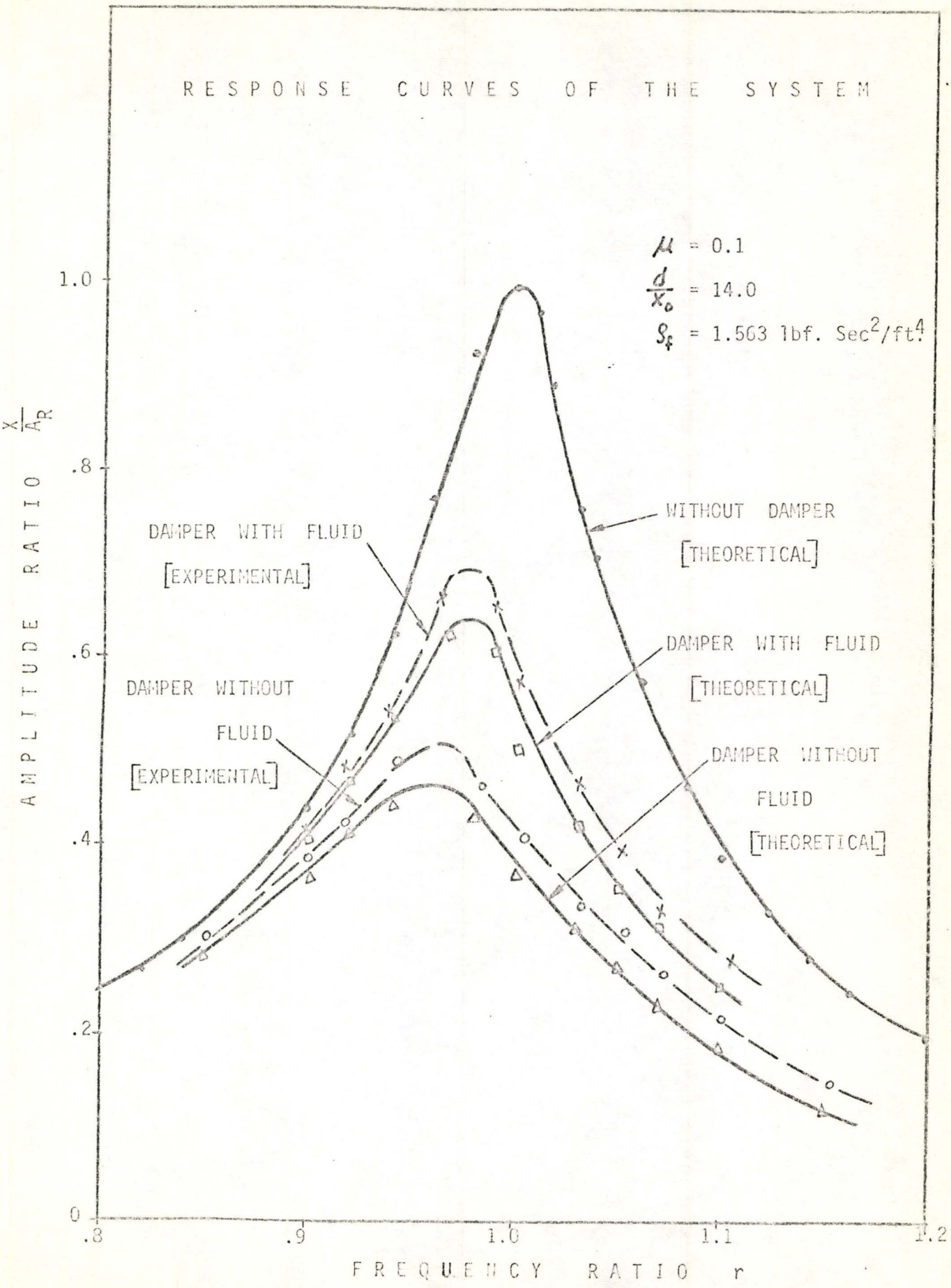
RESPONSE CURVES OF THE SYSTEM
μ = 0.1
$\frac{d}{x_o}$ = 14.0
ρ_f = 1.563 lbf. Sec^2/ft^4
WITHOUT DAMPER [THEORETICAL]
DAMPER WITH FLUID [EXPERIMENTAL]
DAMPER WITH FLUID [THEORETICAL]
DAMPER WITHOUT FLUID [EXPERIMENTAL]
DAMPER WITHOUT FLUID [THEORETICAL]
AMPLITUDE RATIO $\frac{X}{A_R}$
1.0
.8
.6
.4
.2
0
.8
.9
1.0
1.1
1.2
FREQUENCY RATIO r

FIG. A1

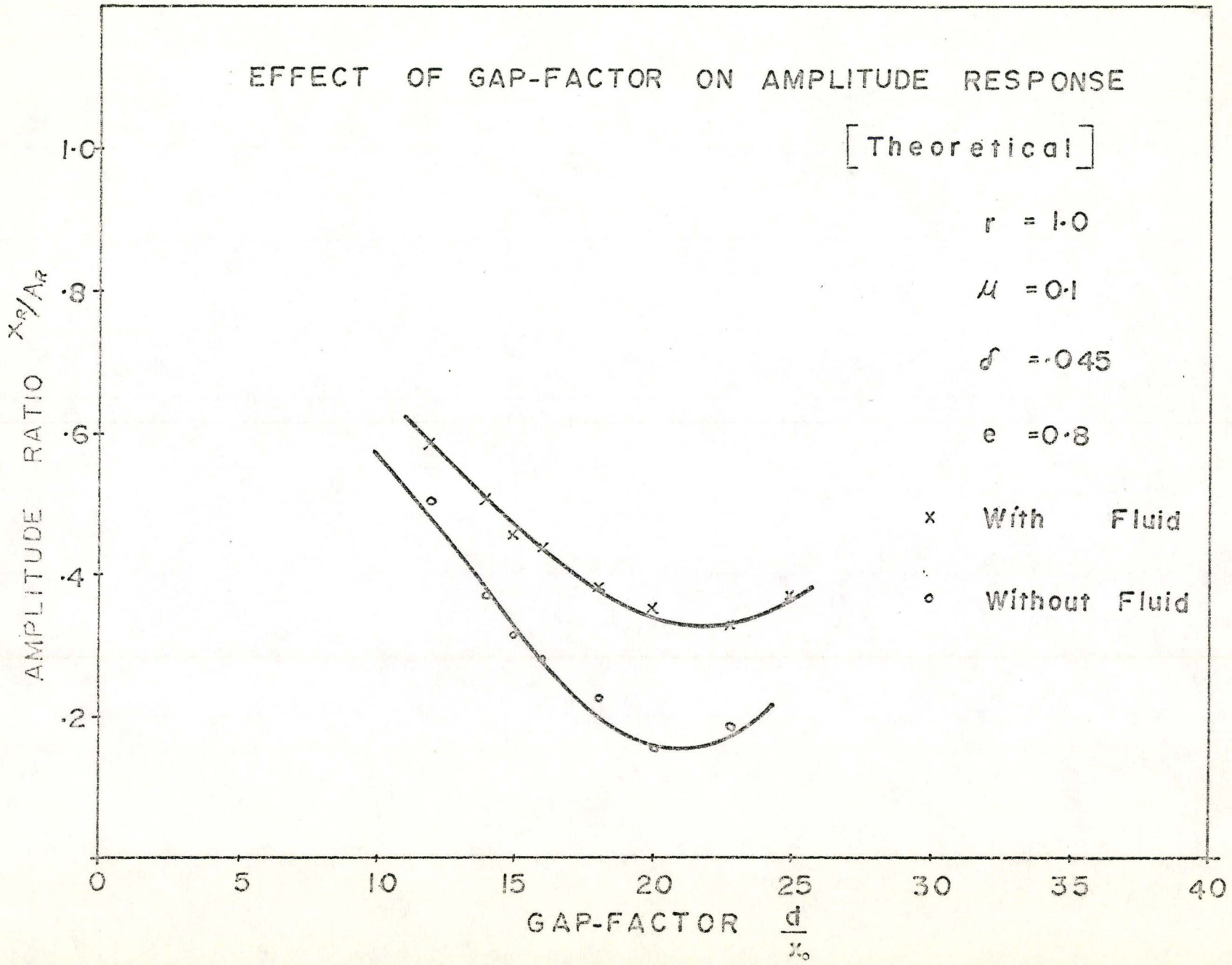
EFFECT OF GAP-FACTOR ON AMPLITUDE RESPONSE
[Theoretical]
r = 1·0
μ = 0·1
δ = ·045
e = 0·8
× With Fluid
○ Without Fluid
AMPLITUDE RATIO X_p/A_r
1·0
·8
·6
·4
·2
0
5
10
15
20
25
30
35
40
GAP-FACTOR $\frac{d}{\lambda_0}$

APPENDIX AII

DIGITAL COMPUTER OUTPUT FOR THE SYSTEM WITHOUT FLUID

ω = 46.47 δ = 0.045 μ = 0.1 e = 0.8 ω_n = 46.47 $\frac{F_o}{K}$ 1.0 $\frac{d}{F_{o/K}}$ = 16.0

Impact (i)	t_i	X_i	Y_i	$\dot{X}_{i+}$	$\dot{Y}_{i+}$	$\frac{X_{max}}{A}$ $t_{i-1} \leq t \leq t_i$
1	0.67	-7.9999	8.00	-100.9629	-96.5732	-0.7299
2	0.71	0.1481	-8.00	296.3541	472.4167	-0.7321
3	0.74	6.5505	8.00	184.5966	-558.6798	0.5945
4	0.82	-7.9393	-8.00	-9.3901	348.7412	-0.7212
5	0.91	5.1182	8.00	-202.6083	-518.3959	0.7332
6	0.94	-5.3915	-8.00	-295.1243	407.3634	-0.5409
7	0.99	0.3585	-8.00	348.7453	226.2233	-0.7313
8	1.03	6.9387	8.00	-8.6158	-558.2111	0.6626
9	1.08	-5.5466	-8.00	-270.4099	283.5293	-0.6242
10	1.12	-5.1007	-8.00	244.0137	220.8554	-0.6944
11	1.18	6.3003	8.00	-64.3862	-506.2442	0.6451
12	1.22	-5.5169	-8.00	-228.7095	327.0548	-0.5138
13	1.27	-1.3400	-8.00	304.0573	196.7680	-0.6345
14	1.31	5.6230	8.00	-36.0674	-513.5495	0.5585
15	1.36	-4.4454	-8.00	-230.9094	304.8506	-0.4357
16	1.40	-1.1762	-8.00	270.2466	187.7703	-0.5656
17	1.45	4.6108	8.00	-52.2303	-486.0624	0.4869
18	1.50	-3.7252	-8.00	-206.6249	319.1605	-0.3872
19	1.56	2.9553	-8.00	209.1012	92.3671	-0.4881
20	1.60	0.9858	8.00	-163.4000	-444.6567	0.4605
21	1.64	-3.5358	-8.00	-126.3382	460.7741	-0.3200
22	1.71	4.3929	8.00	75.2681	-247.8996	0.3907
23	1.82	1.8406	-8.00	166.4887	324.3759	-0.4295
24	1.85	3.1494	8.00	-20.7907	-489.4094	0.3534
25	1.89	-2.4618	-8.00	-194.0908	302.3654	-0.2948
26	2.03	-4.1281	8.00	-125.5141	-223.6240	-0.4619
27	2.06	-1.3711	-8.00	141.4514	469.2403	-0.4390
28	2.10	3.5198	8.00	157.5002	-433.4684	0.3399
29	2.19	-4.7138	-8.00	49.0896	310.9248	-0.4704
30	2.26	4.5333	8.00	-49.9265	-392.1173	0.4715
31	2.31	-4.9785	-8.00	-83.2245	343.2184	-0.4479
32	2.40	2.6904	8.00	-156.1763	-398.0759	0.4916
33	2.45	-4.3217	-8.00	-130.3855	405.4377	-0.3898
34	2.53	3.9096	8.00	-98.4088	-357.2236	0.4603
35	2.59	-4.5857	-8.00	-70.2933	368.5853	-0.4071
36	2.67	3.8176	8.00	-80.4608	-362.2853	0.4394
37	2.72	-4.2953	-8.00	-70.4340	356.1246	-0.3778
38	2.81	3.3803	8.00	-84.9143	-354.4916	0.4112
39	2.86	-3.9283	-8.00	-67.9512	355.3045	-0.3506
40	2.94	3.3301	8.00	-64.4584	-336.5154	0.3785

41	3.00	-3.6711	-8.00	-39.1218	346.1193	-0.3276
42	3.07	3.3575	8.00	-31.8499	-324.1149	0.3363
43	3.14	-3.3697	-8.00	-6.4464	334.3220	-0.3186
44	3.21	3.2442	8.00	-6.1218	-319.4758	0.3165
45	3.27	-3.0662	-8.00	12.8581	323.7402	-0.3078
46	3.34	3.0523	8.00	3.1357	-318.9643	0.2940
47	3.41	-2.8990	-8.00	13.6700	315.1726	-0.2933
48	3.48	2.8757	8.00	-2.6401	-317.0704	0.2822
49	3.54	-2.8269	-8.00	6.3813	311.9139	-0.2812
50	3.61	2.7681	8.00	-9.2369	-313.2915	0.2785
51	3.68	-2.7759	-8.00	3.9782	312.3106	-0.2746
52	3.75	2.7472	8.00	-8.7805	-310.9359	0.2762
53	3.81	-2.7508	-8.00	6.7707	312.2920	-0.2747
54	3.88	2.7640	8.00	-6.4057	-311.3176	0.2756
55	3.95	-2.7637	-8.00	8.3472	311.8935	-0.2773
56	4.02	2.7867	8.00	-6.4463	-312.4832	0.2776
57	4.08	-2.7992	-8.00	7.5929	312.3257	-0.2798
58	4.15	2.8139	8.00	-7.5034	-313.1862	0.2810
59	4.22	-2.8337	-8.00	6.9140	313.3599	-0.2822
60	4.29	2.8444	8.00	-7.6890	-313.7036	0.2839
61	4.35	-2.8595	-8.00	7.0951	314.2057	-0.2847
62	4.42	2.8703	8.00	-7.2905	-314.3048	0.2858
63	4.49	-2.8782	-8.00	7.3772	314.6694	-0.2866
64	4.56	2.8868	8.00	-7.0891	-314.8255	0.2871
65	4.62	-2.8908	-8.00	7.3335	314.9329	-0.2877
66	4.69	2.8948	8.00	-7.1568	-315.1005	0.2879
67	4.76	-2.8970	-8.00	7.1694	315.1038	-0.2881
68	4.83	2.8974	8.00	-7.2193	-315.1668	0.2882
69	4.90	-2.8978	-8.00	7.1096	315.1698	-0.2881
70	4.96	2.8966	8.00	-7.1822	-315.1373	0.2881
71	5.03	-2.8954	-8.00	7.1355	315.1309	-0.2879
72	5.10	2.8938	8.00	-7.1293	-315.0742	0.2878
73	5.17	-2.8918	-8.00	7.1536	315.0372	-0.2876
74	5.23	2.8900	8.00	-7.1199	-314.9929	0.2874
75	5.30	-2.8881	-8.00	7.1436	314.9409	-0.2873
76	5.37	2.8865	8.00	-7.1351	-314.9058	0.2871
77	5.44	-2.8850	-8.00	7.1328	314.8619	-0.2870
78	5.50	2.8837	8.00	-7.1471	-314.8313	0.2869
79	5.57	-2.8828	-8.00	7.1364	314.8054	-0.2868
80	5.64	2.8819	8.00	-7.1488	-314.7823	0.2867
81	5.71	-2.8814	-8.00	7.1442	314.7677	-0.2867
82	5.77	2.8810	8.00	-7.1501	-314.7551	0.2867
83	5.84	-2.8807	-8.00	7.1503	314.7487	-0.2866
84	5.91	2.8807	8.00	-7.1529	-314.7453	0.2866
85	5.98	-2.8807	-8.00	7.1533	314.7449	-0.2866
86	6.04	2.8808	8.00	-7.1552	-314.7466	0.2866
87	6.11	-2.8809	-8.00	7.1552	314.7502	-0.2867
88	6.18	2.8812	8.00	-7.1560	-314.7543	0.2867
89	6.25	-2.8814	-8.00	7.1573	314.7603	-0.2867
90	6.31	2.8816	8.00	-7.1555	-314.7656	0.2867
91	6.38	-2.8818	-8.00	7.1570	314.7703	-0.2867
92	6.45	2.8820	8.00	-7.1559	-314.7753	0.2867
93	6.52	-2.8821	-8.00	7.1575	314.7804	-0.2868
94	6.59	2.8823	8.00	-7.1538	-314.7834	0.2868

95	6.65	-2.8824	-8.00	7.1571	314.7858	-0.2868
96	6.72	2.8825	8.00	-7.1561	-314.7903	0.2868
97	6.79	-2.8826	-8.00	7.1532	314.7908	-0.2868
98	6.86	2.8826	8.00	-7.1563	-314.7916	0.2868
99	6.92	-2.8826	-8.00	7.1551	314.7942	-0.2868
100	6.99	2.8826	8.00	-7.1523	-314.7928	0.2868
101	7.06	-2.8826	-8.00	7.1570	314.7934	-0.2868
102	7.13	2.8826	8.00	-7.1516	-314.7934	0.2868
103	7.19	-2.8826	-8.00	7.1552	314.7917	-0.2868

APPENDIX AII

DIGITAL COMPUTER OUTPUT FOR THE SYSTEM WITH FLUID

$\omega = 46.47$ $\delta = 0.045$ $\mu = 0.1$ $e = 0.8$ $\omega_n = 46.47$ $\frac{F_o}{K}$ 1.0 $\frac{d}{F_{o/K}} = 16.0$

$\mu_1 = 0.951$ $\frac{X_{max}}{A}$

Impact (i)	t_i	X_i	Y_i	X_{i+}	Y_{i+}	$t_{i-1} \leq t \leq t_i$
1	0.81	-8.8889	8.00	-73.1817	-61.7909	-1.1426
2	0.85	2.6741	-8.00	327.9988	396.7067	-1.0907
3	0.88	7.6556	8.00	70.8947	-589.2626	0.9620
4	0.93	-5.5116	-8.00	-327.2044	216.6915	0.9453
5	0.96	-7.9967	-8.00	143.8073	194.4059	-1.1193
6	1.04	3.8510	8.00	-267.9083	-530.0170	1.1067
7	1.08	-5.6437	-8.00	-303.7184	467.0079	-0.8679
8	1.19	1.0493	8.00	-319.1050	-451.1228	1.0739
9	1.22	-6.7626	-8.00	-191.2584	531.1754	-0.8668
10	1.30	7.7509	8.00	-15.3741	-349.8230	-0.9862
11	1.38	-6.0887	-8.00	143.1710	462.0596	-0.9667
12	1.43	6.1313	8.00	224.2268	-365.0494	0.8363
13	1.48	-4.4185	8.00	-283.7730	-86.4524	0.9530
14	1.53	-2.9335	-8.00	223.0237	509.0204	-0.9227
15	1.56	4.7303	8.00	241.3877	-462.0401	0.6937
16	1.66	-4.3116	-8.00	180.6966	382.2260	-0.8597
17	1.70	5.7049	8.00	131.8780	-399.8115	0.7300
18	1.79	-4.3288	-8.00	146.1244	387.1187	0.7913
19	1.84	5.2434	8.00	126.6665	-379.4421	0.6711
20	1.93	-3.6278	-8.00	149.0470	374.7079	0.7328
21	1.98	4.7712	8.00	111.5518	-383.1973	0.6063
22	2.06	-4.1248	-8.00	93.9513	344.6418	-0.6629
23	2.12	4.6115	8.00	53.6552	-357.3553	0.5717
24	2.19	-4.1178	-8.00	52.8230	334.5560	-0.5925
25	2.26	4.2253	8.00	20.0191	-341.5671	0.5404
26	2.33	-3.9078	-8.00	25.8696	325.3866	-0.5345
27	2.39	3.7975	8.00	-3.4904	-330.0569	0.5087
28	2.46	-3.6401	-8.00	7.8437	319.2182	-0.4921
29	2.53	3.4335	8.00	-15.8585	-319.4926	0.4760
30	2.60	-3.3635	-8.00	3.4560	316.0454	-0.4546
31	2.67	3.2133	8.00	-14.1411	-311.3613	0.4468
32	2.73	-3.1365	-8.00	9.4929	312.0640	-0.4325
33	2.80	3.0817	8.00	-8.8881	-308.2879	0.4252
34	2.87	-3.0090	-8.00	12.9665	307.6782	-0.4208
35	2.93	2.9928	8.00	-9.3699	-307.5130	0.4145
36	3.00	-2.9715	-8.00	11.1716	305.8426	-0.4141
37	3.07	2.9579	8.00	-11.9161	-306.4254	0.4132
38	3.14	-2.9704	-8.00	10.3464	306.2753	-0.4129

39	3.20	2.9746	8.00	-11.8474	-306.0766	0.4153
40	3.27	-2.9895	-8.00	11.4659	306.8353	-0.4166
41	3.34	3.0107	8.00	-11.1016	-306.9174	0.4188
42	3.41	-3.0259	-8.00	11.8685	307.3343	-0.4216
43	3.47	3.0473	8.00	-11.3393	-307.9262	0.4236
44	3.54	-3.0661	-8.00	11.4763	308.1502	-0.4261
45	3.61	3.0817	8.00	-11.6730	-308.6422	0.4282
46	3.68	-3.0985	-8.00	11.3521	308.9990	-0.4299
47	3.75	3.1108	8.00	-11.5568	-309.2355	0.4317
48	3.81	-3.1217	-8.00	11.4863	309.5708	-0.4330
49	3.88	3.1311	8.00	-11.3868	-309.7417	0.4340
50	3.95	-3.1372	-8.00	11.4914	309.9064	-0.4349
51	4.02	3.1425	8.00	-11.3816	-310.0566	0.4354
52	4.08	-3.1458	-8.00	11.3910	310.1127	-0.4358
53	4.15	3.1474	8.00	-11.4022	-310.1827	0.4361
54	4.22	-3.1484	-8.00	11.3423	310.2072	-0.4361
55	4.29	3.1481	8.00	-11.3687	-310.2020	0.4361
56	4.35	-3.1473	-8.00	11.3456	310.1998	-0.4360
57	4.42	3.1461	8.00	-11.3331	-310.1678	0.4358
58	4.49	-3.1443	-8.00	11.3433	310.1358	-0.4356
59	4.56	3.1426	8.00	-11.3260	-310.0998	0.4354
60	4.62	-3.1408	-8.00	11.3320	310.0565	-0.4351
61	4.69	3.1390	8.00	-11.3297	-310.0189	0.4349
62	4.76	-3.1373	-8.00	11.3281	309.9804	-0.4347
63	4.83	3.1358	8.00	-11.3313	-309.9456	0.4345
64	4.89	-3.1345	-8.00	11.3315	309.9158	-0.4344
65	4.96	3.1334	8.00	-11.3323	-309.8888	0.4342
66	5.03	-3.1325	-8.00	11.3361	309.8672	-0.4341
67	5.10	3.1318	8.00	-11.3367	-309.8508	0.4340
68	5.17	-3.1312	-8.00	11.3385	309.8374	-0.4340
69	5.23	3.1309	8.00	-11.3406	-309.8281	0.4339
70	5.30	-3.1307	-8.00	11.3417	309.8221	-0.4339
71	5.37	3.1306	8.00	-11.3432	-309.8187	0.4339
72	5.44	-3.1305	-8.00	11.3445	309.8178	-0.4339
73	5.50	3.1306	8.00	-11.3449	-309.8184	0.4339
74	5.57	-3.1308	-8.00	11.3460	309.8202	-0.4339
75	5.64	3.1309	8.00	-11.3482	-309.8247	0.4339
76	5.71	-3.1311	-8.00	11.3442	309.8274	-0.4340
77	5.77	3.1312	8.00	-11.3494	-309.8309	0.4340
78	5.84	-3.1314	-8.00	11.3460	309.8358	-0.4340
79	5.91	3.1316	8.00	-11.3457	-309.8372	0.4340
80	5.98	-3.1317	-8.00	11.3504	309.8423	-0.4341
81	6.04	3.1318	8.00	-11.3442	-309.8457	0.4341
82	6.11	-3.1320	-8.00	11.3473	309.8464	-0.4341
83	6.18	3.1320	8.00	-11.3480	-309.8502	0.4341
84	6.25	-3.1321	-8.00	11.3444	309.8513	-0.4341
85	6.31	3.1322	8.00	-11.3473	-309.8517	0.4341
86	6.38	-3.1322	-8.00	11.3473	309.8546	-0.4341
87	6.45	3.1322	8.00	-11.3435	-309.8541	0.4341
88	6.52	-3.1322	-8.00	11.3482	309.8545	-0.4341
89	6.58	3.1323	8.00	-11.3438	-309.8550	0.4341
90	6.65	-3.1322	-8.00	11.3473	309.8547	-0.4341

APPENDIX B

METHOD AND CALCULATIONS FOR COEFFICIENT OF RESTITUTION

The following method was used to calculate the coefficient of restitution.

Reducing to single particle system equation (21) and (22) will become ;

$$X_b + \frac{\pi}{2\Omega}\left(\frac{1+e}{1-e+2\mu}\right)\dot{X}_b = -\frac{d}{2} \qquad \text{(B-1)}$$

$$X_b + \frac{\pi}{2\Omega}\left(\frac{1+e}{1-e-2\mu e}\right)\dot{X}_a = -\frac{d}{2} \qquad \text{(B-2)}$$

Substracting equation (B-2) from equation (B-1)

$$\frac{\pi}{2\Omega}\left(\frac{1+e}{1-e+2\mu}\right)\dot{X}_b - \frac{\pi}{2\Omega}\left(\frac{1+e}{1-e-2\mu e}\right)\dot{X}_a = 0$$

or $$\dot{X}_b(1-e-2\mu e) = \dot{X}_a(1-e+2\mu)$$

or $$e\left(1+2\mu - \frac{\dot{X}_a}{\dot{X}_b}\right) = 1-(1+2\mu)\frac{\dot{X}_a}{\dot{X}_b}$$

or $$e = \frac{1-(1+2\mu)\frac{\dot{X}_a}{\dot{X}_b}}{(1+2\mu)-\dot{X}_a/\dot{X}_b} \qquad \text{(B-3)}$$

This gives the relation for coefficient of restitution in terms of known quantities. The ratio $\dot{x}_a/\dot{X}_b$ is calculated from the $\dot{X}$ wave forms obtained.

Figure B1 shows the X-$\dot{X}$ wave forms for three different rubber pads used. The three pads are named B1, B2 and R.

The average ratio $\dot{x}_a/\dot{X}_b$ is observed as follows:

Pad	$\dot{x}_a/\dot{X}_b$	μ
B2	.5616	.112
B1	.5895	.112
R	.651	.112

Now

$$e = \frac{1-(1+2\mu)\,\dot{x}_a/\dot{x}_b}{(1+2\mu)-\dot{x}_a/\dot{x}_b}$$

$$= \frac{1-1.224\,\frac{\dot{x}_a}{\dot{x}_b}}{1.224-\frac{\dot{x}_a}{\dot{x}_b}}$$

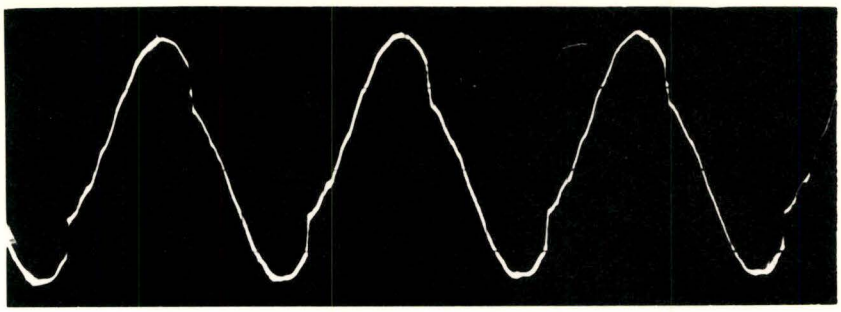

(a)

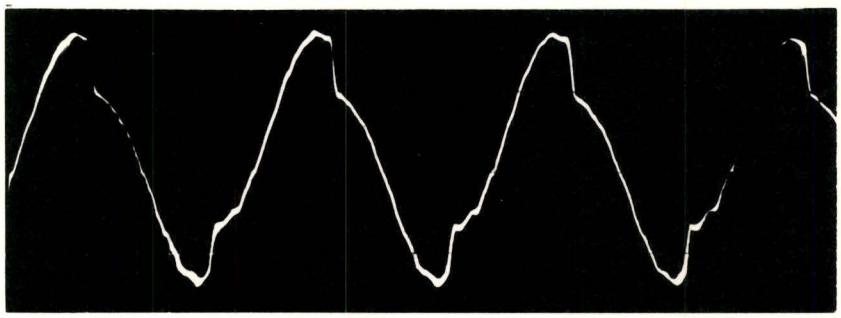

(b)

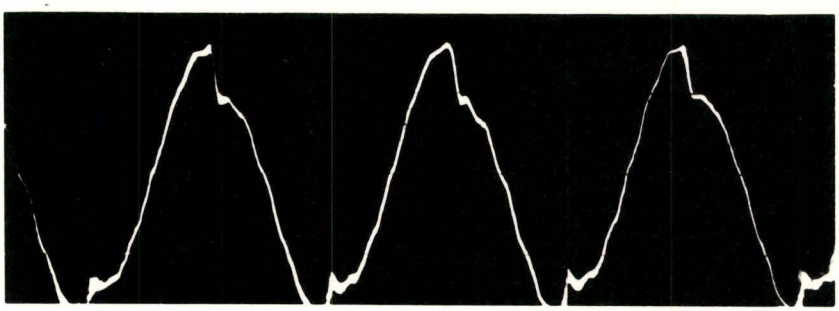

(c)

Figure B1. $\dot{X}$ Wave Form With $\mu = 0.112$
(a) Rubber Pad B2, (b) Rubber Pad B1
(c) Rubber Pad R

$$e_{B2} = \frac{1 - 1.224 \times .5616}{1.224 - .5616} = \frac{.3120}{.6624} = .471$$

$$e_{B1} = \frac{1 - 1.224 \times .5895}{1.224 - .5895} = \frac{.28}{.6345} = .442$$

$$e_{R} = \frac{1 - 1.224 \times .651}{1.224 - .651} = \frac{.203}{.573} = .355$$

APPENDIX C

GENERAL EXPERIMENTAL DATA

Primary Mass:

$$M = 4.4/386 = .0114 \quad lb.sec^2/in.$$

Natural Frequency of the System:

$$f_n = 7.4 \text{ cycles/sec.}$$

Equivalent Spring Constant:

$$K = 24.5 \text{ lbs./in.}$$

Critical Damping Ratio:

$$\delta = .0146$$

Amplitude of Sinusoidal Driving Force:

$$F = 0.49 \text{ lbs.}$$

Ball Size (inches)	Weight (lbs.)	Mass Ratio (μ) Single-Particle System	Mass Ratio (μ) Double-Particle System
1/2	0.0183	0.0042	0.0084
5/8	0.0357	0.0081	0.0162
3/4	0.0621	0.0141	0.0282
7/8	0.0988	0.0224	0.0448
1	0.147	0.0334	0.0668
1-1/8	0.208	0.0474	0.0948
1-1/4	0.284	0.0647	0.1294
1-3/8	0.386	0.0878	0.1756
1-1/2	0.495	0.112	0.2240

LIST OF THE EQUIPMENT

1. 1, Frequency Generator, "RC-Generator, type Z9 060 69", Philips Gloeilampenfabrieken, Eindhoven, Holland.
2. 1, Amplifier Unit, "250 VA Amplifier, type 119567", Philips.
3. 1, Ammeter, Range 0-5 Amps, Conway Electronic Enterprises.
4. 1, Vibration Generator (exciter)", Moving Coil Vibration Generator Model 790", Goodmans Industries Ltd., Wimbley, England.
5. 2, Capacitance Transducers (1, type 51 D04-204 with a tuning plug type 51C02; 1, proximity Vibration Transducer type 51D11). Disa Electronik, Herlev, Denmark.
6. 2, Oscillators, type 51E02-103, Disa Electronik.
7. 2, Reactance converters, type 51E01, Disa Electronik.
8. 1, Cathod Ray Oscilloscope, type 564 storage oscilloscope, Tektronix Inc. S.W. Millikan Way, Beaverton, Oregon, U.S.A.
9. 1, Analog Computer, Electronic Pace Associates Inc.
10. 1, Amplifier Model 2616B, Endevco Corporation, Pasadena, California.
11. 1, Accelerometer Model 2221, Endevco Corporation.
12. 1, Oscilloscope Camera C-12 Serial 007109, Tektronix, Inc., Portland, U. S. A.

APPENDIX D

COMPUTER PROGRAMMES

PROGRAMME 1

1. With proper change in read statements the same programme was used for computing the effect of different parameters.

2. By inserting the write statement x and $\dot{x}$, at proper place, results were obtained for phase-plane plot.

PROGRAMME 1 and 2

3. Replacing statements C_3 and C_4 by σ_1 and σ_2, with formulae for single-particle system, the same programme was used for single-particle system computations.

PROGRAMME 3

4. The same programme was used, for the system without fluid with proper change in formulae.

PROGRAMME 1

```
003727 M D SHAH
$IBFTC
C       TWO PARTICLE IMPACT DAMPER
C       STEADY STATE SOLUTION
C      TO STUDY THE EFFECT OF COEFFICIENT OF RESTITUTION
       READ%5,2␣FF,D,U,E3
       WN#1.0
       W#1.0
       R#W/WN
       A#FF/SQRT%%1.-R*R□**2&%2.*D*R□**2␣
       ETA#SQRT%1. D*D␣
       RP#3.14/R
       DRP#-D*RP
       ERP#ETA*RP
       EX#EXP%DRP□
       SI#SIN%ERP□
       CO#COS%ERP□
       H1#EX*SI
       H2#EX*CO
       TH1#WN*EX*% D*SI&ETA*CO□
       TH2#WN*EX*% D*CO-ETA*SI□
       DO 50 I#1,1
       DO#0.0
       READ%5,2␣E
       U1#2.*U
       WRITE%6,1□FF,D,E,U1,R,A
       ALPO#3.14*E3/%1.&E3□
       C9#%1.-E3□/%3.&E3␣
       C10#-%1.&3.*E3␣/%3.&E3□
       AK7#%E-U␣/%1.&E␣
       AK8#%1.&U□/%1.&E□
       AK9#E*%1.&U␣/%1.&E␣
       AK10#%1.-U*E␣/%1.&E□
       C19#%ALPO&3.14*C9/2.□/%W*%AK7*C10&AK8□□
       C20#%ALPO&3.14*C9/2.□/%W*%AK9*C10&AK10␣□
       SG1#C19
       SG2#C20
       H#2.*W*%%%SG2-SG1□&SG1*SG2*%D*WN-TH2␣□*H1&%SG1*SG2*%TH1&ETA*WN␣□*%
     11.&H2□□/%%D*SG2*WN-SG1*TH2␣*H1&%SG1*TH1&ETA*SG2*WN␣*%1.&H2□□
       N#0
    10 ROH#DO/A
       N#N&1
       IF%N.GT.100□ GO TO 25
       GAP#DO/FF
       ARG#H**2&4. ROH**2
       IF%ARG.LT.0.0□GO TO 25
       ARG#SQRT%ARG␣
```

```
      TO1#ATAN%%-2.*ROH&H*ARG□/%-ROH*-2.*ARG□□
      TO#TO1
   11 S#SIN%TO□
      C#W*COS%TO□
      BN#DO/2.*%SG2-SG1□*C
      BN1#BN*%1.&H2□
      BN2#-BN*H1
      AN#DO/2.*%H1*%SG1*TH2-SG2*WN*D□-%SG1*TH1&ETA*SG2*WN□*%1.&H2□□
      WT#0.0
      X1#0.0
   15 XBYA#EXP%-D*WT/R□/AN*%BN1*SIN%ETA*WT/R□&BN2*COS%ETA*WT/R□□&SIN%WT&
     1TO□
      IF%ABS%X1□.GT.ABS%XBYA□□GO TO 20
      X1#XBYA
   20 IF%WT.GT.3.14□GO TO 21
      WT#WT&0.02
      GO TO 15
   21 WRITE%6,1□TO,X1,GAP
   24 DO#DO&0.02
      GO TO 10
   25 WRITE%6,3□
   50 CONTINUE
    1 FORMAT%5X,8F10.4□
    2 FORMAT%5F10.4□
    3 FORMAT%/,5X,27HGAP TOO BIG,UNSTEADY MOTION    /□
      STOP
      END
```

PROGRAMME 2

```
003727 M D SHAH
$IBFTC
C       TWO PARTICLE IMPACT DAMPER
C       STEADY STATE SOLUTION
C       FREQUENCY RESPONSE
C                       1.      VARING MASS RATIO
C                       2.      VARING GAP FACTOR
C                       3.      VARING COEFFICIENT OF RESTITUTION
        DIMENSION FREQ%25␣
C       READ IN PARAMETERS
        READ%5,2□%FREQ%I□,I#1,20□
        READ%5,2␣FF,D,E3
        DO 50 J#1,42
        READ%5,2␣E,U,DO
        GAP#DO/FF
        U1#2.*U
        WRITE%6,1□FF,D,E,U1,GAP
        WN#7.4*6.28
        DO 50 I#1,2
        W#6.28*FREQ%I□
        R#W/WN
        A#FF/SQRT%%1.-R*R□**2&%2.*D*R□**2□
        ROH#DO/A
        ETA#SQRT%1. D*D␣
        RP#3.14/R
        DRP#-D*RP
        ERP#ETA*RP
        EX#EXP%ERP□
        SI#SIN%ERP□
        CO#COS%ERP□
        H1#EX*SI
        H2#EX*CO
        TH1#WN*EX*% D*SI&ETA*CO□
        TH2#WN*EX*% D*CO□
        ALPO#3.14*E3/%1.&E3□
        C9#%1.-E3□/%3.&E3␣
        C10#-%1.&3.%E3␣/%3.&E3␣
        AK7#%E-U□/%1.&E□
        AK8#%1.&U□/%1.&E□
        AK9#E*%1.&U□/%1.&E□
        AK10#%1.-U*E□/%1.&E□
        C19#%ALPO&3.14*C9/2.□/%W*%AK7*C10&AK8␣␣
        C20#%ALPO&3.14*C9/2.□/%W*%AK9*C10&AK10□□
        SG1#C19
        SG2#C20
        H#2.*W*%%%SG2-SG1□&SG1*SG2*%D*WN-TH2␣□*H1&%SG1*SG2*%TH1&ETA*WN␣□*%
       11.&H2□□/%%D*SG2*WN-SG1*TH2␣*H1&%SG1*TH1&ETA*SG2*WN␣*%1.&H2␣□
```

```
C       CHECKING FOR THE REAL ROOTS
        ARG#H**2&4. ROH**2
        IF%ARG.LT.0.0□GO TO 25
        ARG#SQRT%ARG□
        TO#ATAN%%-2.*ROH&H*ARG□/%-ROH*H-2.*ARG□□
        S#SIN%TO□
        C#W*COS%TO□
        BN#DO/2.*%SG2-SG□*C
        BN1#BN*%1.&H2□
        BN2#-BN*H1
        AN#DO/2.*%H1*%SG1*TH2-SG2*WN*D□-%SG1*TH1&ETA*SG2*WN□*%1.&H2□□
        WT#0.0
        X1#0.0
   15   XBYA#EXP%-D*WT/R□/AN*%BN1*SIN%ETA*WT/R□&BN2*COS%ETA*WT/R□□&SIN%WT&
       1TO□
        IF%ABS%X1□.GT.ABS%XBYA□□GO TO 20
        X1#XBYA
   20   IF%WT.GT.3.14□GO TO 21
        WT#WT&0.02
        GO TO 15
   21   X#X1*A
        WRITE□6,1*FREQ□I*,W,R,X,X1,A,TO
        GO TO 50
   25   WRITE%6,3□
   50   CONTINUE
    1   FORMAT%5X,8F10.4□
    2   FORMAT%5F10.4□
    3   FORMAT%/,5X,27HGAP TOO BIG,UNSTEADY MOTION  /□
        STOP
        END
```

```
$JOB            003727 M D SHAH
$IBJOB          NODECK
$IBFTC
C       IMPACT DAMPER WITH FLUID
        DO 60 MD=1,4
C       READ IN PARAMETERS
        READ(5,4)WN,D,U,E,W,FF,DO,U1
    4   FORMAT(8F10.4)
        R=W/WN
        IF(R.EQ.1.0) GO TO 6
        PSI=ATAN(2.*D*R/(1.-R*R))
        GO TO 8
    6   PSI=1.57
    8   A=FF/SQRT((1.-R*R)**2+(2.*D*R)**2)
        WRITE(6,4)U1,R,E,U,D,FF,DO,A
        IF(DO/A.GT.2.0) GO TO 60
C       INITIAL CONDITIONS
        ETA=SQRT(1.-D*D)
        TI=0.0
        XI=0.0
        YI=0.0
        DXI=0.0
        DYI=0.0
        YY=DO/2.0
        T=TI
        MM=0
        XX=0.0
        DO 50 I=1,250
        AK=0.01
        X1=0.0
C       SOLUTION BETWEEN TWO CONSECUTIVE IMPACTS
        EI=XI-A*SIN(W*TI-PSI)
        DI=(D*EI+DXI/WN-A*R*COS(W*TI-PSI))/ETA
         N=0
    5   T=TI+AK
        X =EXP(-D*WN*(T-TI))*(DI*SIN(ETA*WN*(T-TI))+EI*COS(ETA*WN*(T-TI)))
       1+A*SIN(W*T-PSI)
        Y=-U1*X+YI+U1*XI+(DYI+U1*DXI)*(T-TI)
C       CHECKING IF THE NEXT IMPACT IS REACHED
        ARG=DO/2.-ABS(Y)
        IF(ABS(X1).GT.ABS(X))GO TO 7
        X1=X
    7   IF(ARG.LT.0.0)GO TO 10
        AK=AK+0.01
        N=N+1
        GO TO 5
   10   IF(Y.GT.0.0) GO TO 11
        YY=-DO/2.
```

```
      GO TO 12
   11 YY=DO/2.
   12 CONTINUE
    9 FORMAT(3F10.4)
      K=0
C     NEWTON-RAPHSON METHOD FOR SOLVING TRANSCENDENTAL EQUATION
   14 T2=T
      M=0
   15 T3=T-TI
      WNT=WN*T3
      DWNT=-D*WNT
      IF(ABS(DWNT).GT.85.0) GO TO 50
      EW=ETA*WNT
      EX=EXP(DWNT)
      SI=SIN(EW)
      CO=COS(EW)
      FT=-YY-U1*(EX*(DI*SI+EI*CO)+A*SIN(W*T-PSI))+YI+U1*XI+(DYI+U1*DXI)*
     1T3
      DX=EX*(ETA*WN*(DI*CO-EI*SI)-D*WN*(DI*SI+EI*CO))+A*W*COS(W*T-PSI)
      FDFT=-U1*DX+DYI+U1*DXI
      T1=FT/FDFT
      T=T-T1
      IF(ABS(T1).LT.0.0001)GO TO 21
      IF(M.EQ.100)GO TO 22
      M=M+1
      GO TO 15
   22 WRITE(6,2)
      GO TO 48
   21 YI=YY
      IF(T.LT.TI)GO TO 49
C     COMPUTING THE CONDITIONS AT IMPACT
   20 XI=EXP(-D*WN*(T-TI))*(DI*SIN(ETA*WN*(T-TI))+EI*COS(ETA*WN*(T-TI)))
     1+A*SIN(W*T-PSI)
      DX=EXP(-D*WN*(T-TI))*(ETA*WN*(DI*COS(ETA*WN*(T-TI))-EI*SIN(ETA*WN*
     1(T-TI)))-D*WN*(DI*SIN(ETA*WN*(T-TI))+EI*COS(ETA*WN*(T-TI))))+A*W*C
     2OS(W*T-PSI)
      FDFT=-U1*DX+DYI+U1*DXI
      DXI=DX+U*(1.+E)/(1.+U)*FDFT
      DYI=-E*FDFT
      TI=T
      X1=X1/A
      IF(ABS(ABS(XX)-ABS(X1)).LT.0.00001) GO TO 70
      XX=X1
      GO TO 71
   70 MM=MM+1
      IF(MM.GT.10) GO TO 60
   71 WRITE(6,1)I,TI,XI,YI,DXI,DYI,X1
      GO TO 50
   49 WRITE(6,3)
   48 T=T2+0.2
      K=K+1
      IF(K.GT.15) GO TO 50
```

```
      GO TO 14
   50 CONTINUE
   60 WRITE(6,1)I,T,X,Y
    1 FORMAT(I5,F10.2,F10.4,F10.2,3F10.4)
    2 FORMAT(5X,41HMETHOD DOES NOT CONVERGE IN 50 ITERATIONS )
    3 FORMAT(5X,27HT FOUND LESS THAN T1)
      STOP
      END
$ENTRY
$IBSYS
```

REFERENCES

1. Paget, A., "The Acceleration Damper", Engineering 1934, 557.

2. Lieber, P. and Jensen, D.P., "An Acceleration Damper: Development, Design and Some Applications", Trans. ASME, Vol. 67 (1945), pp. 523 - 530.

3. Grubin, C., "On The Theory of Acceleration Damper", Journal of Applied Mechanics, Vol. 23, Trans. ASME, Vol. 78 (1956), pp. 373 - 378.

4. Arnold, R. N., "Response of an Impact Vibration Absorber to Forced Vibrations", Ninth International Congress of Applied Mechanics (1956).

5. Warburton, G.B., Discussion of "On The Theory of Acceleration Damper", Journal of Applied Mechanics, Vol. 24, Trans. ASME, Vol. 79 (1957), pp. 322 - 324.

6. Masri, S. F., "Analytical and Experimental Studies of Impact Dampers", Ph.D. Thesis, California Institute of Technology (1965).

7. Marsi, S. F., "Electric-Analog Studies of Impact Dampers", Experimental Mechanics, February 1967.

8. Masri, S. F. Brief Note on "Motion and Stability of Two-Particle, Single-Container Impact Dampers", Journal of Applied Mechanics, June 1967, pp. 506 - 507.

9. Kaper, H. G., "The Behaviour of a Mass -Spring System Provided with a Discontinuous Dynamic Vibration Absorber", Journal of Appl. Sci. Vol. 10, Section A, pp. 369 - 383.

10. Egle, D.M., "An Investigation of An Impact Vibration Absorber", ASME Paper No. 67, Vibr. 10.

11. Sadek, M. M., "The Behaviour of the Impact Damper", The Institution of Mechanical Engineers, Proceedings 1965-66, Vol. 180, Part 1.

12. Sakaguchi, R. L., "Particle Damping of Forced Vibrations", M.A.Sc. Thesis, University of Toronto, 1964.

13. McGoldric, R. T., "Experiments with An Impact Vibration Damper", David Taylor Model Basin Report, No. 816.

14. Lieber, P. and Tripp, F., "Experimental Results on The Acceleration Damper", Rensselaer Polytechnic Institute Aeronautical Laboratory, Report No. TRAE 5401 (1954).

15. Sankey, G. O., "Some Experiments on a Particle or 'Shot' Damper", Memorandum, Westinghouse Research Labs. (1954).

16. Duckwald, C. S., " Impact Damping for Turbine Buckets", General Engineering Laboratory, General Electric, Report No. R55 GL 108 (1955).

17. Estabrook, L. H. and Plunkett, R., "Design Parameters for Impact Dampers", General Engineering Laboratory, General Electric, Report No. R55 GL 250 (1955).

18. Jha, S. K. "Steady State Response of a Non-Linear Mechanical System Provided with an Impact Vibration Absorber", M.Eng. Thesis, McMaster University, 1966.

19. Nielsen, K. L., "Methods in Numerical Analysis", The Mcmillan Company, Second Edition, 1964.